Using these forces, the effective vertical load, $D_{effective}$, calculation is described below.

Reactor Building Effective Dead Weight with Water Table Buoyancy

The effective dead weight, or buoyant weight, is calculated using the following equation:

$$D_{effective} = W_{RXB} - R_{buoyancy} \quad \text{Eq. 3.8-3}$$

where,

W_{RXB} = 587,147 kips.

Therefore,

$D_{effective}$ = 587,147 - 279,445 = 307,702 kips

Control Building Effective Dead Weight with Water Table Buoyancy

The effective dead weight, or buoyant weight, is calculated using the following equation:

$D_{effective} = W_{CRB} - R_{buoyancy}$, where

W_{CRB} = 45,774 kips.

Therefore,

$D_{effective}$ = 45774 - 40,500 = 5,274 kips

3.8.5.4 Design and Analysis Procedures

3.8.5.4.1 Foundation Basemat Analysis

Foundation basemats are analyzed and designed for static and seismic loads. Forces and moments in the basemat and pressures below the basemat are evaluated. Where a linear analysis did not provide acceptable results, a nonlinear analysis showed satisfatory conclusions.

3.8.5.4.1.1 Analysis of Reactor Building Basemat

RXB Basemat and Stability Linear Analysis

The design input parameters used to perform the flotation, sliding, and overturning evaluations are listed in Table 3.8.5-1.

3.8.5.4.1.2 RXB Basemat Analysis Model Description

The envelope of the soil bearing pressure due to the seismic loads is calculated using the two SASSI2010 models, and the soil bearing pressure envelope due to the static loads is calculated using the two SAP2000 models. A separate SAP2000 model was developed for the RXB basemat model. The two layers of the solid elements modeling the RXB concrete foundation were replaced by a single layer of shell elements. The thickness of the shell elements is the same as the foundation thickness (i.e., 120") and the centerline of the shell elements is at the bottom of the basemat. The pilasters on the building perimeter and walls within the footprint were connected to the shell elements, thereby acting as inverted supports to the basemat. All the pilaster and wall joints at the top of the foundation (i.e., Z = 120") are restrained for the six degrees of freedom. Elements above the elevation Z = 120" were deleted. The shell elements of the basemat model are subjected to out-of-plane loading. The purpose of restraining the nodes associated with the walls is to hold the basemat in the vertical direction to apply the out-of-plane loads. Under vertical soil pressure loads, walls are expected to provide sufficient vertical support to create "fixed-node" behavior at nodes shared by walls and basemat. The applied loads on the basemat shell model are the out-of-plane soil pressure extracted from static and dynamic analyses of the RXB. After the soil pressure is calculated from the static and dynamic analysis, these soil pressures are applied as out-of-plane pressure to the basemat shell elements. The results of this analysis would provide the internal moments and shear for the design of the basemat.

Table 3.8.5-16 shows a summary of the RXB basemat model.

Figure 3.8.5-1 shows the SAP2000 RXB basemat model. The area elements shown in light red tinge are shell elements representing the base slab.

Figure 3.8.5-2 and Figure 3.8.5-3 show the static and seismic base pressure contours on the shell foundation in the RXB basemat model.

Figure 3.8.5-4 and Figure 3.8.5-5 show the main bending moments due to static base pressures in the RXB basemat model.

Figure 3.8.5-6 and Figure 3.8.5-7 show the main bending moments due to seismic base pressures in the RXB basemat model.

For both the seismic and static base pressures, the applied base pressures will directly give the forces and moments for the foundation. The demands obtained thus are acceptable for foundation solid elements that are not connected to any wall or pilaster. However, for foundation solid elements that are connected to walls or pilasters, the demands will be much higher than what is obtained by the application of base pressures. In view of this, for solid elements that are connected to the walls and pilasters, the fixed end forces and moments are added to the affected foundation shell element responses.

The static forces and moments in the basemat are calculated with both the standalone and the combined building SAP2000 models.

The seismic forces, moments and stresses in all structural elements such as walls, pilasters, and basemat were calculated using the standalone and combined SASSI2010 models. The enveloped base pressures were applied to the solid foundation model to evaluate the responses. To be consistent with the SASSI2010 analysis, absolute values of all responses obtained by applying base pressures from SASSI2010 were used together with the fixed end forces and moments from walls and pilasters to arrive at the seismic demands.

As shown in Table 3.8.5-5, the linear analysis for stability gave factors of safety less than 1 for sliding. Therefore a nonlinear analysis was performed for RXB Sliding.

Nonlinear Analysis Approach for RXB Sliding where Linear Analysis is too conservative

Where the RXB linear sliding analyses did not yield acceptable factors of safety results for sliding, detailed nonlinear sliding analyses were performed using ANSYS. The fixed base boundary conditions for this analysis were compared favorably with the SAP2000 linear analysis boundary conditions, and the model is shown in Figure 3.8.5-8. The nonlinear ANSYS analysis uncoupled the soil domain from the building to permit simulation of sliding under seismic conditions by creating two coincident joint/nodes in the finite element mesh, one belonging to the RXB and one belonging to the backfill soil. The coincident nodes were used to define a nonlinear contact region as shown on Figure 3.8.5-9. A coefficient of friction of 0.5 was used so that the tangential force required for overcoming compressive normal force resistance to allow the building to slide and uplift relative to the soil is equal to half of the normal force between the RXB walls and soil.

The seismic analyses were performed in SASSI for Soil Type 11 backfill. The SASSI results yielded acceleration versus time in the global N-S, E-W, and vertical direction for each node on the external surface of the RXB and the backfill soil. The SSI seismic input acceleration histories in the three orthogonal directions obtained at representative skin node 946 were applied to 5,822 RXB and backfill soil nodes in contact with the in-situ soil. These nodes are shown on Figure 3.8.5-11 and Figure 3.8.5-12. There were a total of three time histories for each soil type considered.

Rather than directly applying the SASSI accelerations to the RXB and backfill soil, coincident nodes were created. Nonlinear node-to-node CONTA178 elements were defined between the coincident nodes as shown in Figure 3.8.5-13 and Figure 3.8.5-14. Figure 3.8.5-15 illustrates the CONTA178 definition wherein forces are transferred between the end node-I and node node-J only when the gap is closed, i.e., transmitting compression but not tension. The elements directly under the RXB basemat have a coefficient of friction of 0.58 defined to resist sliding.

A pressure of 36.92 psi was applied to the bottom of the basemat to account for buoyancy effects as shown on Figure 3.8.5-16. The static surcharge effects from the backfill soil against the RXB outer wall are ignored.

Table 3.8.5-6 shows the number of elements in the ANSYS structural analysis model including joints, frame elements, shell elements, solid elements, and links/supports.

East-west and north-south unidirectional, horizontal time-history analyses were performed for each of the surrounding Soil Types 7, 8, and 11. For all cases, the respective acceleration time-history from the SASSI representative skin node 946 was applied uniformly to all the boundary nodes in the ANSYS model, while the displacements in the other two directions were constrained. Thus, for each soil type, the cases performed were acceleration time history in the east-west direction, with the displacements in the vertical and north-south directions fixed and acceleration time history in the north-south direction, with the displacements in the vertical and east-west directions fixed.

Figure 3.8.5-17 through Figure 3.8.5-19 show the input acceleration time histories for each of the Soil Type 7 cases.

Figure 3.8.5-20 through Figure 3.8.5-22 show the input acceleration time histories for each of the Soil Type 8 cases.

Figure 3.8.5-23 through Figure 3.8.5-25 show the input acceleration time histories for each of the Soil Type 11 cases.

3.8.5.4.1.3 Analysis of Control Building Basemat

The static load results are obtained from the SAP2000 model of the CRB. Both the stand-alone and the combined CRB SAP2000 models are used to obtain the static forces and moments in the basemat, using the most critical static load combination for the calculation of structural responses. Bending moments, axial and shear forces in the basemat are extracted from the SAP2000 CRB global model. To do this, the foundation's solid elements' nodal forces from the CRB model are converted into axial and shear forces, and moments, by applying equilibrium along the solid faces perpendicular to the global X and Y axes. Final bending moments include the effect of the twisting moments.

For dynamic loads, the basemat solid element stresses obtained from the SASSI analysis are used. The axial and shear forces are obtained by multiplying the axial and shear stresses by the solid element thickness. The bending moments are calculated using a separate SAP2000 shell element basemat model. In this model, the nodes along the base of the concrete walls are fixed and the soil pressure from the SASSI analysis results are applied as out-of-plane pressure to the basemat shell elements. For the shell elements on the perimeter of the basemat, the end moments of the perimeter walls, obtained from SASSI results, are used.

For the tunnel basemat, the bending moments are also estimated by considering the tunnel basemat as a simple-supported one-way slab spanning between the exterior and middle tunnel walls. Conservatively, the ends moments of the exterior and middle walls are averaged and added to the

simple-supported moments at the center of the span. The resultant moment is used for both global X and Y axes.

The solid element seismic stresses are calculated using the stand-alone and combined SASSI2010 models. Figure 3.8.5-2a and Figure 3.8.5-3a show the CRB basemat contour pressure for static and seismic load combinations. Figure 3.8.5-4a and Figure 3.8.5-5a show the CRB basemat static Myy and Mxx from the standalone SAP2000 model. Figure 3.8.5-6a and Figure 3.8.5-7a show the CRB basemat seismic Myy and Mxx. The enveloped seismic pressures are obtained as a result of the four-step, post-processing method described in Section 3.7.2. Absolute values of the responses are used.

Control Building Basemat and Stability Linear Analysis

Acceptance criteria for flotation/ uplift, sliding, and overturning is based on a factor of safety (FOS) determined from the ratio of the driving force to the resisting force. These analyses are performed statically using the maximum forces from the combinations of soil profiles, time histories, and cracked/uncracked conditions discussed in Section 3.7. The FOS performed for the CRB yielded unacceptable results (less than 1.1 FOS) for uplift stability; therefore, the uplift, sliding and overturning of the CRB is determined by a nonlinear sliding and uplift analysis.

3.8.5.4.1.4 Control Building Basemat Nonlinear Analysis Model Description

For the nonlinear analysis, the ANSYS CRB model with fixed-base boundary sliding and uplift conditions was changed to:

1) Provide independence of the building and soil domain by establishing coincident joints/nodes for the building and soil in the finite element mesh.

2) Define a nonlinear frictional contact region with the coincident nodes as shown in Figure 3.8.5-26. A coefficient of friction of 0.5 (between the CRB walls and soil) was used so that the tangential force required to overcome the resistance from any compressive normal force is equal to half the normal force, allowing the building to slide and uplift relative to the soil.

3) Obtain, at a typical skin node near the CRB basemat, the seismic input acceleration time histories in the three orthogonal directions for the Soil Type 11 backfill in combination with the surrounding Soil Type 7 and Soil Type 11. Three time histories for each soil type were considered by uniformly applying the time histories from the typical skin node to the CRB and backfill soil nodes, as shown in Figure 3.8.5-27, which are in contact with the in-situ soil. The SASSI time histories for the Capitola input case were selected since that case produced the largest horizontal base reactions, as shown in Table 3.8.5-3. The three time histories are shown in

    - Acceleration time history for each of the Soil Type 11 cases (Figure 3.8.5-28 through Figure 3.8.5-30)

- Acceleration time history for each of the Soil Type 7 cases. (Figure 3.8.5-31 through Figure 3.8.5-33)

4) Create coincident nodes and define nonlinear node-to-node CONTA178 elements as shown on Figure 3.8.5-34 and Figure 3.8.5-35 to accurately model the contact gap between CRB and soil. The typical definition of CONTA178 elements is shown in Figure 3.8.5-15, where forces are transferred between node-I and node-J only when the gap is closed. The elements directly under the CRB foundation have a coefficient of friction of 0.55 defined to resist sliding, i.e., transmitting compression but not tension. The elements on the sides of the CRB have a coefficient of friction of 0.50 defined to resist sliding.

5) Account for buoyancy effects by applying a pressure of 29.399 psi to the bottom of the basemat, as shown in Figure 3.8.5-36. The buoyancy pressure was determined as follows:

   Total modeled area = basemat area + tunnel area = 78' × 116.667' + 25' × 18.667'

   = 9,100 ft^2 + 466.67 ft^2 = 9,566.67 ft^2

   Buoyancy pressure = 40,500,000 lbs / (9,566.67×144) in^2 = 29.399 psi

6) Include Poisson's ratio effect in the static soil pressure profile due to the deadweight of the backfill soil on the CRB walls as a conservative measure. The pressure profile is shown in Figure 3.8.5-37. The Poisson's ratio effect produces a complex pressure distribution depending on the local flexibility of the walls (Figure 3.8.5-38 and Figure 3.8.5-39).

The model summary showing quantity of elements in the ANSYS structural analysis model including joints, frame elements, shell elements, and solid elements is shown in Table 3.8.5-10. A comparison of the SAP2000, SASSI2010, and ANSYS models also is shown in Table 3.8.5-10.

The coordinate system for the nonlinear analysis is represented by the CRB SAP2000 model as shown in Figure 3.8.5-40. The X axis points to the East, the Y axis point to the North, and the Z axis points vertically upward. The X-coordinate of the west side of the CRB tunnel is 350'-0" (4,200") in the global X-direction (East-West) from the origin of the global SAP2000 coordinate system.

COL Item 3.8-3: A COL applicant that references the NuScale Power Plant design certification will identify local stiff and soft spots in the foundation soil and address these in the design, as necessary.

3.8.5.5 Evaluation Criteria for Stability Analysis

3.8.5.5.1 Flotation and Uplift Stability Analysis Approach

Flotation is calculated for static conditions and uplift is calculated with the earthquake present.

The factor of safety is calculated as follows, with load combination E for flotation and load combination C for uplift:

$$FOS = \frac{F_{resisting}}{F_{driving}} \quad \text{Eq. 3.8-1}$$

$$FOS_{flotation} = \frac{D}{B} \quad \text{Eq. 3.8-2}$$

$$FOS_{uplift} = \frac{D + F}{B + Rz} \quad \text{Eq. 3.8-3}$$

Where

$F_{resisting}$ is the resistance of the buried portion of the structure. This includes two components:

D= the weight of the building

F = Vertical friction due to static soil pressure

The driving forces for uplift are from groundwater and seismic motion. This includes two components:

B = the buoyant force from groundwater or floodwater at grade.

Rz = Upward inertia = Seismic vertical base reaction (when soil moves downward in the direction of gravity).

3.8.5.5.2 Sliding Stability Analysis Approach

The sliding stability evaluation is done with load combination C as described in Section 3.8.5.3.

The stability evaluation is determined by comparing the total resisting sliding forces and the total driving sliding forces. A sliding evaluation is performed for both directions separately; one for east-west movement (Global X-direction) and one for North-South movement (Global Y-direction).

The RXB and CRB are deeply embedded structures, therefore, the frictional resistance provided by the interaction of soil and structure on the exterior walls and basemats is considered.

The sliding driving force is the inertia force due to seismic. By neglecting insignificant damping forces, the total inertia force equals the sum of all reaction forces on walls and basemat. The inertia force is thus calculated by adding seismic reactions.

Friction Resistance to N-S Sliding

Two force components result in frictional resistance against North-South sliding:

- Friction resistance between foundation and soil.
- Frictional resistance on East and West walls from effective static soil pressure. See Section 3.8.5.3.2 for the definition of effective static soil pressure.

Friction Resistance to E-W Sliding

Two force components result in frictional resistance against East-West sliding:

- Friction resistance between foundation and soil
- Frictional resistance on North and South walls from effective static soil pressure. See Section 3.8.5.3.2 for the definition of effective static soil pressure.

Friction between Basemat and Soil due to Effective (or Buoyant) Dead Weight

For sliding stability evaluation, the effective dead weight, or buoyant weight, of the RXB is an important stabilizing force.

The RXB buoyant dead weight is calculated in Section 3.8.5.3.3 as:

$D_{effective}$ = 307,702 kips

The RXB friction resistance R_sliding between basemat and soil against N-S or E-W sliding is calculated by multiplying the buoyant weight and the friction coefficient as follows:

$R_{sliding} = D_{effective} \times \mu$ (Eq 3.8-6) = 307,702 × 0.58 = 178,467 kips

Similarly, the CRB buoyant dead weight, calculated in Section 3.8.5.3.3, is 5,274, kips. The frictional resistance $R_{sliding}$ between the basemat and soil against N-S or E-W sliding is:

$R_{sliding} = D_{effective} \times \mu$ = 5,274 x 0.58 = 3,059 kips

3.8.5.5.3 Overturning Stability Analysis Approach

The overturning stability evaluation is done with load combination C as described in Section 3.8.5.3. The factor of safety for overturning is calculated as follows:

$$FOS_{overturning} = \frac{M_{restoring}}{M_{overturning}} \quad \text{Eq. 3.8-4}$$

The overturning evaluation is determined by comparing the total resisting overturning moment and the total driving overturning moments. An overturning evaluation is performed for both directions separately; one for the North-South movement (moment about Global X-direction) and one for the East-West movement (moment about Global Y-direction).

The RXB is a deeply embedded structure, therefore, the frictional resisting moments provided by the interaction between soil and structure on the exterior walls and basemat are considered. The restoring moment due to the effective vertical load is also included in the evaluation.

Three components result in resistance to overturning:

- Friction on Parallel Walls
- Friction on Perpendicular Walls
- Effective Dead Weight

The North-South overturning pivot for the RXB is the north edge of the foundation. The East-West overturning pivot is the west wall edge of the foundation.

RXB Resistance to North-South Overturning

The resisting moment resulting from friction on the East and West walls is:

$$M_1 = (F_{EAST} + F_{WEST}) \times r_{cg} \quad \text{Eq. 3.8-5}$$

where

F_{EAST} = total friction force on the East wall

F_{WEST} = total friction force on the West wall

r_{cg} = Moment arm = perpendicular distance from pivot point (edge of North wall) to line of friction force = (150.5'/2) + 6' = 81.25' (Table 3.8.5-7)

The resisting moment resulting from friction on the South wall is:

$$M_2 = (F_{SOUTH}) \times L_{NS} \quad \text{Eq. 3.8-6}$$

where

F_{SOUTH} = total friction on the south wall

L_{NS} = moment arm = North-South width of the foundation = 156.5'

The resisting moment resulting from buoyant dead weight is:

$$M_3 = (D_{effective}) \times L_{NS1} \quad \text{Eq. 3.8-7}$$

where

$D_{effective}$ = 307,702 (Section 3.8.5.3.3)

L_{NS1} = moment arm = half width of North-South width of foundation = 81.25'

M_3 = 307,702 x 81.25 = 25,000,824 kip-ft

The resultant frictional resistance to North-South overturning is:

$M_{NS} = M_1 + M_2 + M_3$

RXB Resistance to East-West Overturning

The resisting moment resulting from friction on the North and South walls is:

$$M_4 = (F_{NORTH} + F_{SOUTH}) \times r_{cg} \quad \text{Eq. 3.8-8}$$

where

F_{NORTH} = total friction on the North wall

F_{SOUTH} = total friction on the South wall

r_{cg} = moments arm = perpendicular distance from pivot (edge of West Wall) to line of friction force = (346'/2) + 6' =179'

The resistant moment resulting from friction on the East wall:

$$M_5 = (F_{EAST}) \times L_{EW} \quad \text{Eq. 3.8-9}$$

where

F_{EAST} = Total friction on the East wall

L_{EW} = moment arm = East-West width of the foundation = 352'

The resisting moment resulting from buoyant dead weight is:

$$M_6 = (D_{effective}) \times L_{EW} \quad \text{Eq. 3.8-10}$$

where

$D_{effective}$ = 307,702 kips (Section 3.8.5.3.3)

L_{EW} = moment arm = half of East-West width of foundation = 179'

M_6 = 307,702 X 179 = 55,078,739 kip-ft

The resultant resistance to East-West overturning is:

$$M_{EW} = M_4 + M_5 + M_6$$

3.8.5.5.4 Bearing Pressure Approach

Average Bearing Pressure

Average static bearing pressure is calculated by dividing the building weight by the building footprint. Seismic average bearing pressure is calculated by the algebraic summation of reaction time histories in the rigid springs below the basemat. The springs connect the basemat with the free-field soil. The algebraic summation yields three time histories of total basemat reactions in the three global directions due to each seismic input. From the time histories, the maximum reactions can be obtained. The vertical reaction divided by the total area of the basemat yields the average bearing pressure.

Localized Bearing Pressure

Localized bearing pressure under each building's basemat is calculated using the forces in the rigid springs, which connect the RXB and the CRB basemats to the excavated free-field soil (or to a fixed support for the static case). The vertical force in a spring is divided by the tributary area of the spring to obtain the localized nodal soil pressure. For the seismic case, reactions are obtained as a result of the four-step post-processing method described in Section 3.7.2.4.1.

3.8.5.5.5 Settlement Approach

A large-scale SAP2000 finite element model is used to determine the effect of foundation differential movements. To maximize the effect of the differential movements, the soil is modeled using the softest soil profile, i.e., Soil Type 11. In addition, the soil stiffnesses are further reduced by 50 percent to amplify the effect of differential movements or settlements. The 50 percent reduction in soil stiffness includes the areas below the triple building basemats and is extended to the entire free-field soil model. The size of the soil included in the model is so large that the static displacements induced by the static loads of the structures become

negligible on the edges of the freefield soil model. The model is analyzed for both the cracked and uncracked concrete conditions.

The size of the freefield soil block in the model is 2005.5' long, 768.5' wide, and 360' deep. Figure 3.8.5-41 shows the overall size of the freefield soil block with the three embedded buildings.

As discussed in Section 3.8.4, Load combination 10 using Equation 9-6 of ACI 349 governs

$$U = D + F + H + 0.8L + C_{cr} + T_o + R_o + E_{sse}$$

For the dynamic analyses, the dead weight of the building was increased to account for the effect of live and snow loads.

The results presented in the NuScale Power Plant design certification application for which the soil stiffness is reduced by 50 percent include the following:

1) Determination of static demand forces for the RXB foundation design.

2) Determination of static demand forces for the CRB building and foundation design.

3) Determination of maximum differential displacements within each building foundation over 50 feet in length and maximum foundation bottom tilt angle of the CRB.

Results presented in the FSAR which include the effects of the 50 percent reduction in soil stiffness can be found in Table 3B-36 through Table 3B-38.

3.8.5.6 Results Compared with Structural Acceptance Criteria

3.8.5.6.1 RXB Stability

Factors of safety (FOS) were determined for 16 cases for the RXB. The cases include enveloping seismic loads from two RXB models (a standalone RXB model and an integrated RWB+RXB+CRB triple building model), two concrete conditions (cracked and uncracked with 7 percent damping) and four soil profiles (Soil Types 7, 8, 9, and 11) and are shown in Table 3.8.5-5. The results in this table indicate that the linear analysis for RXB sliding stability did not yield a FOS of greater than 1.

The minimum acceptable factor of safety for flotation, uplift, sliding and overturning is 1.1. This was not achieved for RXB sliding. Table 3.8.5-5 summarizes the factors of safety for the RXB.

A nonlinear analysis was performed for the RXB to show sliding was insignificant.

Bearing pressure is used to establish a design parameter for bearing capacity for site selection. The bearing capacity of the soil should provide a factor of safety of 3.0 for the static bearing pressure and a factor of safety of 2.0 for dynamic bearing

pressure. The maximum allowable tilt settlement for the Reactor Building is 1" total or ½" per 50 feet in any direction at any point in the structure. The maximum allowable total settlement at any foundation node is four inches.

3.8.5.6.1.1 RXB Uplift

As shown in Section 3.8.5.5.1,

$$FOS = \frac{F_{resisting}}{F_{driving}} \qquad FOS_{flotation} = \frac{D}{B} \qquad FOS_{uplift} = \frac{D + F}{B + Rz}$$

The FOS for flotation is shown in Table 3.8.5-5 for each of the 16 cases considered, including cracked and uncracked conditions, Soil Types 7, 8, 9 and 11, and for RXB model and the triple building model. For each of the cases, an acceptable FOS for overturning was met.

3.8.5.6.1.1.1 Dynamic RXB Uplift Ratio

The effect of foundation uplift has been evaluated for the RXB. The linear SSI analysis methods are acceptable if the ground contact ratio is equal to or greater than 80 percent. The ground contact ratio can be calculated from the linear SSI analysis using the minimum basemat area that remains in compression with the soil. The seismic total vertical base reactions are calculated by the time step-by-time step algebraic summation of all nodal vertical reactions of the nodes of the RXB basemat. The maximum seismic vertical reactions for the cracked and uncracked concrete conditions for the two models are summarized in Table 3.8.5-4. The base vertical reaction results for the uncracked condition are similar to those for the cracked concrete condition.

As shown in Table 3.8.5-4, the seismic reactions are much less than the total dead weight reaction of 471,487 kips over the rectangle basemat area. The dead weight reaction corresponds to the self-weight of the concrete structures, equipment, and water weight. Thus, the net reactions are always in compression.

The typical total basemat vertical reaction time histories are shown in Figure 3.8.5-42 through Figure 3.8.5-47. Figure 3.8.5-42 and Figure 3.8.5-43 show the reactions for comparison between the cracked and uncracked concrete conditions. Each of the CSDRS- and CSDRS-HF-compatible seismic inputs contain three acceleration components, X (EW), Y (NS), and Z (vertical).

Figure 3.8.5-44 through Figure 3.8.5-47 are for the cracked concrete condition for the CSDRS Capitola input and CSDRS-HF Lucerne input. As can be seen in these figures, the total reactions are always in compression. The cracked and uncracked total reactions can be compared using Figure 3.8.5-42 for the cracked reaction and Figure 3.8.5-43 for the uncracked reaction due to Capitola input for Soil Type 7. The differences in

total reactions are small because the differences between the cracked and uncracked seismic reactions and between standalone RXB and triple building models are small as shown in Table 3.8.5-4.

Based on the examination of the total vertical reaction force underneath the basemat, all net vertical reactions are in compression. Thus, the basemat is 100 percent in contact.

3.8.5.6.1.2 Reactor Building Sliding

As shown in Section 3.8.5.5.1,

$$FOS_{sliding} = \frac{R_{resisting}}{R_{driving}} \qquad \text{Eq. 3.8-11}$$

Linear evaluations have shown that an acceptable FOS for sliding is not met, as shown on Table 3.8.5-5. Therefore, a nonlinear sliding analysis has been performed to show that sliding is insignificant.

Nonlinear Analysis

Figure 3.8.5-52 shows the designations used (A through D) for the locations on the RXB basemat where lateral displacements (sliding) were assessed between two end nodes of CONTA178 elements.

Figure 3.8.5-53 through Figure 3.8.5-60 show the E-W and N-S sliding displacements for Soil Type 7 for the four foundation locations (A, B, C, and D).

Figure 3.8.5-61 through Figure 3.8.5-68 show the E-W and N-S sliding displacements for Soil Type 11 for the four foundation locations (A, B, C, and D).

Figure 3.8.5-69 through Figure 3.8.5-76 show the E-W and N-S sliding displacements for Soil Type 8 for the four foundation locations (A, B, C, and D).

A detailed summary of the sliding displacement results are provided in Table 3.8.5-11. The results indicate that the deeply embedded RXB experiences less than 1/8" of sliding horizontal displacement. The magnitude of the displacements presented is insignificant.

3.8.5.6.1.3 RXB Overturning

As shown in Section 3.8.5.5.3,

$$FOS_{overturning} = \frac{M_{restoring}}{M_{overturning}}$$

The FOS for overturning is shown in Table 3.8.5-5 for each of the 16 cases considered, including cracked and uncracked conditions, Soil Types 7, 8, 9, and

11, and for RXB model and the triple building model. For each of the cases, an acceptable FOS for overturning was met.

3.8.5.6.2 CRB Stability

The minimum acceptable factor of safety for flotation, uplift, sliding, and overturning is 1.1. This was not achieved for the CRB uplift.

Linear analyses were overly conservative and showed unsatisfactory results for the CRB Stability Analyses, so nonlinear evaluation was used. The uplift, sliding, and overturning stability analysis of the Control Building is performed using a nonlinear sliding and uplift analysis. A nonlinear sliding, overturning, and uplift analysis was performed for the CRB to show that sliding, overturning, and uplift are insignificant.

Figure 3.8.5-48 shows the designations used (A through I) for the locations on the CRB basemat where the relative vertical displacements (uplift) and lateral displacements (sliding) were assessed between the two end nodes of the CONTA178 elements.

Bearing pressure is used to establish a design parameter for bearing capacity for site selection. The bearing capacity of the soil should provide a factor of safety of 3.0 for the static bearing pressure and a factor of safety of 2.0 for dynamic bearing pressure. The maximum allowable tilt settlement for the Control Building is 1" total or 1/2" per 50 feet in any direction at any point in the structure. The maximum allowable total settlement at any foundation node is 4 inches.

3.8.5.6.2.1 CRB Uplift

The key results are:

The relative displacements between the nodes at the basemat of the CRB are considered as actual uplift between CRB and surrounding soil. (Negative displacement values are considered as penetrations; a negligible amount of penetration is expected for penalty stiffness based contact algorithms.)

The elements transfer loads only when the contact is made. Therefore, the reactions drop to zero when there is a contact gap or uplift. This can be clearly seen from the force versus uplift comparison at location A in Figure 3.8.5-49 and Figure 3.8.5-50. The CRB is in an uplifted state at this corner location A for an infinitesimal duration of time just before the 10 seconds mark, resulting in zero reaction forces. The maximum uplift at location A is less than 1/64". The magnitude of this displacement is insignificant. Thus, the potential for uplift is insignificant.

3.8.5.6.2.1.1 Dynamic CRB Uplift Ratio

The effect of the foundation uplift has been evaluated for the CRB. The linear SSI analysis methods are acceptable if the ground contact ratio is equal to or greater than 80 percent. The ground contact ratio can be calculated from the linear SSI analysis using the minimum basemat area

that remains in compression with the soil. The seismic total vertical base reactions are calculated by the time step-by-time step algebraic summation of all nodal vertical reactions of the nodes of the CRB basemat. The maximum seismic vertical reactions for the cracked and uncracked concrete conditions are summarized in Table 3.8.5-14. The base vertical reaction results for the uncracked condition are similar to those for the cracked concrete condition.

As shown in Table 3.8.5-14, the seismic reactions are much less than the total dead weight reaction over the rectangle basemat area of 45,774 kips. The dead weight reaction corresponds to the self-weight of the concrete and steel structures, and equipment (based on SAP2000 calculations). Thus, the net reactions are always in compression.

The typical total basemat vertical reaction time histories are shown in Figure 3.8.5-77 through Figure 3.8.5-82. The first two show the reactions for comparison between the cracked and uncracked concrete conditions. Others are all for the cracked concrete condition for the CSDRS Capitola input and CSDRS-HF Lucerne input. As can be seen in these figures, the total reactions are always in compression. Each of the CSDRS- and CSDRS-HF-compatible seismic inputs contain three acceleration components, X (EW), Y (NS), and Z (vertical).

The cracked and uncracked total reactions can be compared using Figure 3.8.5-77 for the cracked reaction and Figure 3.8.5-78 uncracked reaction due to Capitola input for Soil Type 7. The differences in total reactions are small because the differences between the cracked and uncracked seismic reactions are small as shown in Table 3.8.5-14.

Based on the examination of the total vertical reaction force underneath the basemat, all net vertical reactions are in compression. Thus, the basemat is 100 percent in contact.

3.8.5.6.2.2 Control Building Sliding

Figure 3.8.5-51 shows the relative sliding between the nodes at location A. In contrast to penetration compatibility, sliding can exhibit both positive and negative values equally since the nodes could move away from each other, towards one side or the other. Maximum sliding at A is approximately 0.006".

A summary of the results is provided in Table 3.8.5-12. The magnitudes of these displacements are insignificant. Thus, the potential for sliding is insignificant.

3.8.5.6.2.3 Control Building Overturning

The results provided in Table 3.8.5-12 show that the deeply embedded Control Building experiences less than 1/10" of sliding displacement and less than 1/64" of total vertical uplift displacement. The magnitudes of these displacements are insignificant. Thus, the potential for overturning is insignificant.

3.8.5.6.3 Average Bearing Pressure

As stated in Section 3.8.5.5.4, the average static bearing pressure is the dead load of the building divided by the footprint.

The seismic weight of the RXB is 587,147 kips and the calculated footprint is 58,175 ft^2. This results in an average pressure of 10.1 ksf. This results in a factor of safety of 7.4 to the minimum soil bearing capacity of 75 ksf specified in Table 2.0-1. The seismic weight of the CRB, including the tunnel, is 49,041 kips. The rectangular basemat area is 11,800 ft^2, the tunnel area is 501 ft^2, which makes a total area of 12,301 ft^2. This results in an average static bearing pressure of 4.0 ksf. This provides a factor of safety of 19 to the minimum soil bearing pressure of 75 ksf provided in Table 2.0-1.

The average dynamic bearing pressure is obtained as described in Section 3.8.5.5.4, with the vertical reaction for the entire basemat computed at each time step. The RXB foundation average dynamic pressure is 4.6 ksf. The CRB average foundation dynamic pressure on the rectangular basemat is 2.3 ksf. The average dynamic pressure on the tunnel area is not calculated. Maximum dynamic pressures across the entire CRB basemat, including the tunnel basemat, are shown on Figure 3.8.5-3a. These pressures are obtained by the post-processing approach indicated in Section 3.7.2.4.1.

3.8.5.6.4 Settlement

Displacement values are provided in Table 3.8.5-7a and Table 3.8.5-7b for selected nodes in the foundation shown in Figure 3.8.5-10. Summaries of different settlement types are given in Table 3.8.5-7c and Table 3.8.5-7d. The calculated angle of foundation rotation in these tables is based upon the building foundation dimensions in Table 3.8.5-19.

Total settlement, tilt settlement, and differential settlement are minimal, as shown in Table 3.8.5-7a through Table 3.8.5-7d. The maximum allowable differential settlement between the RXB and CRB, and between the RXB and RWB is 0.5 inch.

The RXB settles approximately 1¾ inch on the west end and approximately 2 inches on the east end. The tilt settlement of 0.25" is less than 1" as cited in Section 3.8.5.6.1. There is negligible tilt north to south. The east end of the building contains the pool and the NPMs.

The CRB settles approximately 1¾ inch on the west end and approximately 1 inch on the east end. The tilt settlement of 0.75" is less than the 1" limit cited in Section 3.8.5.6.2. North to south tilt is negligible. The CRB tilts toward the RXB. Differential settlement between the two buildings is on the order of ¼ inch. The displacements at the four corners of the tunnel foundation calculated for the cracked concrete condition are provided in Table 3.8.5-17, and the rotation of the tunnel foundation is –0.0361°, as shown in Table 3.8.5-18. The tunnel foundation has negligible differential settlement in the north-south direction, and the differential settlement over 50 ft length in the east-west direction is -0.36."

The Seismic Category II Radioactive Waste Building settles approximately ½ inch on the west end and approximately 1½ inch on the east end. The RWB tilts toward the RXB. The RWB tilts approximately 1/5 inch in the north-south direction. Differential settlement between the RWB and the RXB is also on the order of ¼ inch.

3.8.5.6.5 Thermal Loads

During normal operation or accident conditions, a linear temperature gradient across the RXB foundation may develop. An explicit analysis considering these loads has been performed and described in Section 3.8.4.4.1 and Appendix 3B.1.3.

3.8.5.6.6 Construction Loads

The entire RXB basemat is poured in a very short time. The building is essentially constructed from the bottom up. The main loads (the reactor pool and the NPMs) are not added until the building is complete. Therefore, there are no construction-induced settlement concerns. The CRB basemat is much smaller and will be poured later than the RXB basemat in the construction sequence.

3.8.5.6.7 Basemat Soil Pressures along Basemat Edges (Toe Pressures)

The static deadweight reaction at an edge node is added to the seismic reaction of the node to calculate the total reaction. The seismic reaction is obtained with the approach shown in Section 3.7.2.4.1, for combining seismic analysis results. The bearing pressure is calculated by dividing the total reaction by the tributary area of the node (i.e., localized bearing pressure). The edge bearing pressures, or toe pressures, along the edges are averaged to obtain the average toe pressures of the basemat. The average toe pressures for the RXB and CRB are shown in Table 3.8.5-13 and Table 3.8.5-15, respectively. The values shown in these tables indicate that two times the maximum toe pressure is less than the minimum soil bearing pressure capacity of 75 ksf as specified in Table 2.0-1.

3.8.5.6.8 Leak Detection

Groundwater has the potential to leak through the RXB exterior walls through microscopic concrete cracks. Due to the exterior concrete wall thickness, these leaks will be very slow (<<1 gallon per day (gpd)). This leak rate through the wall is not enough to cause an interior flood in any of the rooms that share an exterior wall. Leaks of this nature will be discovered and dealt with in accordance with plant concrete maintenance specifications. Further reduction of groundwater seepage can be accomplished with a building dewatering system surrounding the RXB.

A leak chase system is provided in the RXB basemat to detect any leakage from the reactor pool.

3.8.5.7 Materials, Quality Control, and Special Construction Techniques

Section 3.8.4.6 describes the materials, quality control, and special construction techniques applicable to the RXB and CRB including the foundations.

3.8.5.8 Testing and Inservice Inspection Requirements

Section 3.8.4.7 identifies the testing and inservice surveillances applicable to the RXB and CRB including the foundations.

Table 3.8.5-1: RXB Stability Evaluation Input Parameters

Data Description	Value
RXB Seismic Weight (kips)	**587,147**
RXB East-West Length (ft) (between exterior faces of walls)	**346**
RXB North-South Length (ft) (between exterior faces of walls)	**150.5**
RXB Height (ft)	**167**
RXB Embedment Depth (ft)	**86**
Foundation East-West Length (ft)	**358**
Foundation North-South Length (ft)	**162.5**
Foundation Area (ft^2)	**58,175**
Soil Density, γ_{soil} (pcf)	**130**
Coefficient of Friction between Wall and Soil	**0.5**
Coefficient of Friction between Basemat and Soil	**0.58**
Effective Soil Density, $\gamma_{eff} = \gamma_{soil} - \gamma_{water}$ (pcf)	**67.6**
Angle of Internal Friction	**30°**
Soil Coefficient of Pressure at Rest, K_o	**0.5**
Surcharge (psf)	**250**

Table 3.8.5-2: Reactor Building Static Effective Soil Force

Definition	Symbol	Results	Units
Reactor Building			
Total Effective Soil Force on North Wall	F_{y1}	46,967	Kips
Total Effective Force on South Wall	F_{y2}	46,967	Kips
Total Effective Force on West Wall	F_{x1}	20,429	Kips
Total Effective Force on East Wall	F_{x2}	20,429	Kips
Total Static Wall Force	Ftotal	**134,792**	Kips

Table 3.8.5-3: Seismic Base Reactions

Model	Concrete Case	Soil Type	Seismic Load Case	Global FX (kips)	Global Fy (kips)	Global Fz (kips)
Reactor Building	Cracked 7% Damping	S7 CSDRS	Capitola	326528	177221	222932
			Chi Chi	303442	185109	254142
			El Centro	253932	190969	264163
			Izmit	273116	171747	234397
			Yermo	277421	196458	254684
		S8 CSDRS	Capitola	306274	206799	205032
			Chi Chi	318687	200201	229313
			El Centro	250271	212788	234071
			Izmit	298958	211286	226435
			Yermo	268717	235929	233072
		S11 CSDRS	Capitola	151960	135837	185963
			Chi Chi	188520	126654	182918
			El Centro	143366	166150	191453
			Izmit	146440	168663	199958
			Yermo	171040	135521	199400
		S7 CSDRS- HF	Lucerne	119790	77946	147529
		S9 CSDRS- HF	Lucerne	126622	82652	162443
	Uncracked 7% Damping	S7 CSDRS	Capitola	331587	203856	225014
			Chi Chi	306830	192224	258618
			El Centro	271625	197785	254444
			Izmit	272082	190891	242807
			Yermo	281972	190668	257452
		S8 CSDRS	Capitola	311880	212752	208268
			Chi Chi	320551	215363	234958
			El Centro	263147	219067	230481
			Izmit	296880	212060	228292
			Yermo	281020	234460	238766
		S11 CSDRS	Capitola	152056	138287	186456
			Chi Chi	188000	128106	185511
			El Centro	143524	167620	189535
			Izmit	147560	170244	201724
			Yermo	172026	135712	201374
		S7 CSDRS- HF	Lucerne	114361	82076	156119
		S9 CSDRS- HF	Lucerne	155572	99573	167031
Control Building	Cracked 7% Damping	S7 CSDRS	Capitola	23416	31065	22228
			Chi-Chi	22129	26172	26415
			El Centro	20588	25473	27118
			Izmit	21529	29205	24628
			Yermo	21544	27899	25374
		S9 CSDRS-HF	Lucerne	15018	19859	21209
	Uncracked 7% Damping	S7 CSDRS	Capitola	25705	32251	23455
			Chi Chi	23304	28272	26333
			El Centro	21920	26926	26885
			Ismit	23147	31104	25146
			Yermo	23161	28982	23616
		S9 CSDRD-HF	Lucerne	16523	20795	21017

Table 3.8.5-3: Seismic Base Reactions (Continued)

Model	Concrete Case	Soil Type	Seismic Load Case	Global FX (kips)	Global Fy (kips)	Global Fz (kips)
Triple Building	Cracked 7% Damping	S7 CSDRS	Capitola	343944	244056	231397
			Chi Chi	336167	239971	250624
			El Centro	267968	269922	256483
			Izmit	297510	245331	251341
			Yermo	297715	236510	263351
		S8 CSDRS	Capitola	290751	274276	196053
			Chi Chi	303767	234230	223377
			El Centro	248628	267201	229007
			Izmit	287011	252901	216609
			Yermo	263706	265195	232279
		S11 CSDRS	Capitola	168396	119565	181518
			Chi Chi	199376	117941	179024
			El Centro	149150	165393	186060
			Izmit	152976	161973	193875
			Yermo	173035	120733	195737
		S7 CSDRS- HF	Lucerne	110986	91038	139697
		S9 CSDRS- HF	Lucerne	129899	98212	162049
	Uncracked 7% Damping	S7 CSDRS	Capitola	**345847**	277296	233754
			Chi Chi	340014	239492	255071
			El Centro	284727	**285248**	253962
			Izmit	289695	248614	241686
			Yermo	300881	233505	**267641**
		S8 CSDRS	Capitola	292384	271970	202190
			Chi Chi	305827	241469	226832
			El Centro	259244	267925	221740
			Izmit	284855	249438	219512
			Yermo	273286	261749	236003
		S11 CSDRS	Capitola	170042	122301	180745
			Chi Chi	200463	119167	180987
			El Centro	151215	166685	183803
			Izmit	153733	163189	195697
			Yermo	174920	125096	196915
		S7 CSDRS- HF	Lucerne	105895	95761	134547
		S9 CSDRS- HF	Lucerne	143621	102666	165813
			Maximum:	**345847**	**285248**	**267641**

These loads are the maximums of the total base reaction time histories obtained by the step-by-step combination of the reactions in all springs below the foundation

Table 3.8.5-4: Seismic Vertical RXB Base Reactions and Dead Weight

Soil Type	Seismic Load Case	Standalone Model		Triple Building Model		Dead Weight (kips)
		Cracked Seismic Vertical Reaction (kips)	Uncracked Seismic Vertical Reaction (kips)	Cracked Seismic Vertical Reaction (kips)	Uncracked Seismic Vertical Reaction (kips)	
S7† CSDRS	Capitola	222,932	225,014	231397	233754	471,487
	Chi-Chi	254,142	258,618	250624	255071	471,487
	El Centro	264,163	254,444	256483	253962	471,487
	Izmit	234,397	242,807	251341	241686	471,487
	Yermo	254,684	257,452	263351	267641	471,487
S8 CSDRS	Capitola	205,032	208,268	196053	202190	471,487
	Chi-Chi	229,313	234,958	223377	226832	471,487
	El Centro	234,071	230,481	229007	221740	471,487
	Izmit	226,435	228,292	216609	219512	471,487
	Yermo	233,072	238,766	232279	236003	471,487
S11 CSDRS	Capitola	185,963	186,456	181518	180745	471,487
	Chi-Chi	182,918	185,511	179024	180987	471,487
	El Centro	191,453	189,535	186060	183803	471,487
	Izmit	199,958	201,724	193875	195697	471,487
	Yermo	199,400	201,374	195737	196915	471,487
S7 CSDRS-HF	Lucerne	147,529	156,119	139697	134547	471,487
S9 CSDRS-HF	Lucerne	162,443	167,031	162049	165813	471,487

†S7, S8, S9, S11 designate Soil Types 7, 8, 9, and 11, respectively.

Table 3.8.5-5: Factors of safety - RXB Stability

Cracked Condition				Uncracked Condition			
Stability	**Vertical**	**N-S**	**E-W**	**Stability**	**Vertical**	**N-S**	**E-W**
Case 1: Cracked RXB Model, Soil Type 7				**Case 2: Uncracked RXB Model, Soil Type 7**			
Flotation	2.34	-	-	Flotation	2.34	-	-
Sliding	-	1.06	0.78	Sliding	-	1.00	0.76
Overturning	-	1.52	1.53	Overturning	-	1.51	1.52
Case 3: Cracked Triple Model, Soil Type 7				**Case 4: Uncracked Triple Model, Soil Type 7**			
Flotation	2.34	-	-	Flotation	2.34	-	-
Sliding	-	0.79	0.76	Sliding	-	0.86	0.75
Overturning	-	1.49	1.50	Overturning	-	1.50	1.50
Case 5: Cracked RXB Model, Soil Type 8				**Case 6: Uncracked RXB Model, Soil Type 8**			
Flotation	2.34	-	-	Flotation	2.34	-	-
Sliding	-	1.03	0.82	Sliding	-	1.00	0.80
Overturning	-	1.66	1.66	Overturning	-	1.64	1.65
Case 7: Cracked Triple Model, Soil Type 8				**Case 8: Uncracked Triple Model, Soil Type 8**			
Flotation	2.34	-	-	Flotation	2.34	-	-
Sliding	-	0.85	0.84	Sliding	-	0.85	0.83
Overturning	-	1.71	1.71	Overturning	-	1.69	1.70
Case 9: Cracked RXB Model, Soil Type 11				**Case 10: Uncracked RXB Model, Soil Type 11**			
Flotation	2.34	-	-	Flotation	2.34	-	-
Sliding	-	1.50	1.47	Sliding	-	1.49	1.47
Overturning	-	1.95	1.96	Overturning	-	1.94	1.95
Case 11: Cracked Triple Model, Soil Type 11				**Case 12: Uncracked Triple Model, Soil Type 11**			
Flotation	2.34	-	-	Flotation	2.34	-	-
Sliding	-	1.60	1.40	Sliding	-	1.58	1.38
Overturning	-	2.00	2.00	Overturning	-	2.00	2.00
Case 13: Cracked RXB Model, Soil Type 9				**Case 14: Uncracked RXB Model, Soil Type 9**			
Flotation	2.34	-	-	Flotation	2.34	-	-
Sliding	-	2.66	1.86	Sliding	-	2.21	1.51
Overturning	-	2.31	2.31	Overturning	-	2.24	2.25
Case 15: Cracked Triple Model, Soil Type 9				**Case 16: Uncracked Triple Model, Soil Type 9**			
Flotation	2.34	-	-	Flotation	2.34	-	-
Sliding	-	2.24	1.81	Sliding	-	2.14	1.64
Overturning	-	2.31	2.32	Overturning	-	2.26	2.26

Table 3.8.5-6: RXB ANSYS Model Summary

Items	ANSYS
Number of Joints	40009
Number of Joint with Restraints	5822
Number of Joint with Lumped Mass	7877
Number of Frame Elements	1541
Number of Shell Elements	15851
Number of Solid Elements	15012
Number of Link/Spring Elements	120
Number of Nonlinear Contact Elements	2100
Number of Nonlinear Gap Elements	5822

Table 3.8.5-7: Overturning Forces and Overturning Arms

Overturning Force	Overturning Moment Arm	Arm Length
Overturning Moment about the Y-Axis (E-W)		
Vertical Seismic Reaction	Half of East-West Width of Basemat	179′
Friction Forces on North and South Walls	Perpendicular Distance between Line of Action of Friction Force Centroid and Pivot	179′
Friction Force on East Wall	East-West Width of Basemat	352′
Effective Structural Dead Weight (Buoyant Weight)	Half of East-West Width of Basemat	179′
Overturning Moment about the X-Axis (N-S)		
Vertical Seismic Reaction	Half of North-South Width of Basemat	81.25′
Friction Forces on East and West Walls	Perpendicular Distance between Line of Action of Friction Force Centroid and Pivot	81.25
Friction Force on South Wall	North-South Width of Basemat	156.5′
Effective Structural Dead Weight (Buoyant Weight)	Half of North-South Width of Basemat	81.25′

Table 3.8.5-7a: Displacement at Bottoms of Foundations of Uncracked Triple Building Model

Building	Node Location	Node No.	Coordinates (inch)			Displacement (inch)		
			X	Y	Z	U1(EW)	U2(NS)	U3(Vert)
RWB	**West**	41173	-2460	-825	570	-0.1	0.01	**-0.6**
		41189	-2460	96	570	-0.1	0.01	**-0.61**
		41206	-2460	1149	570	-0.08	0.02	**-0.52**
	Middle	41887	-1380	-825	570	-0.11	0.01	**-1.04**
		41903	-1380	96	570	-0.1	0.01	**-1.04**
		41920	-1380	1149	570	-0.09	0	**-0.9**
	East	42517	-300	-825	570	-0.12	0.01	**-1.63**
		42533	-300	96	570	-0.11	0.01	**-1.62**
		42550	-300	1149	570	-0.12	0.03	**-1.46**
RXB	**West**	129	0	-873	0	-0.02	-0.03	**-1.75**
		140	0	0	0	-0.03	0	**-1.81**
		151	0	873	0	-0.02	0.04	**-1.75**
	Middle	801	1872	-873	0	-0.01	-0.01	**-1.89**
		812	1872	0	0	-0.02	0.01	**-2.05**
		823	1872	873	0	-0.01	0.03	**-1.88**
	East	1616	4092	-873	0	0.02	-0.02	**-1.95**
		1627	4092	0	0	0.02	0.02	**-2**
		1638	4092	873	0	0.01	0.05	**-1.94**
CRB	**West**	31066	4470	-705	345	0.15	0.01	**-1.75**
		31078	4470	-8	345	0.15	0.01	**-1.78**
		31089	4470	705	345	0.15	0.02	**-1.73**
	Middle	31327	4980	-705	345	0.16	0.01	**-1.36**
		31339	4980	-8	345	0.16	0.01	**-1.36**
		31350	4980	705	345	0.16	0.02	**-1.34**
	East	31559	5406	-705	345	0.16	0.01	**-1.04**
		31571	5406	-8	345	0.16	0.01	**-1.05**
		31582	5406	705	345	0.17	0.02	**-1.02**

Table 3.8.5-7b: Displacement at Bottoms of Foundations of Cracked Triple Building Model

Building	Node Location	Node No.	Coordinates (inch)			Displacement (inch)		
			X	Y	Z	U1(EW)	U2(NS)	U3(Vert)
RWB	**West**	41173	-2460	-825	570	-0.1	0.01	**-0.6**
		41189	-2460	96	570	-0.1	0.01	**-0.61**
		41206	-2460	1149	570	-0.08	0.03	**-0.53**
	Middle	41887	-1380	-825	570	-0.11	0.01	**-1.04**
		41903	-1380	96	570	-0.1	0.01	**-1.04**
		41920	-1380	1149	570	-0.09	0	**-0.89**
	East	42517	-300	-825	570	-0.12	0.01	**-1.64**
		42533	-300	96	570	-0.11	0.01	**-1.63**
		42550	-300	1149	570	-0.12	0.03	**-1.46**
RXB	**West**	129	0	-873	0	-0.02	-0.04	**-1.75**
		140	0	0	0	-0.03	0	**-1.81**
		151	0	873	0	-0.02	0.04	**-1.75**
	Middle	801	1872	-873	0	-0.01	-0.01	**-1.89**
		812	1872	0	0	-0.02	0.01	**-2.06**
		823	1872	873	0	-0.02	0.03	**-1.88**
	East	1616	4092	-873	0	0.02	-0.02	**-1.95**
		1627	4092	0	0	0.02	0.02	**-2**
		1638	4092	873	0	0.01	0.05	**-1.94**
CRB	**West**	31066	4470	-705	345	0.14	0.01	**-1.75**
		31078	4470	-8	345	0.14	0.01	**-1.78**
		31089	4470	705	345	0.15	0.02	**-1.74**
	Middle	31327	4980	-705	345	0.15	0.01	**-1.36**
		31339	4980	-8	345	0.15	0.01	**-1.36**
		31350	4980	705	345	0.16	0.02	**-1.34**
	East	31559	5406	-705	345	0.16	0.01	**-1.04**
		31571	5406	-8	345	0.16	0.01	**-1.05**
		31582	5406	705	345	0.16	0.02	**-1.02**

Table 3.8.5-7c: Summary of Foundation Settlement of Uncracked Triple Building Model

Summary of Foundation Settlements (Uncracked Triple Building Model) Response Combination 9-6: (COMB-Static(1GZ+H+F+S+0.8L)-Concrete							
Building	**Maximum Vertical Settlement[1]**	**Average Vertical Settlement[2]**	**Foundation E-W Tilt[3]**	**Rotation about NS Axis[4]**	**Foundation N-S Tilt[5]**	**Rotation about EW Axis[6]**	**Differential Settlement between Structures [7]**
	(inch)	**(inch)**	**(inch)**	**(degree)**	**(inch)**	**(degree)**	**(inch)**
RWB	-1.63	**-1.05**	0.99	0.0264	0.13	0.0039	0.2 (between RWB and RXB)
RXB	-2.05	**-1.89**	0.19	0.0027	0.004	0.0001	-0.21 (between RXB and CRB)
CRB	-1.78	**-1.38**	-0.72	-0.0442	0.02	0.0008	(n/a)

Notes:

1. Maximum settlement among the 9 selected nodes at the bottom of each foundation
2. The average values of the settlements of the 9 selected nodes
3. A positive tilt for a building implies the east edge of the building is lower and the building is leaning toward the east.
A negative tilt for a building implies the west edge of the building is lower and the building is leaning toward the west.
4. The angle of foundation rotation of a building about the NS axis was calculated by dividing the EW tilt by the EW dimension of the foundation (see Table 3.8.5-19).
5. A Positive tilt for a building implies the south edge of the building is lower and the building is leaning toward the south.
A negative tilt for a building implies the north edge of the building is lower and the building is leaning toward the north.
6. The angle of foundation rotation of a building about the EW axis was calculated by dividing the NS tilt by the NS dimension of the foundation (see Table 3.8.5-19).
7. This is the difference in settlement between two neighboring buildings. It was calculated by subtracting the settlement of the west edge of the east building from the settlement of the east edge of the west building.
A positive value implies that the building in the east settles more than that in the west.

Table 3.8.5-7d: Summary of Foundation Settlement of Cracked Triple Building Model

Summary of Foundation Settlements (Cracked Triple Building Model) Response Combination 9-6: (COMB-Static(1GZ+H+F+S+0.8L)-Concrete							
Building	**Maximum Vertical Settlement[1]**	**Average Vertical Settlement[2]**	**Foundation E-W Tilt[3]**	**Rotation about NS Axis[4]**	**Foundation N-S Tilt[5]**	**Rotation about EW Axis[6]**	**Differential Settlement between Structures [7]**
	(inch)	**(inch)**	**(inch)**	**(degree)**	**(inch)**	**(degree)**	**(inch)**
RWB	-1.64	**-1.05**	0.99	0.0264	0.13	0.0039	0.2 (between RWB and RXB)
RXB	-2.06	**-1.89**	0.2	0.0027	0.005	0.0001	-0.21 (between RXB and CRB)
CRB	-1.78	**-1.38**	-0.72	-0.0443	0.02	0.0007	(n/a)

Notes:

1. Maximum settlement among the 9 selected nodes at the bottom of each foundation
2. The average values of the settlements of the 9 selected nodes
3. A Positive tilt for a building implies the east edge of the building is lower and the building is leaning toward the east.
A negative tilt for a building implies the west edge of the building is lower and the building is leaning toward the west.
4. The angle of foundation rotation of a building about the NS axis was calculated by dividing the EW tilt by the EW dimension of the foundation (see Table 3.8.5-19).
5. A Positive tilt for a building implies the south edge of the building is lower and the building is leaning toward the south.
A negative tilt for a building implies the north edge of the building is lower and the building is leaning toward the north.
6. The angle of foundation rotation of a building about the EW axis was calculated by dividing the NS tilt by the NS dimension of the foundation (see Table 3.8.5-19).
7. This is the difference in settlement between two neighboring buildings. It was calculated by subtracting the settlement of the west edge of the east building from the settlement of the east edge of the west building.
A positive value implies that the building in the east settles more than that in the west.

Table 3.8.5-8: CRB Stability Input Evaluation Parameters

Data Description	Value
CRB Seismic Weight (kips)	49,041
Buoyancy Load (kips)	40,500
CRB East-West Length (ft) (between exterior faces of walls)	81″-0″
CRB North-South Length (ft) (between exterior faces of walls)	119′-8″
CRB Height (ft)	95′-0″
CRB Embedment Depth (ft)	55′-0″
CRB Main Foundation East-West Length (ft)	91′-0″
CRB Main Foundation North-South Length (ft)	129′-8″
Main Foundation Area (ft^2)	11,800
CRB Tunnel Foundation East-West Length (ft)	19'-6"
CRB Tunnel Foundation North-South Length (ft)	25'-8"
Tunnel Foundation Area (ft^2)	500.6
Soil Density, ysoil (pcf)	130
Soil Coefficient of Pressure at Rest, K_o	0.5
Ground water level	Less than plant elevation 98′-0″
Flood level	Less than plant elevation 99′-0″
Surcharge (psf)	250
Coefficient of Friction between Wall and Soil	0.5
Coefficient of Friction between Basemat and Soil (static analysis)	0.58
Coefficient of Friction between Basemat and Soil (nonlinear analysis)	0.55

† Buoyancy load based on the water level at Elevation 100'-0" for conservatism.

Table 3.8.5-9: CRB Total Static Lateral Soil Pressure

Elevation	Lateral Static Soil Pressure (psi)
100′-0″ to 76′-6″	12
76′-6″ to 50′-0″	31
50′-0″ to 45′-0″	38

Note:
The highlighted region at EL 50'-0" & 45'-0" represents the pressure on the 5 ft thick foundation.

Table 3.8.5-10: CRB SAP2000, SASSI2010, and ANSYS Model Summary

Items	SAP2000	SASSI	ANSYS
Number of Joints	8872	17055	12142
Number of Joint with Restraints	864	0	2029
Number of Frame Elements	1393	1393	2098
Number of Shell Elements	4069	4069	3974
Number of Solid Elements	3966	3966	3967

Table 3.8.5-11: Reactor Building Sliding Displacements for Soil Type 7, 8 and 11 (Dead Weight + Buoyancy)

Direction of Input Motion	Description of Results	Maximum Sliding - inch		
		Soil Type 7	Soil Type 11	Soil Type 8
E-W (X)	E-W Sliding (X)	0.11	0.03	0.10
N-S (Y)	N-S Sliding (Y)	0.06	0.04	0.06

Table 3.8.5-12: Control Building Sliding and Uplift Displacements for Soil Type 7 and 11

Description of Results	Maximum Sliding and Uplift Displacement - inch	
	Soil Type 7 (Location/Excitation)	Soil Type 11 (Location/Excitation)
DW+Buoyancy+Static Pressure Vertical (Z) Displacement - Static	0.0353	0.0353
DW+Buoyancy+Static Pressure + Seismic E-W (X)	0.044 (A /E-W)	0.017 (C/E-W)
DW+Buoyancy+Static Pressure + Seismic N-S (Y)	0.08 (D/N-S)	0.029 (D/N-S)
DW+Buoyancy+Static Pressure + Seismic Vertical (Z) Uplift	0.01 (C/E-W)[1]	0.015 (D/Vertical)

[1] Excitation in the E-W direction produces uplift displacement,

Table 3.8.5-13: Average Soil Bearing Pressures (Toe Pressures) along Edges of RXB Basemat

Basemat Edges	WEST	EAST	NORTH	SOUTH
Total Reaction (kips)	61,580	73,004	133,073	133,321
Total Tributary Area (ft^2)	1,869	1,950	4,296	4,296
Average Toe Pressure in ksf	33.0	37.4	31.0	31.0
Average Toe Pressure in psi	229	260	215	216

Table 3.8.5-14: Seismic Vertical CRB Base Reactions and Dead Weight

Concrete Case	Soil Type	Seismic Load Case	Cracked Seismic Vertical Reaction (kips)	Uncracked Seismic Vertical Reaction (kips)	Dead Weight (kips)
Cracked 7% Damping	S7† CSDRS	Capitola	22,228	23,455	45,774
		Chi Chi	26,415	26,333	45,774
		El Centro	27,118	26,885	45,774
		Izmit	24,628	25,146	45,774
		Yermo	26,253	26,015	45,774
	S8 CSDRS	Capitola	22,129	22,284	45,774
		Chi Chi	26,196	26,074	45,774
		El Centro	26,565	26,562	45,774
		Izmit	24,857	25,868	45,774
		Yermo	26,284	26,267	45,774
	S11 CSDRS	Capitola	20,173	20,103	45,774
		Chi Chi	24,121	23,885	45,774
		El Centro	24,400	24,413	45,774
		Izmit	21,793	21,150	45,774
		Yermo	24,260	24,132	45,774
	S7 CSDRS-HF	Lucerne	18,371	19,126	45,774
	S9 CSDRS-HF	Lucerne	21,209	20,637	45,774

†S7, S8, S9, S11 designate Soil Types 7, 8, 9, and 11, respectively.

Table 3.8.5-15: Average Soil Bearing Pressures (Toe Pressures) along Edges of CRB Basemat

Basemat Edges	WEST	EAST	NORTH	SOUTH
Total Reaction (kips)	18,620	21,078	16,974	15,338
Total Tributary Area (ft2)	1,190.4	1,199.4	853.1	853.1
Average Toe Pressure (ksf)	15.64	17.57	19.90	17.98
Average Toe Pressure (Psi)	108.6	122.0	138.2	124.9

Table 3.8.5-16: Reactor Building SAP2000 Basemat Model Summary

Item	RXB Basemat SAP2000
Number of joints	2,360
Number of joints with restraints	559
Number of frame elements	40
Number of shell elements	2,366
Number of solid element	0

Table 3.8.5-17: CRB Tunnel Foundation Corner Displacements

Node No.	Displacement (inch)		
	U1 (EW)	U2 (NS)	U3 (Vertical)
9590	0.05	0.02	**-2**
9594	0.05	0.01	**-2.01**
31071	0.14	0.01	**-1.79**
31075	0.14	0.01	**-1.8**

Table 3.8.5-18: CRB Tunnel Differential Settlement over 50 Feet and Tilt Angle

West Settlement (inch)	East Settlement (inch)	Foundation Tilt over 50' (inch)†	Tilt Angle about NS Axis (degree)
-2	-1.8	-0.36	-0.0361

†-0.36" = [(-2.00")-(-1.80")]/27.5'×50'; EW Tunnel Foundation Model Width = 27.5'

Table 3.8.5-19: Foundation Sizes

Building	E-W Width (ft)†	N-S Width (ft)†
RXB	341	145.5
CRB	78	116.67
CRB Tunnel	27.5‡	18.67‡

† Since the settlements are calculated at the foundation nodes in the centerlines of walls, an E-W or N-S width used for foundation tilting angle calculation is the distance between the centerlines of two exterior walls.
‡ Based on nodal coordinates.

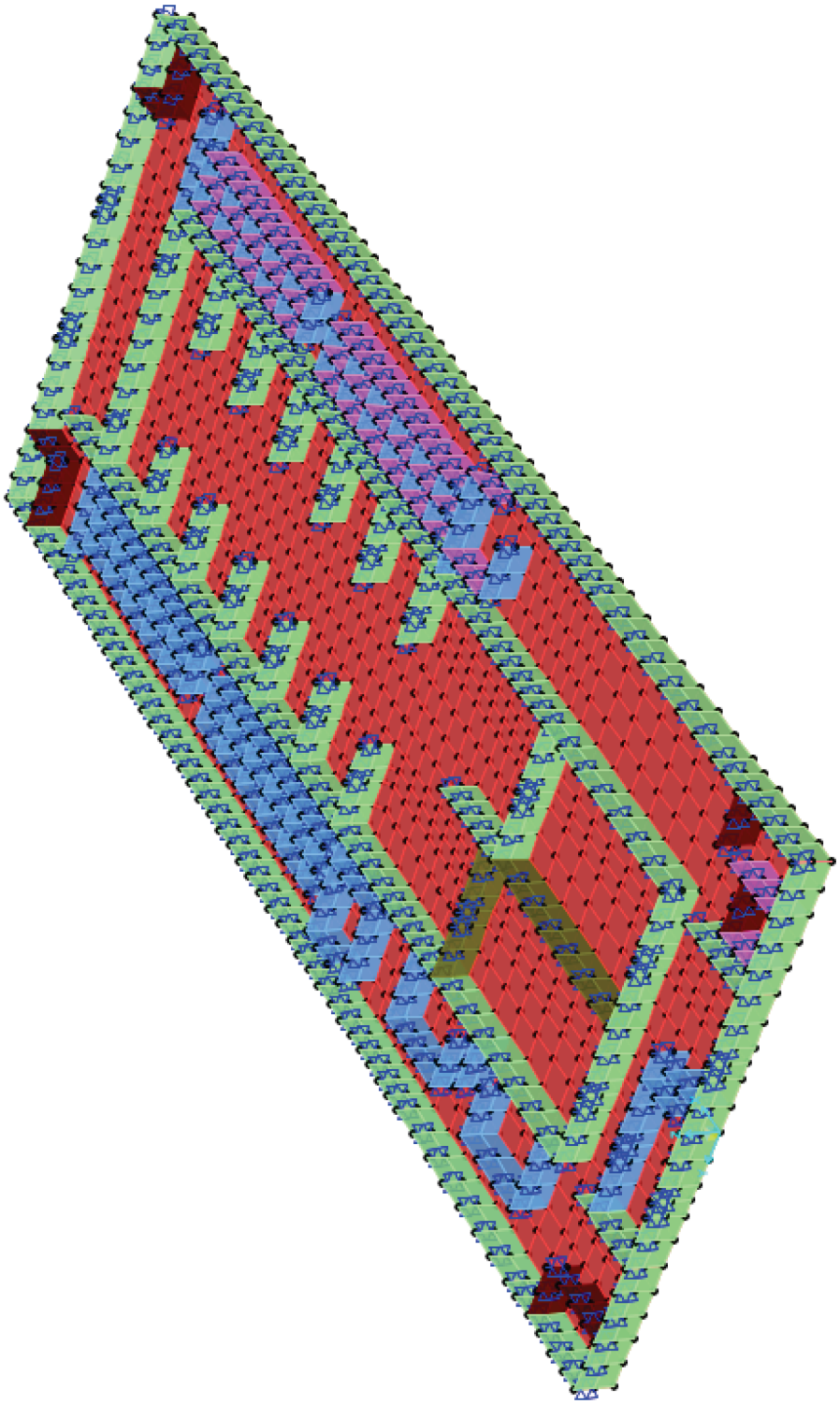

Figure 3.8.5-1: SAP2000 Model for Evaluation of Design Forces in the Reactor Building Basemat Model (X Axis is in the Longitudinal Direction, Y Axis is in the Transverse Direction, and Z Axis in the Vertical Upward Direction)

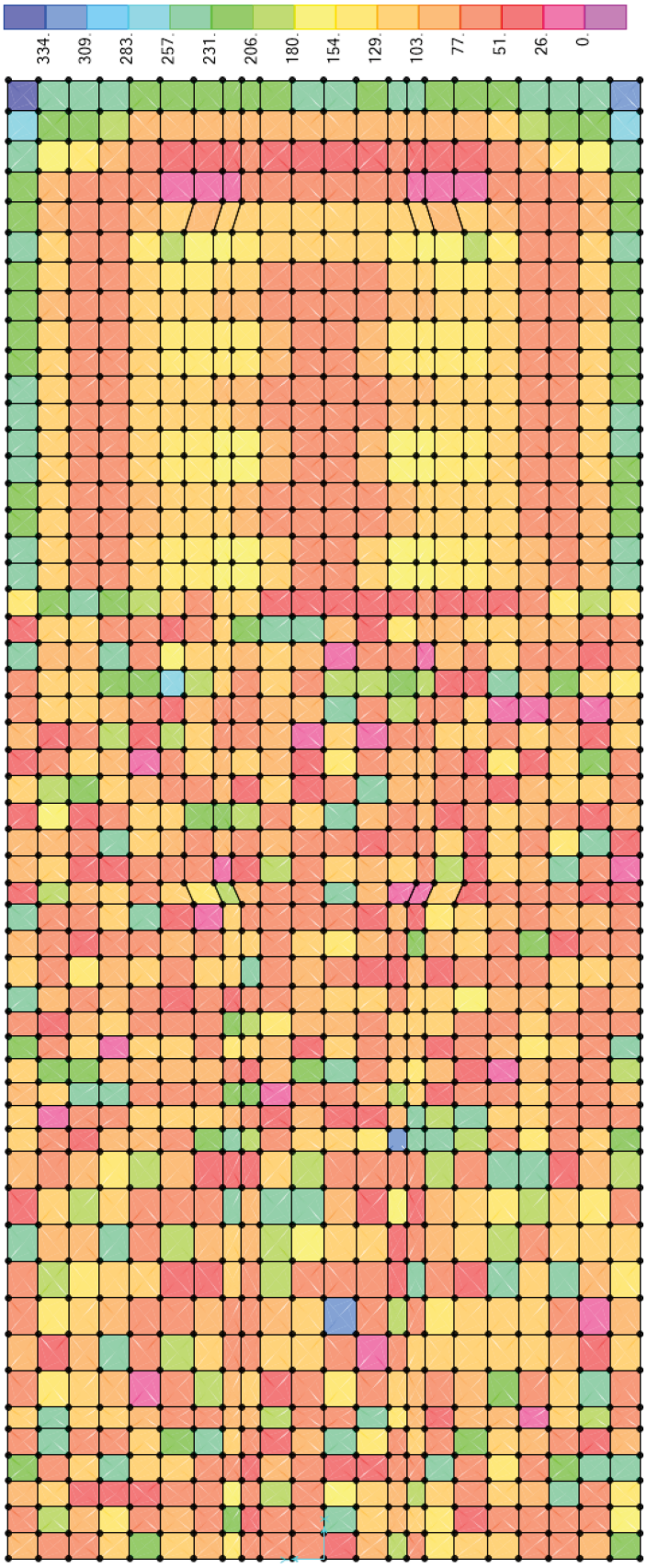

Figure 3.8.5-2: Static Base Pressure Contours for American Concrete Institute Load Combination 9-6 in the Reactor Building Basemat (psi) (Positive X Axis is to the Right of the Image and Positive Y is to the Top of the Image)

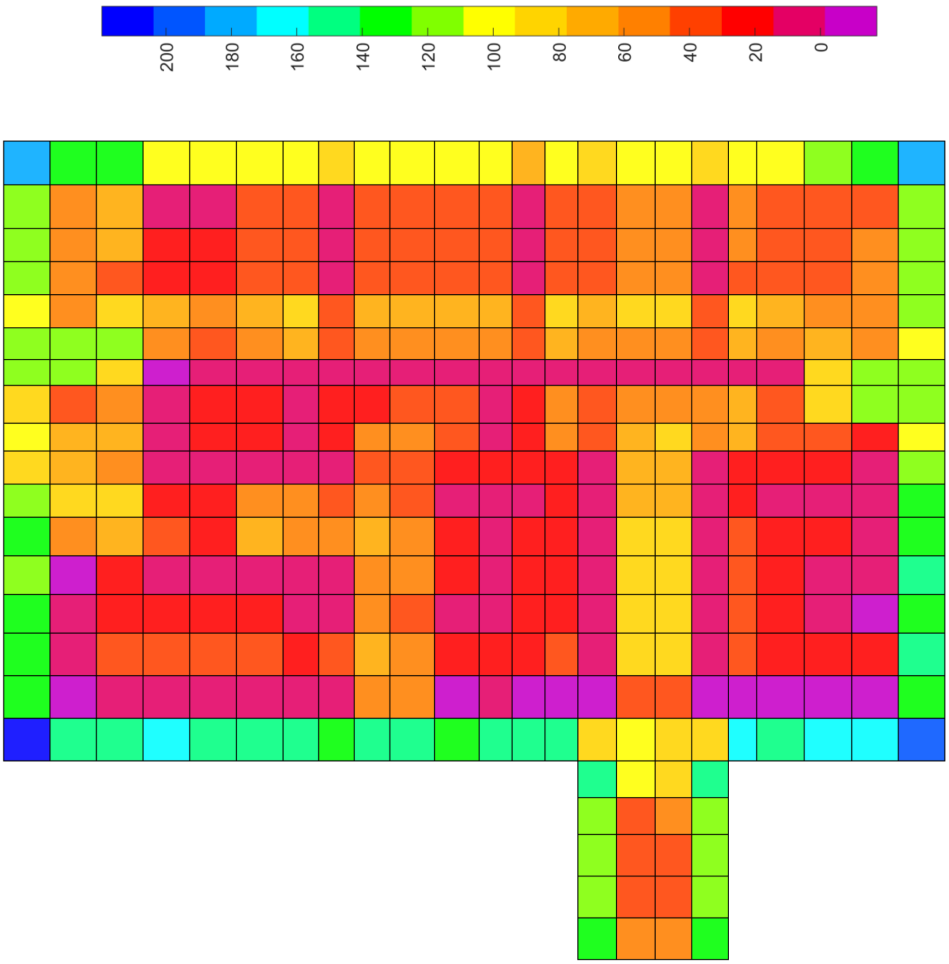

Figure 3.8.5-2a: Static Base Pressure Contours for American Concrete Institute Load Combination 9-6 in the Control Building Basemat (psi) (Positive X Axis is to the Right of the Image and Positive Y is to the Top of the Image)

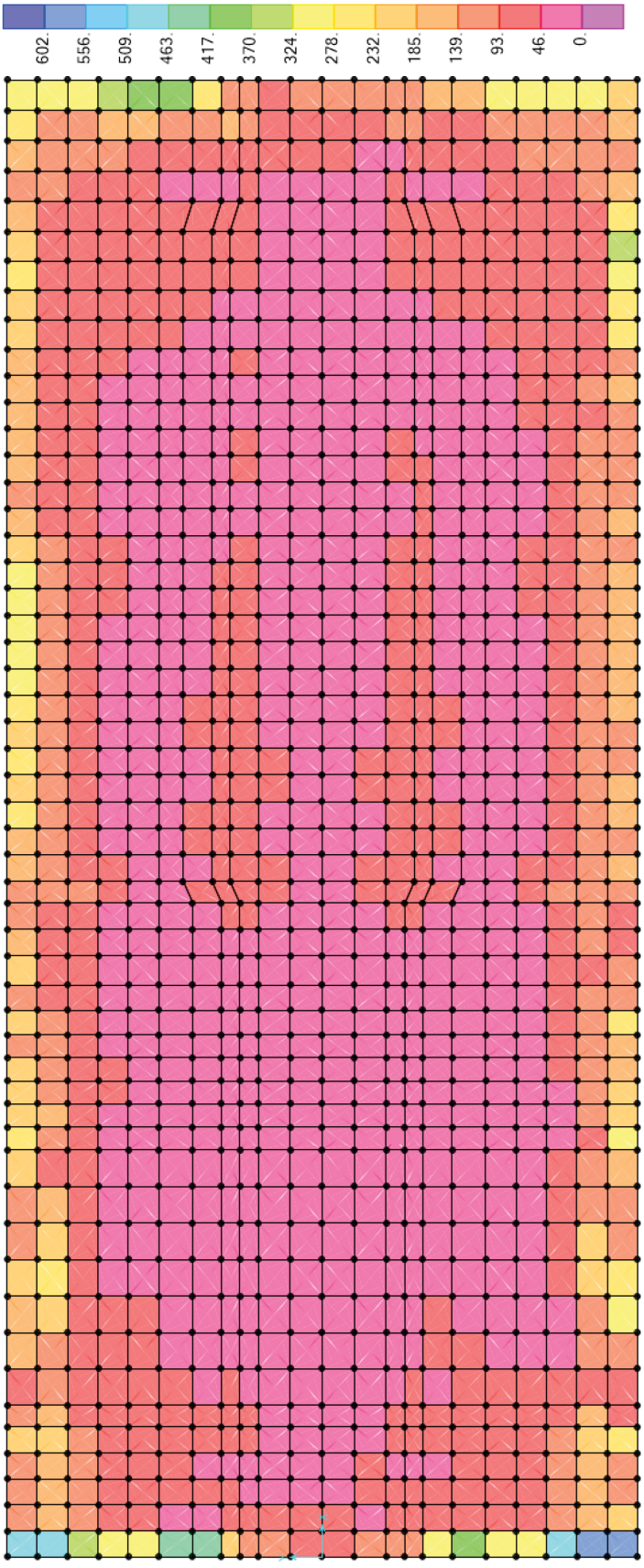

Figure 3.8.5-3: Seismic Base Pressure Contours from SASSI2010 Analysis in the Reactor Building Basemat (psi) (Positive X Axis is to the Right of the Image and Positive Y is to the Top of the Image)

Figure 3.8.5-3a: Dynamic Pressure Contours on Control Building Basemat (psi) (Positive X Axis is to the Right of the Image and Positive Y is to the Top of the Image)

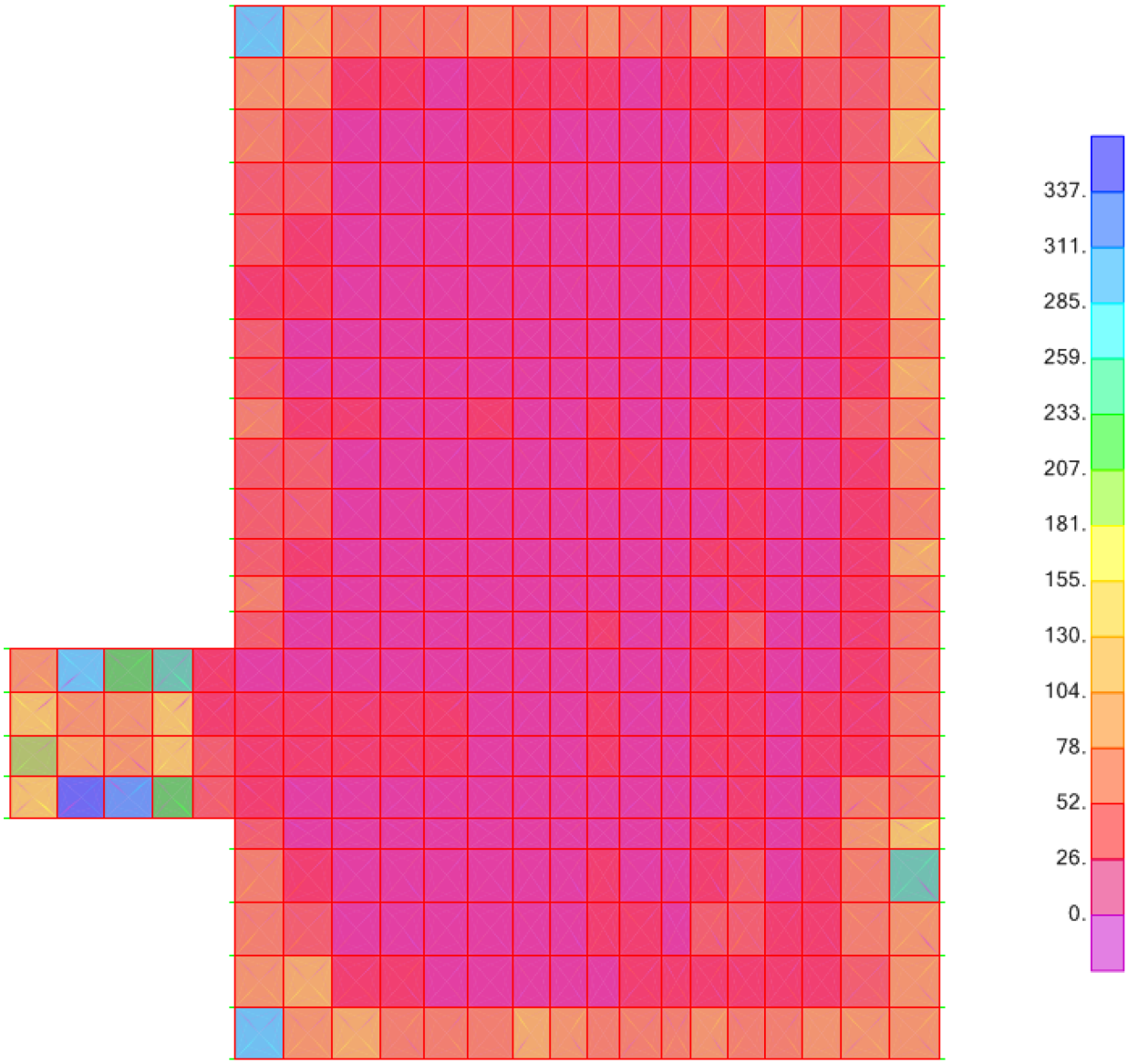

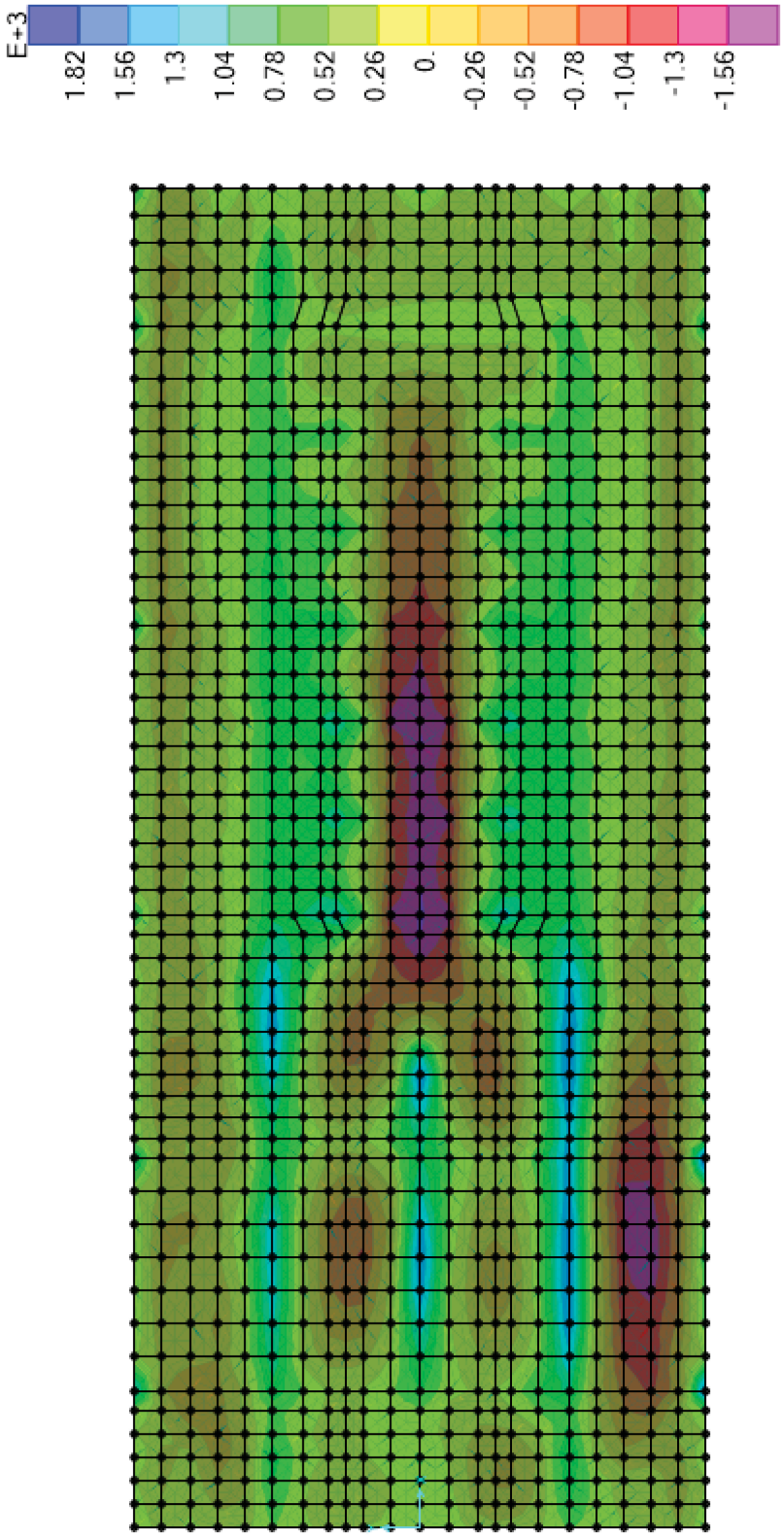

Figure 3.8.5-4: Myy Due to Static Base Pressure on Reactor Building Basemat (kip-ft/ft) in the Reactor Building Basemat Model (Positive X Axis is to the Right of the Image and Positive Y is to the Top of the Image)

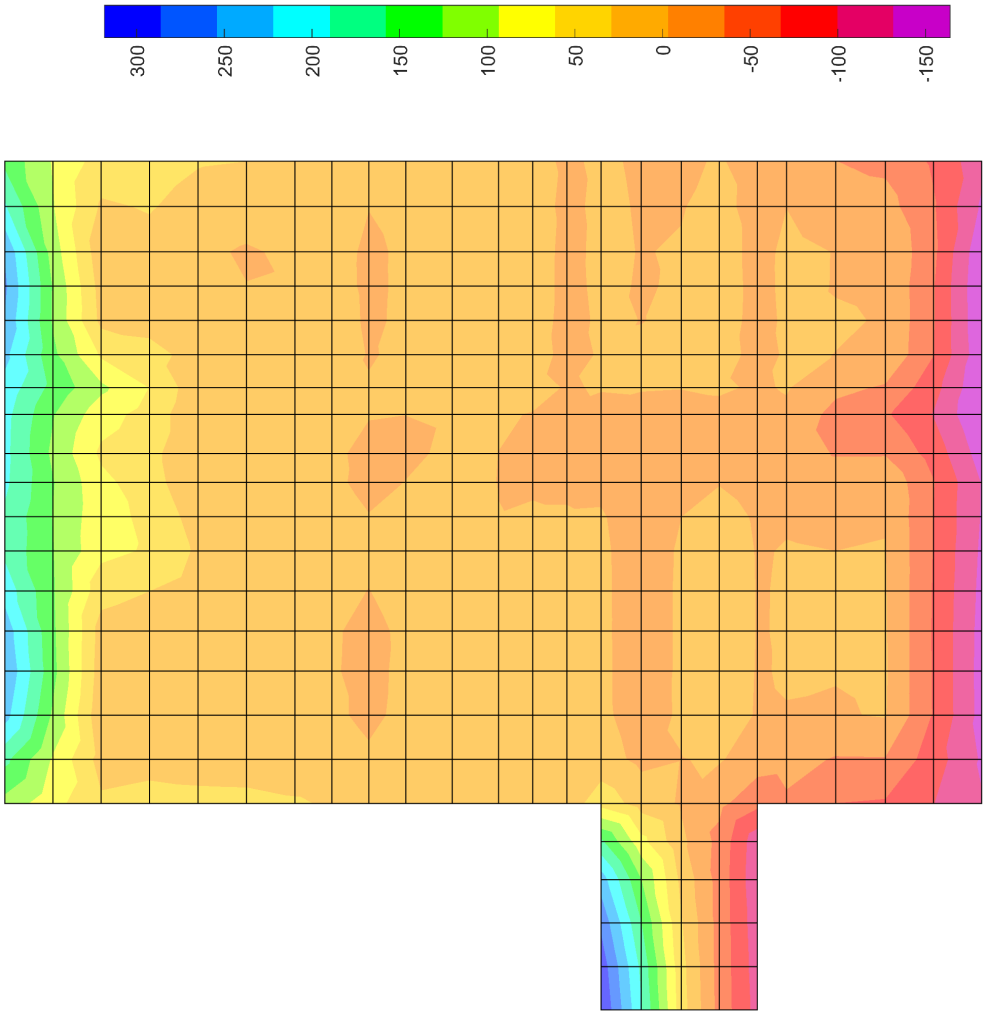

Figure 3.8.5-4a: Myy Due to Static Loads on Control Building Basemat, Stand-Alone SAP2000 Model (kip-ft/ft)
(Positive X Axis is to the Right of the Image and Positive Y is to the Top of the Image)

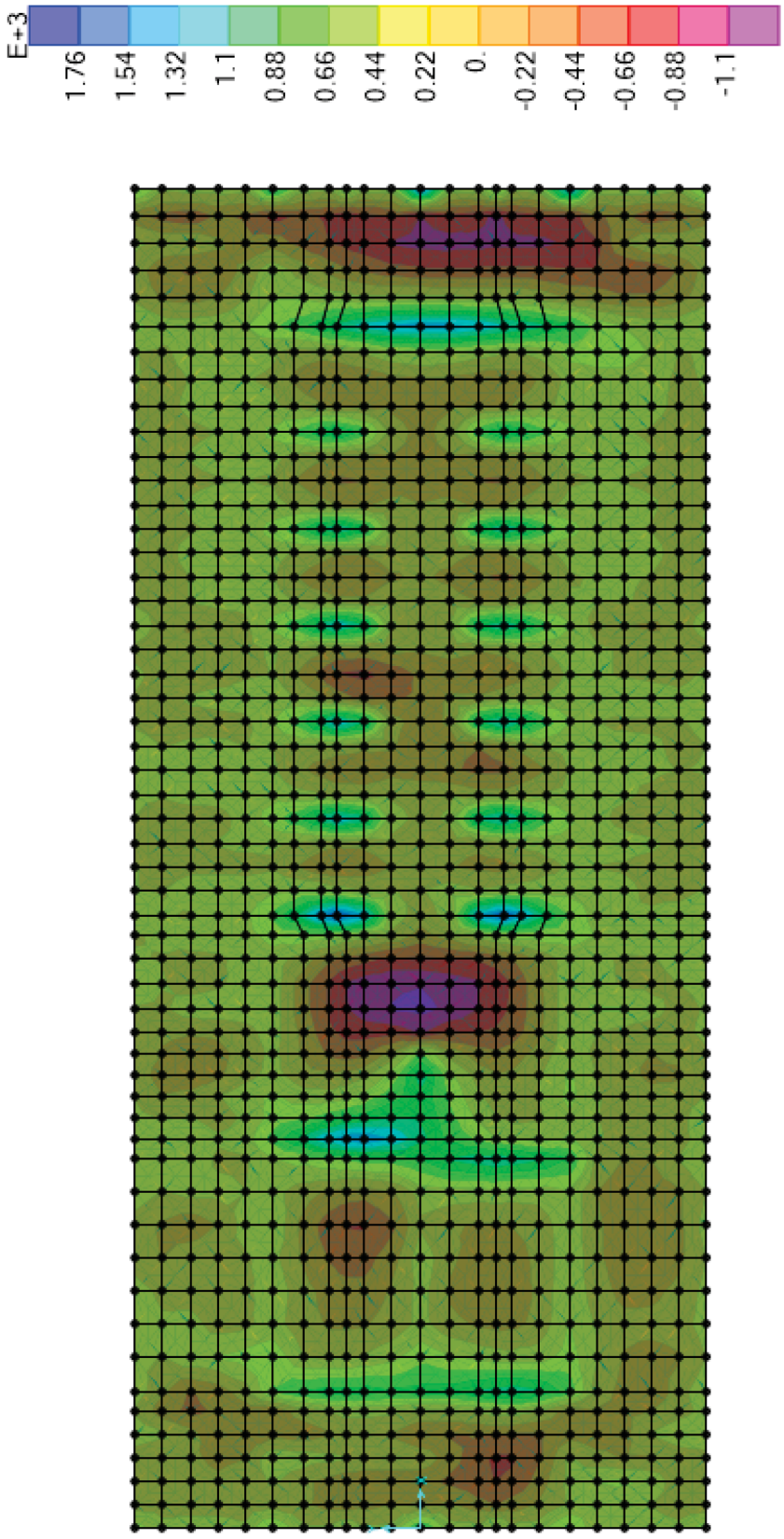

Figure 3.8.5-5: Mxx Due to Static Base Pressure on Reactor Building Basemat (kip-ft/ft) in the Reactor Building Basemat Model (Positive X Axis is to the Right of the Image and Positive Y is to the Top of the Image)

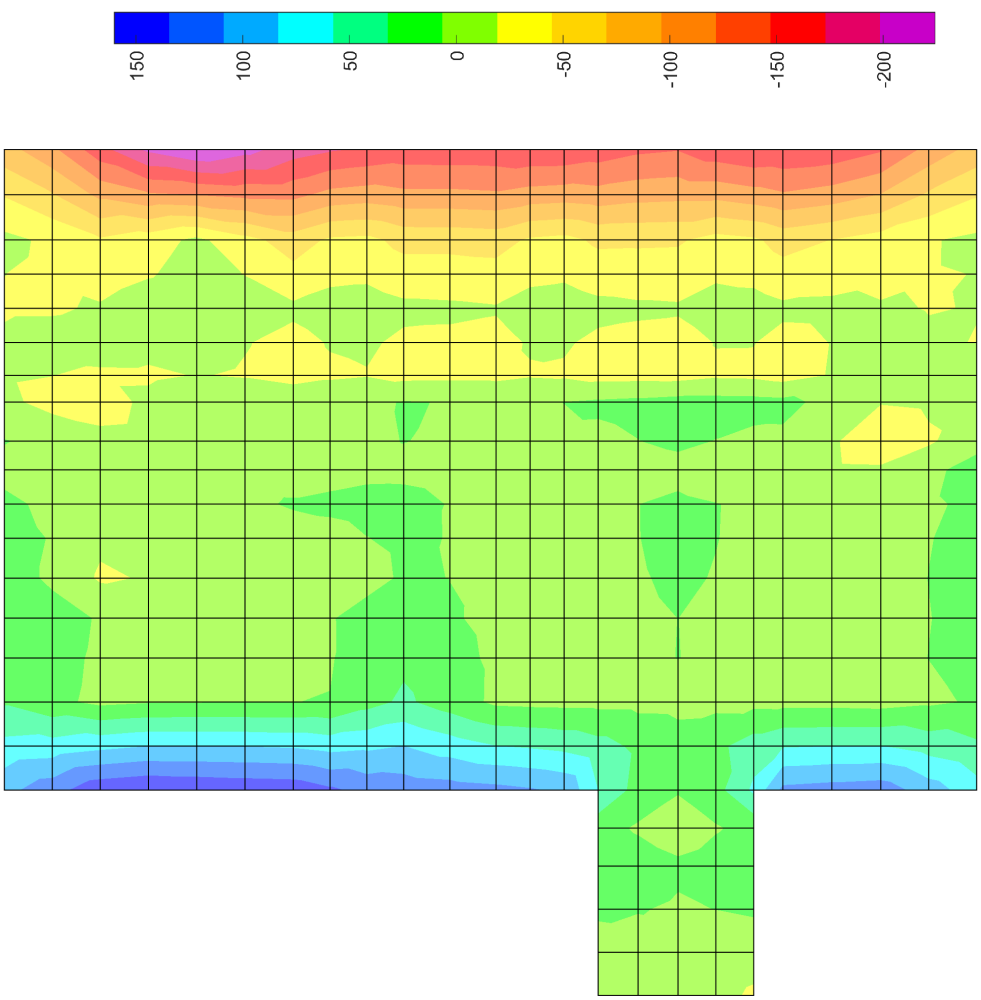

Figure 3.8.5-5a: Mxx Due to Static Loads on Control Building Basemat, Stand-Alone SAP2000 Model (kip-ft/ft)
(Positive X Axis is to the Right of the Image and Positive Y is to the Top of the Image)

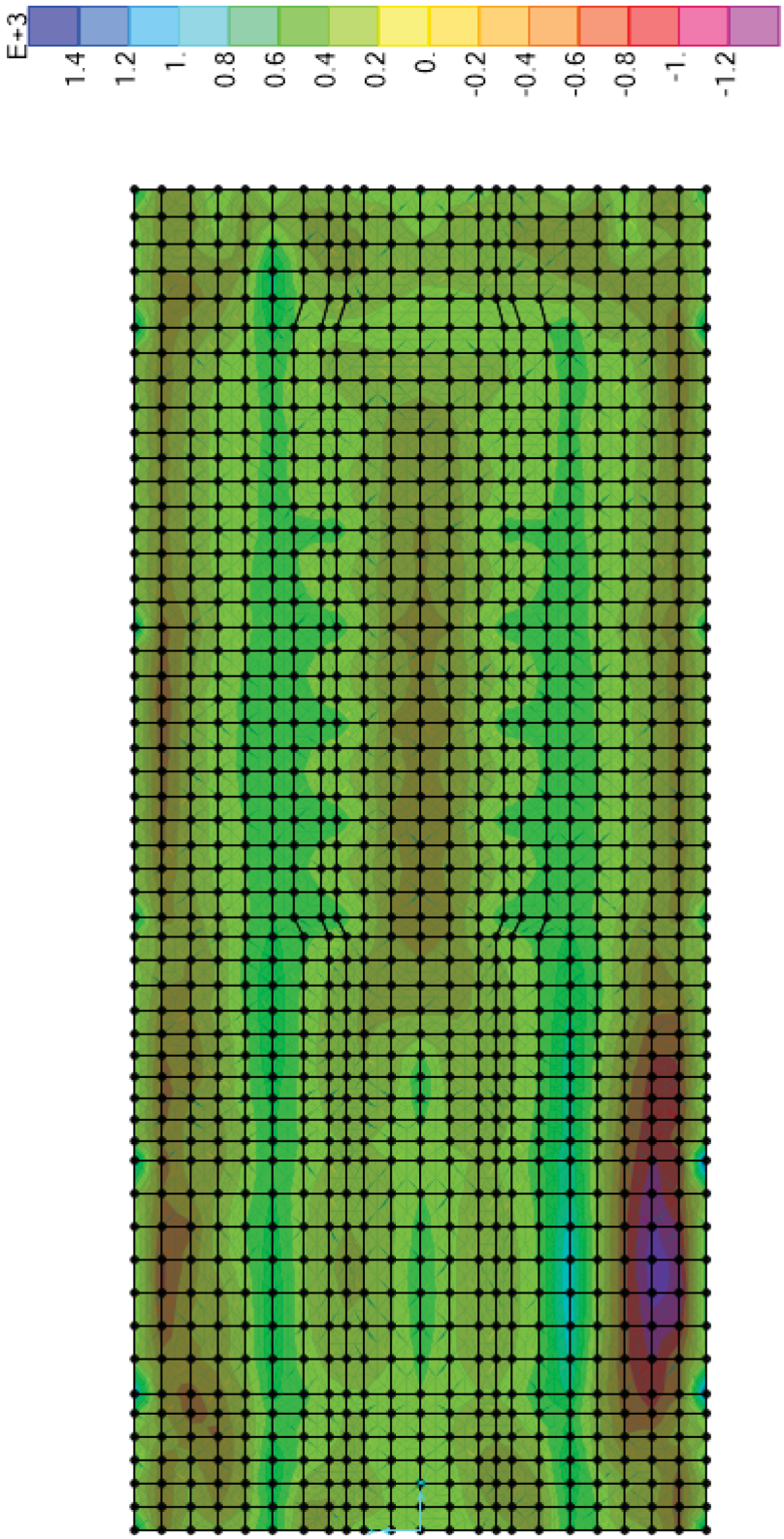

Figure 3.8.5-6: Myy Due to Seismic Base Pressure on Reactor Building Basemat (kip-ft/ft) in the Reactor Building Basemat Model (Positive X Axis is to the Right of the Image and Positive Y is to the Top of the Image)

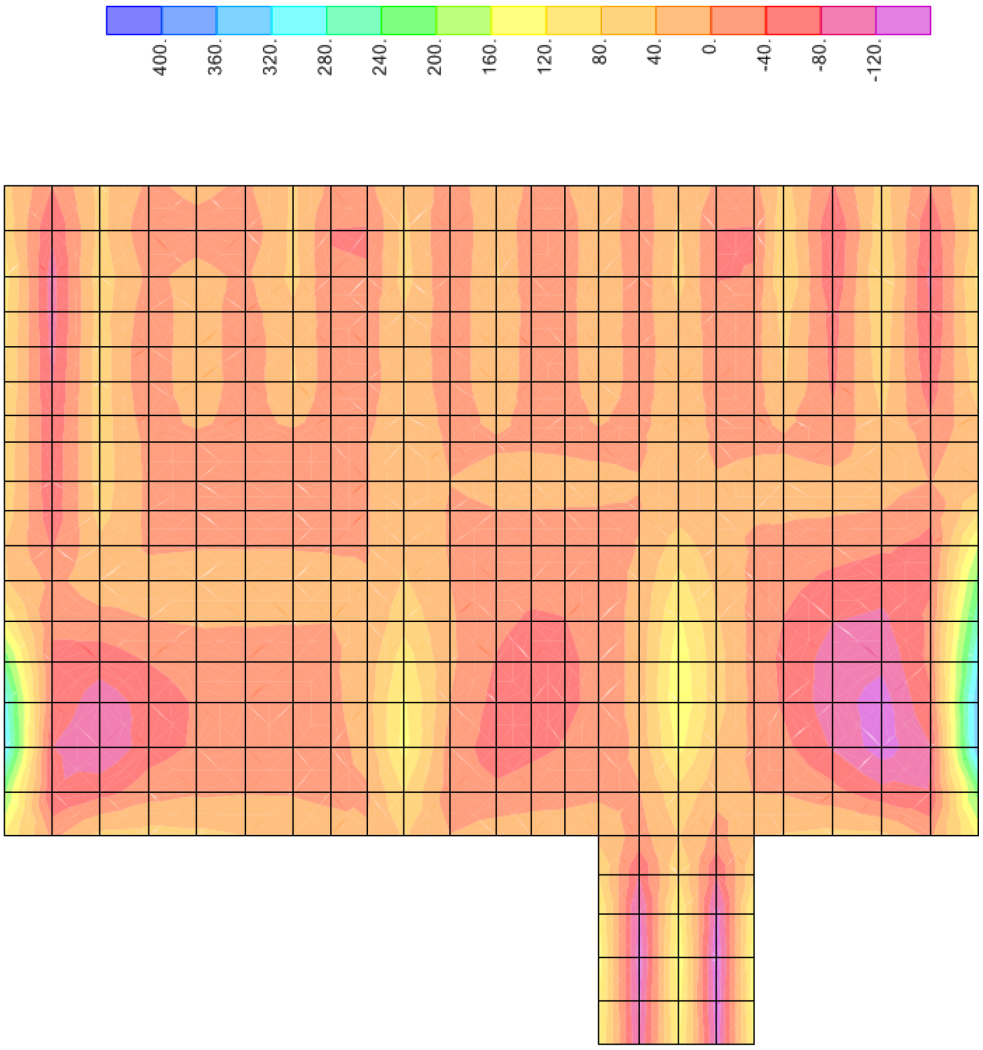

Figure 3.8.5-6a: Myy Due to Seismic Base Pressure on Control Building Basemat (kip-ft/ft) (Positive X Axis is to the Right of the Image and Positive Y is to the Top of the Image)

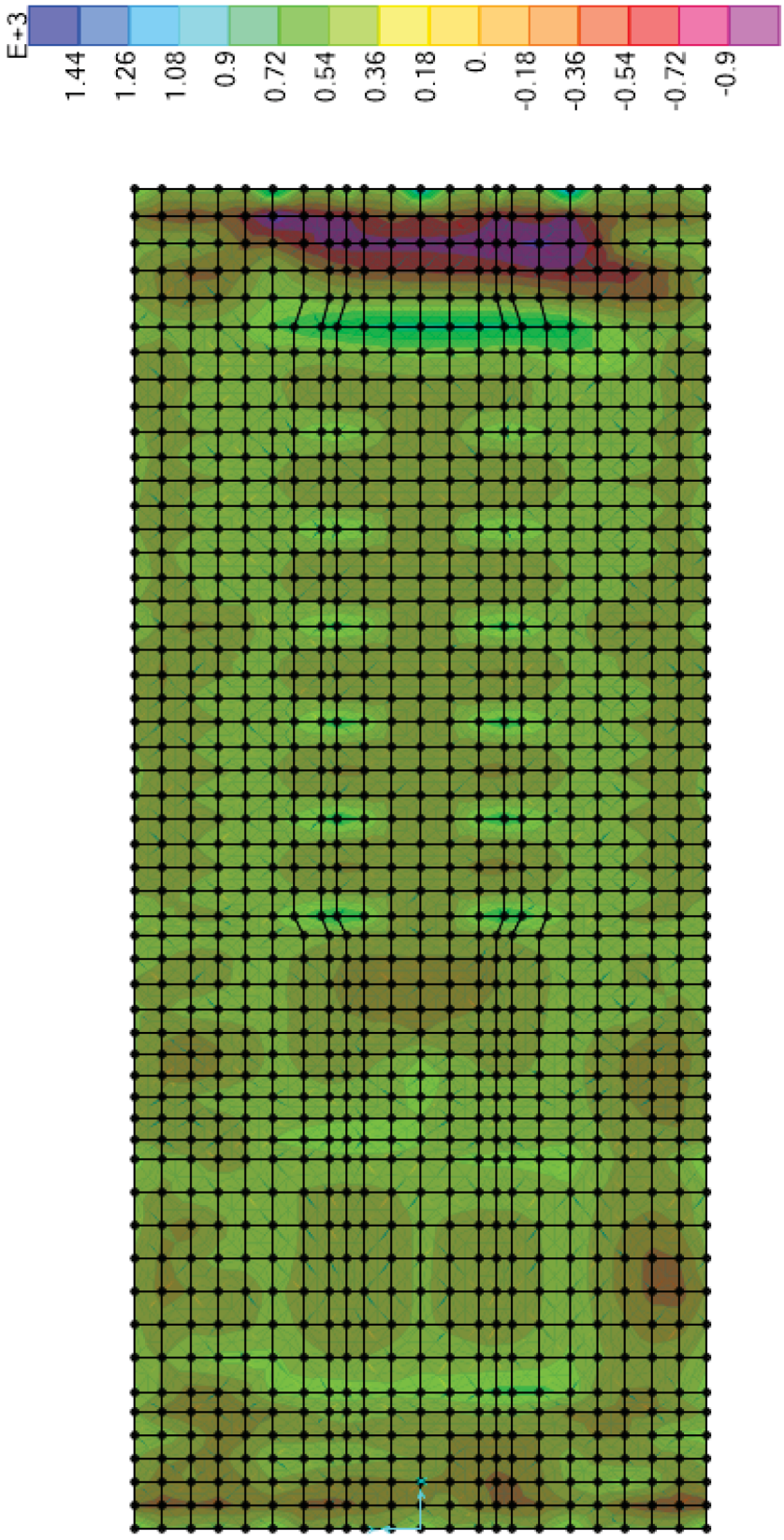

Figure 3.8.5-7: Mxx Due to Seismic Base Pressure on Reactor Building Basemat (kip-ft/ft) in the Reactor Building Basemat Model (Positive X Axis is to the Right of the Image and Positive Y is to the Top of the Image)

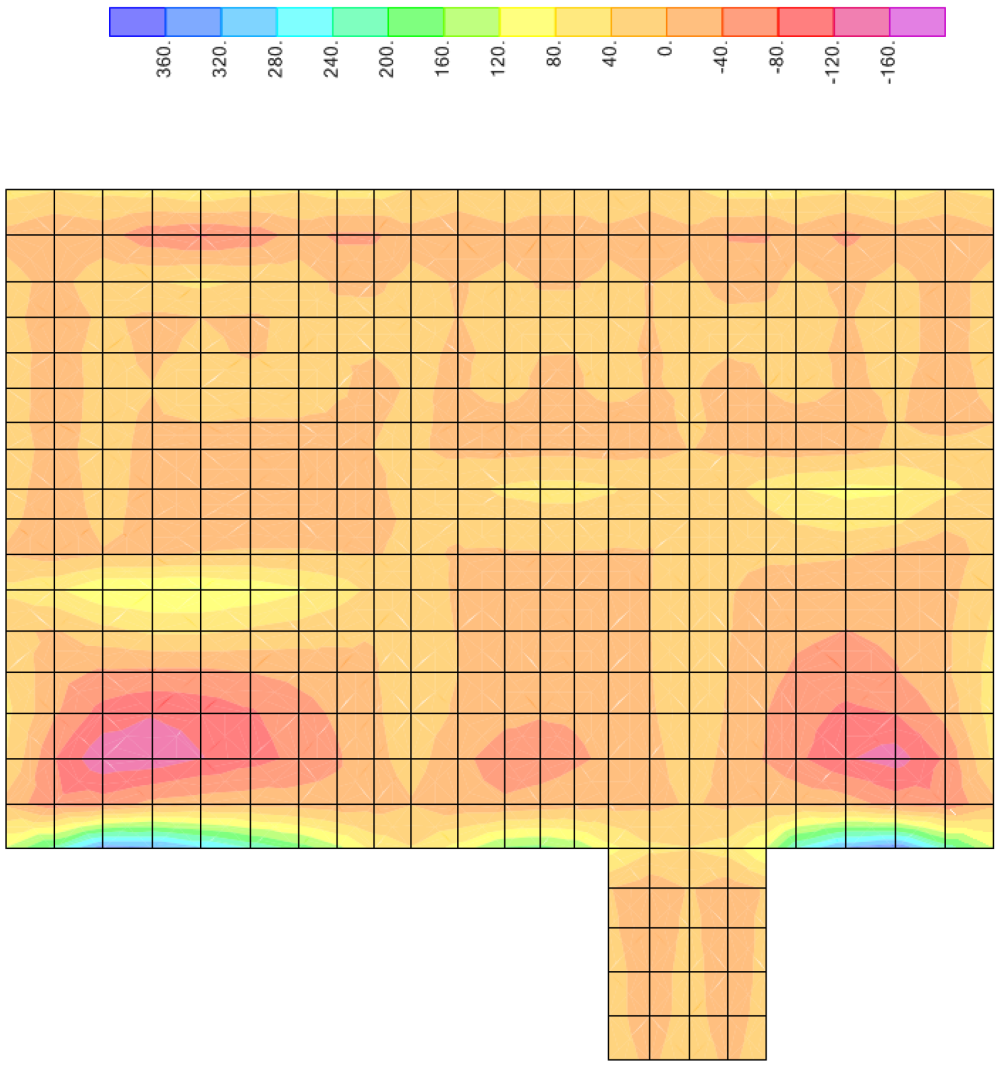

Figure 3.8.5-7a: Mxx Due to Seismic Base Pressure on Control Building Basemat (kip-ft/ft) (Positive X Axis is to the Right of the Image and Positive Y is to the Top of the Image)

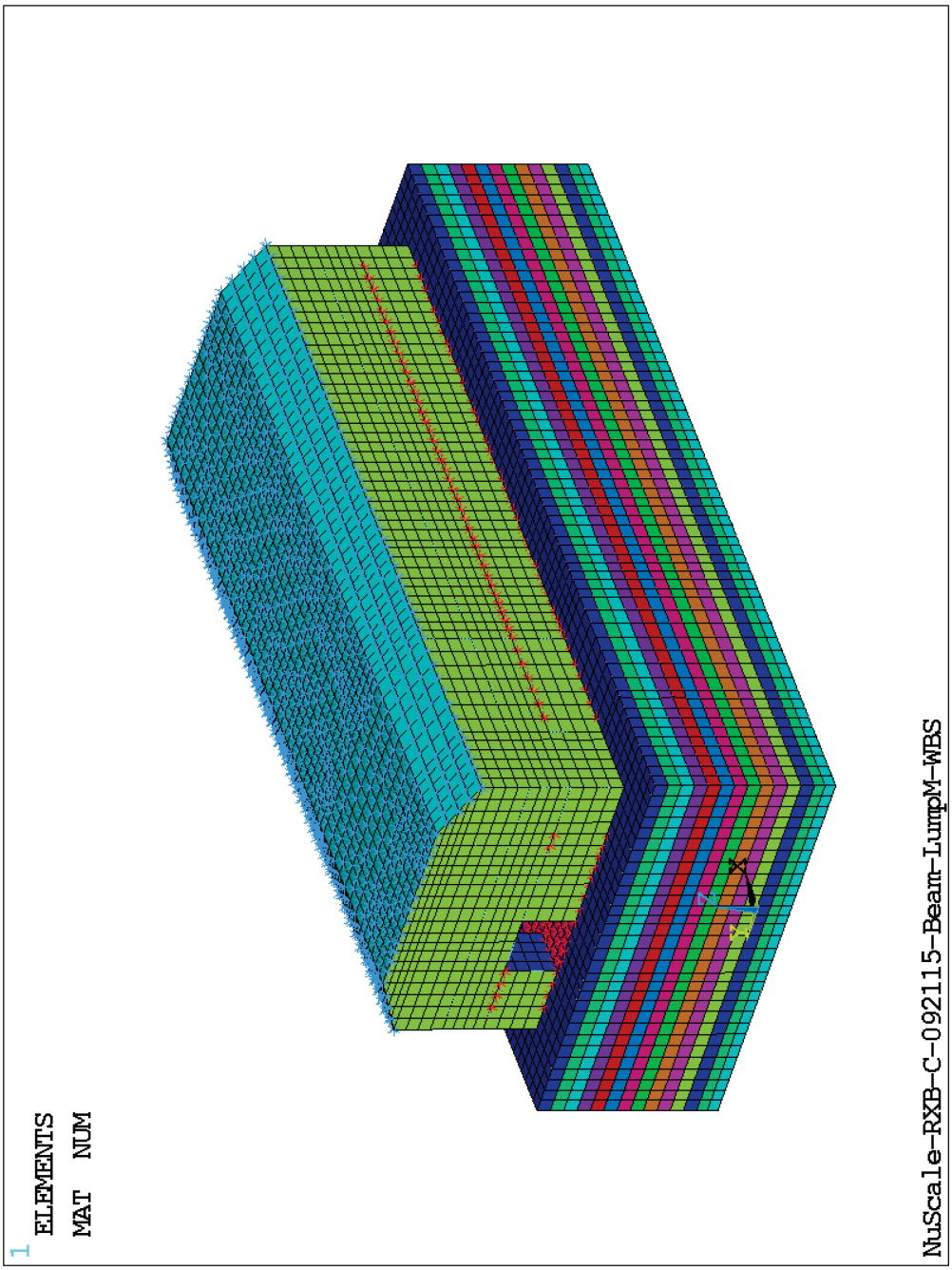

Figure 3.8.5-8: RXB ANSYS Model with Backfill Soil

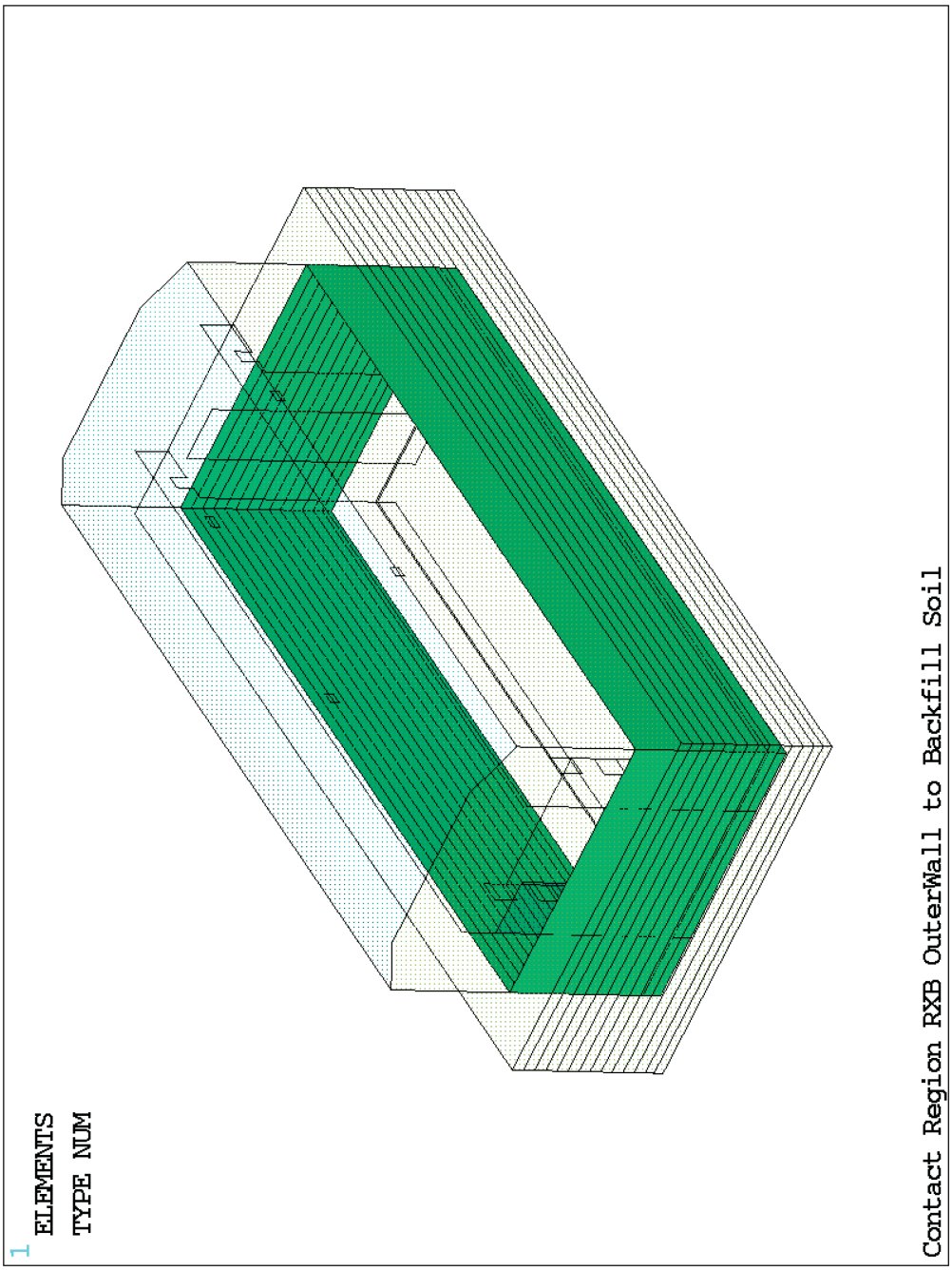

Figure 3.8.5-9: Nonlinear Contact Region between Building and Soil

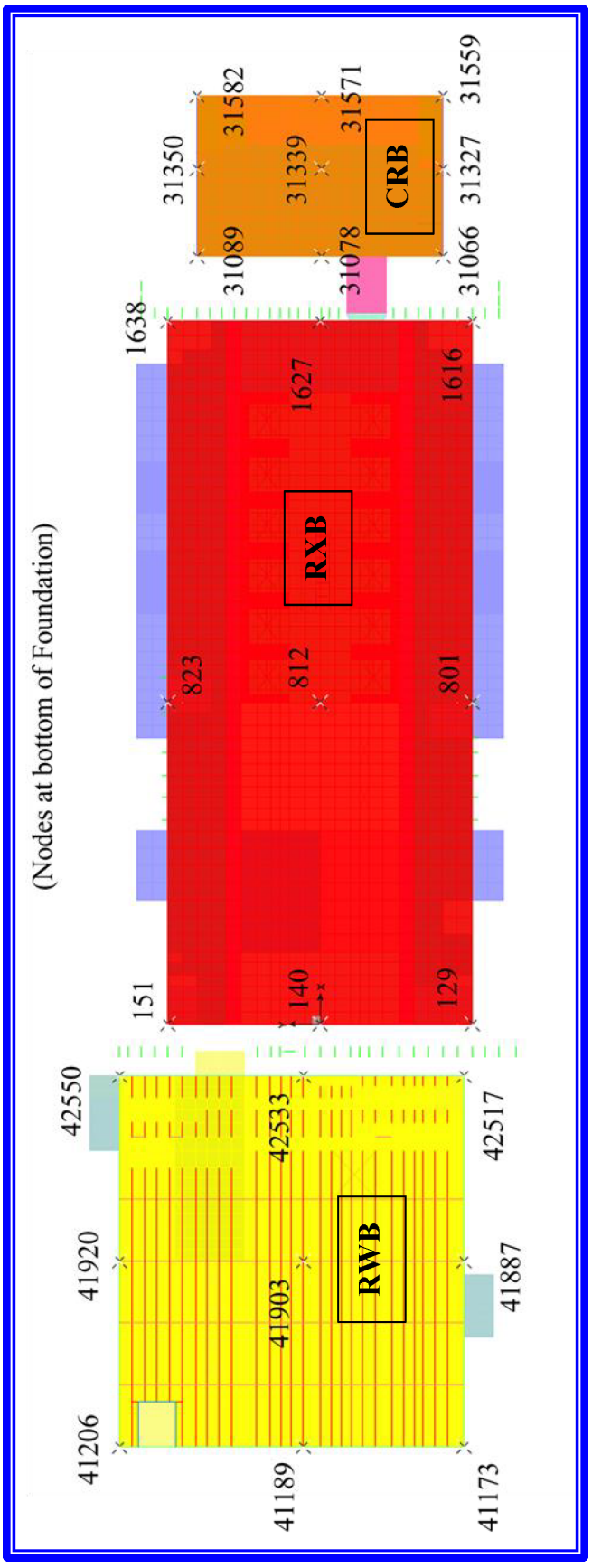

Figure 3.8.5-10: Edge and Center Nodes at Bottom of Foundations Selected for Building Settlement Assessment

Figure 3.8.5-11: RXB Skin Nodes on Backfill Soil Vertical Boundaries for Applying SASSI Acceleration Time Histories

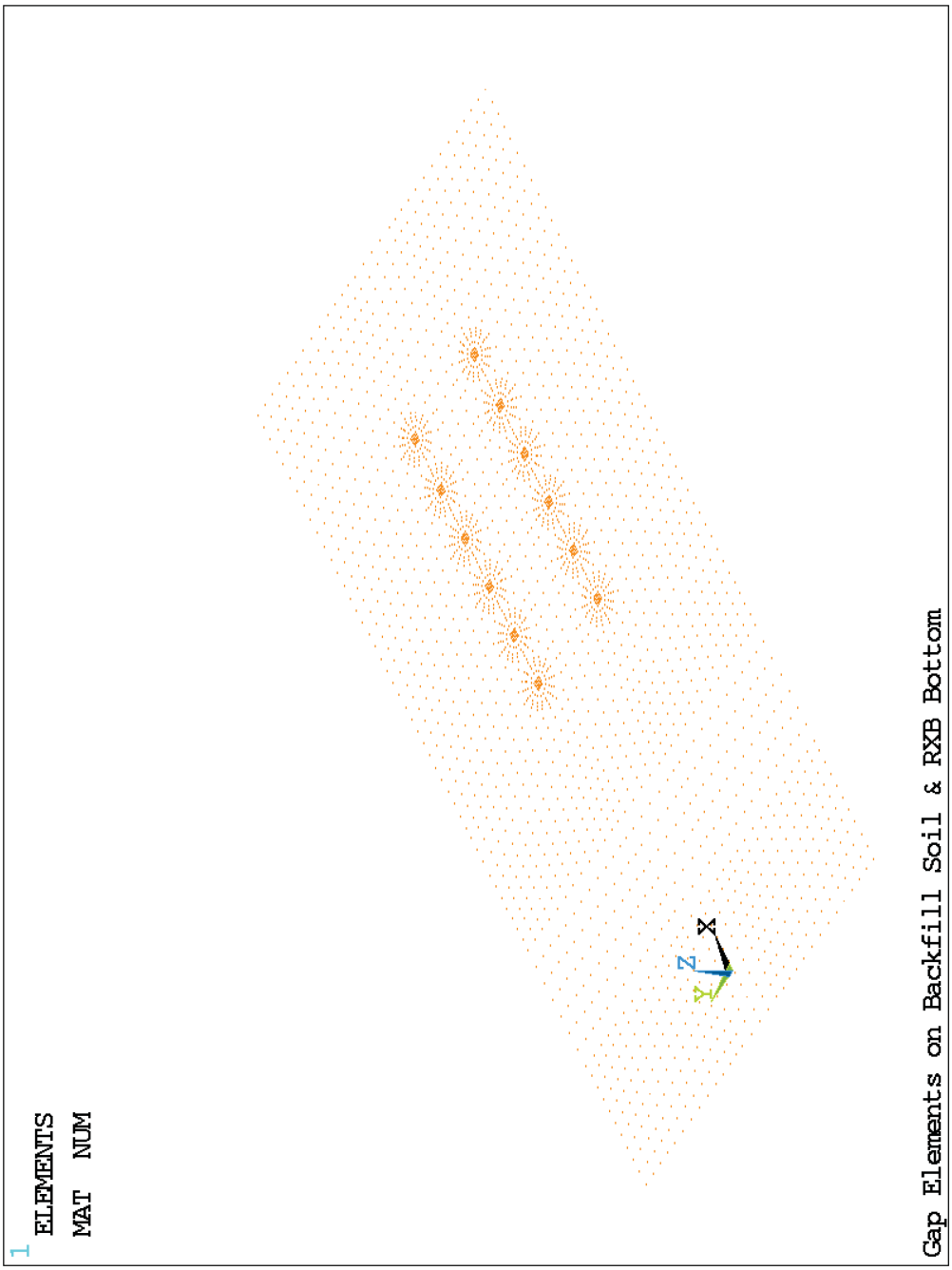

Figure 3.8.5-12: RXB Foundation Bottom Skin Nodes for Applying SASSI Acceleration Time Histories

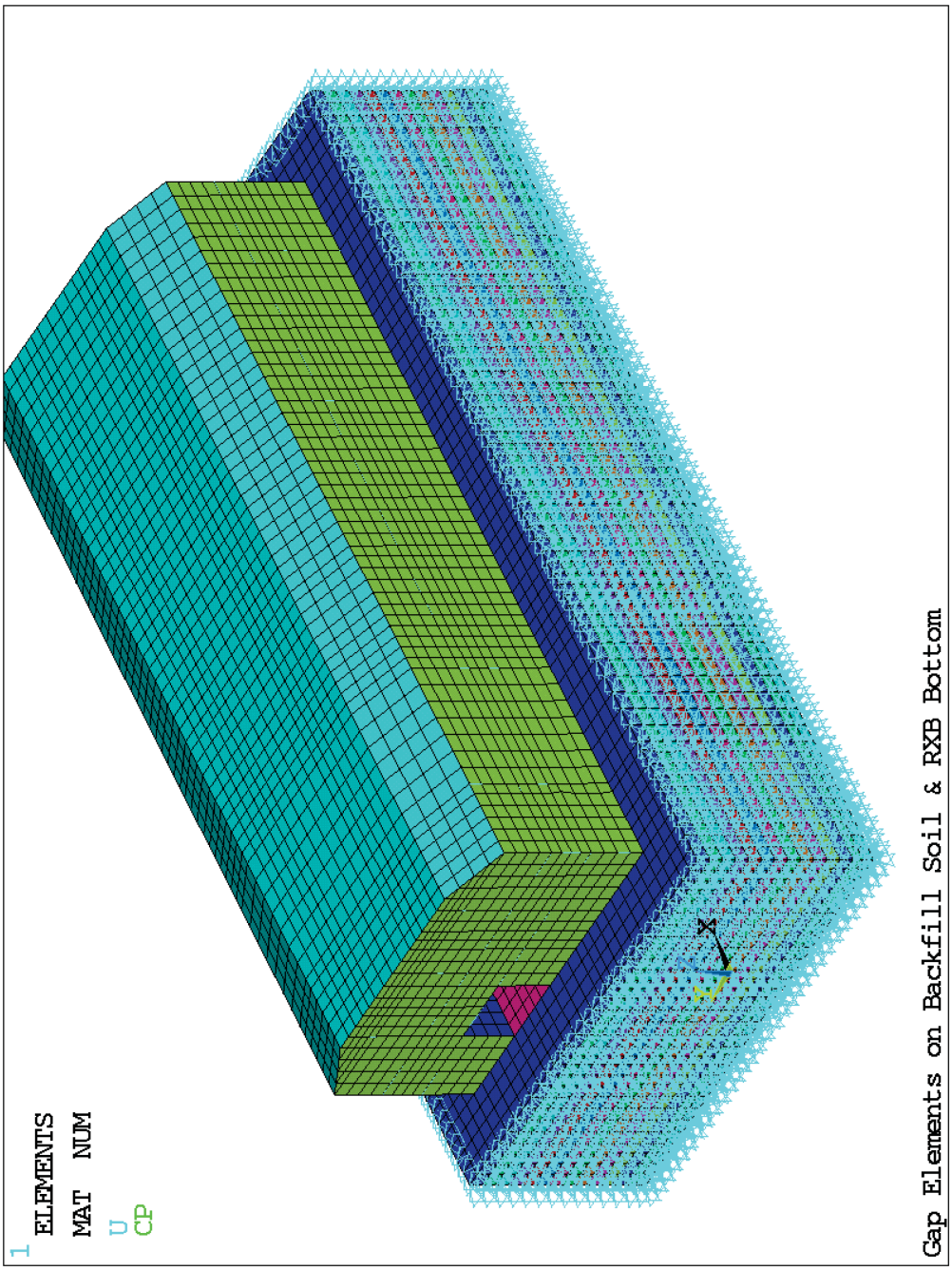

Figure 3.8.5-13: Displacements from SASSI Applied to ANSYS Model Boundary

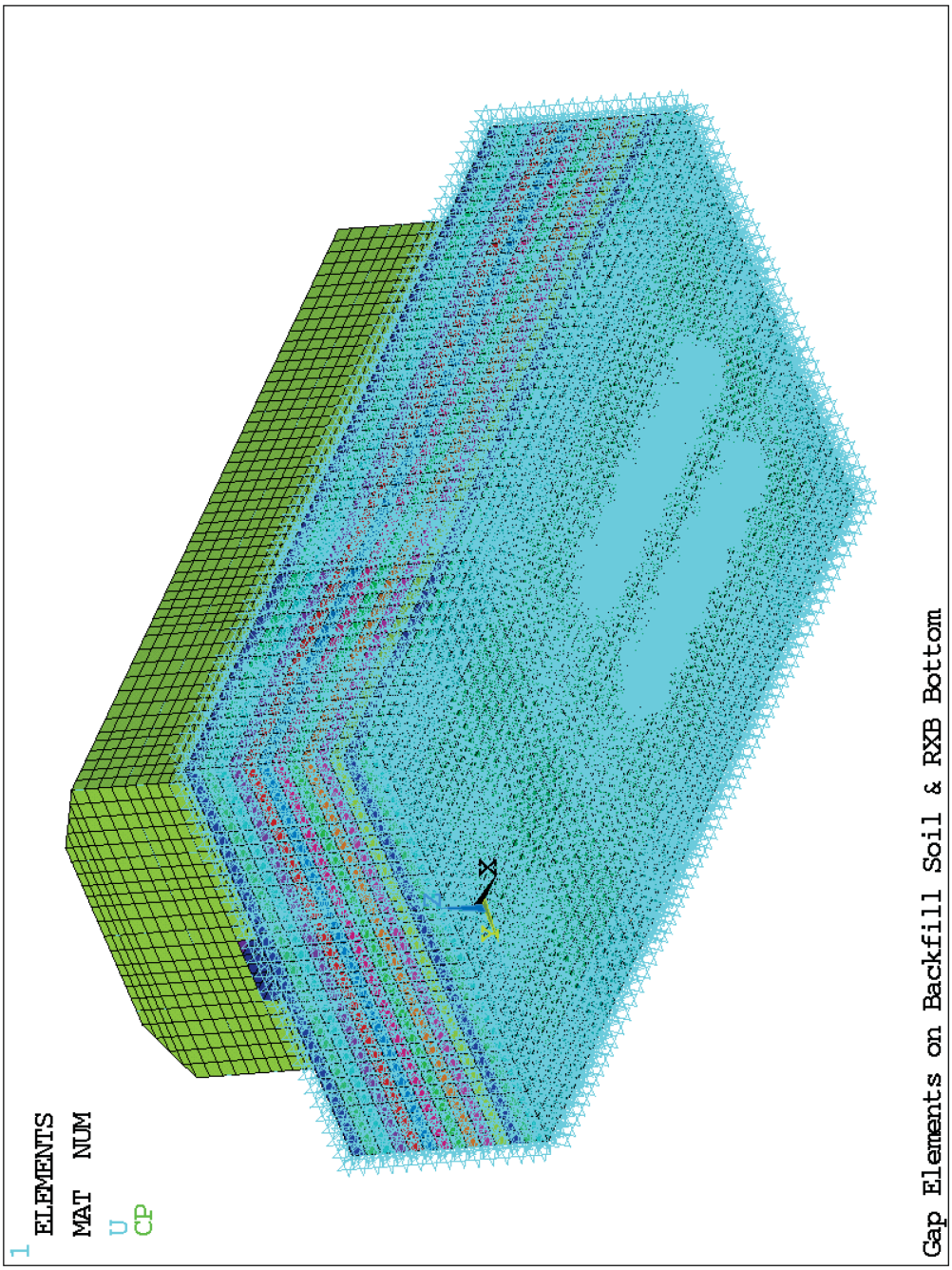

Figure 3.8.5-14: Displacements from SASSI Applied to ANSYS Model Boundary

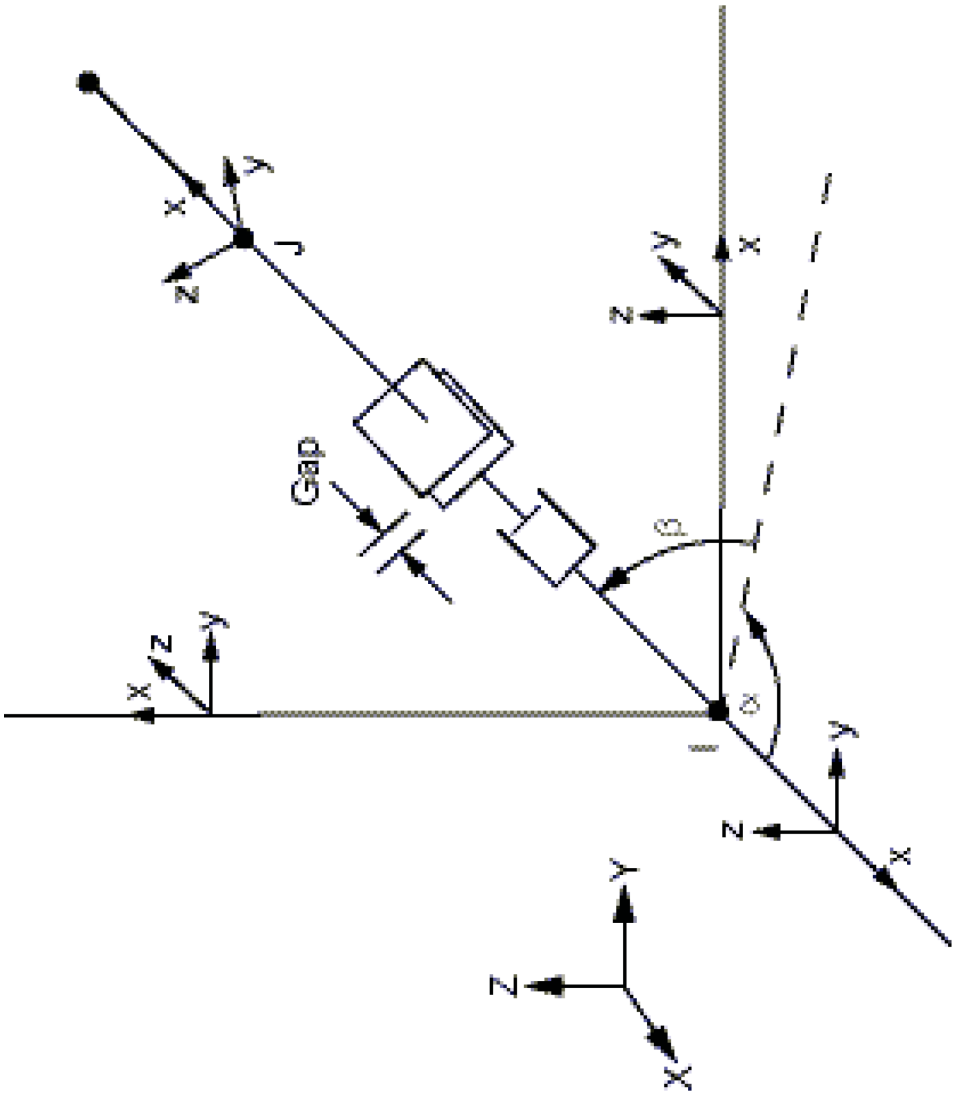

Figure 3.8.5-15: Nonlinear Contact Element between Backfill and Surrounding Soil

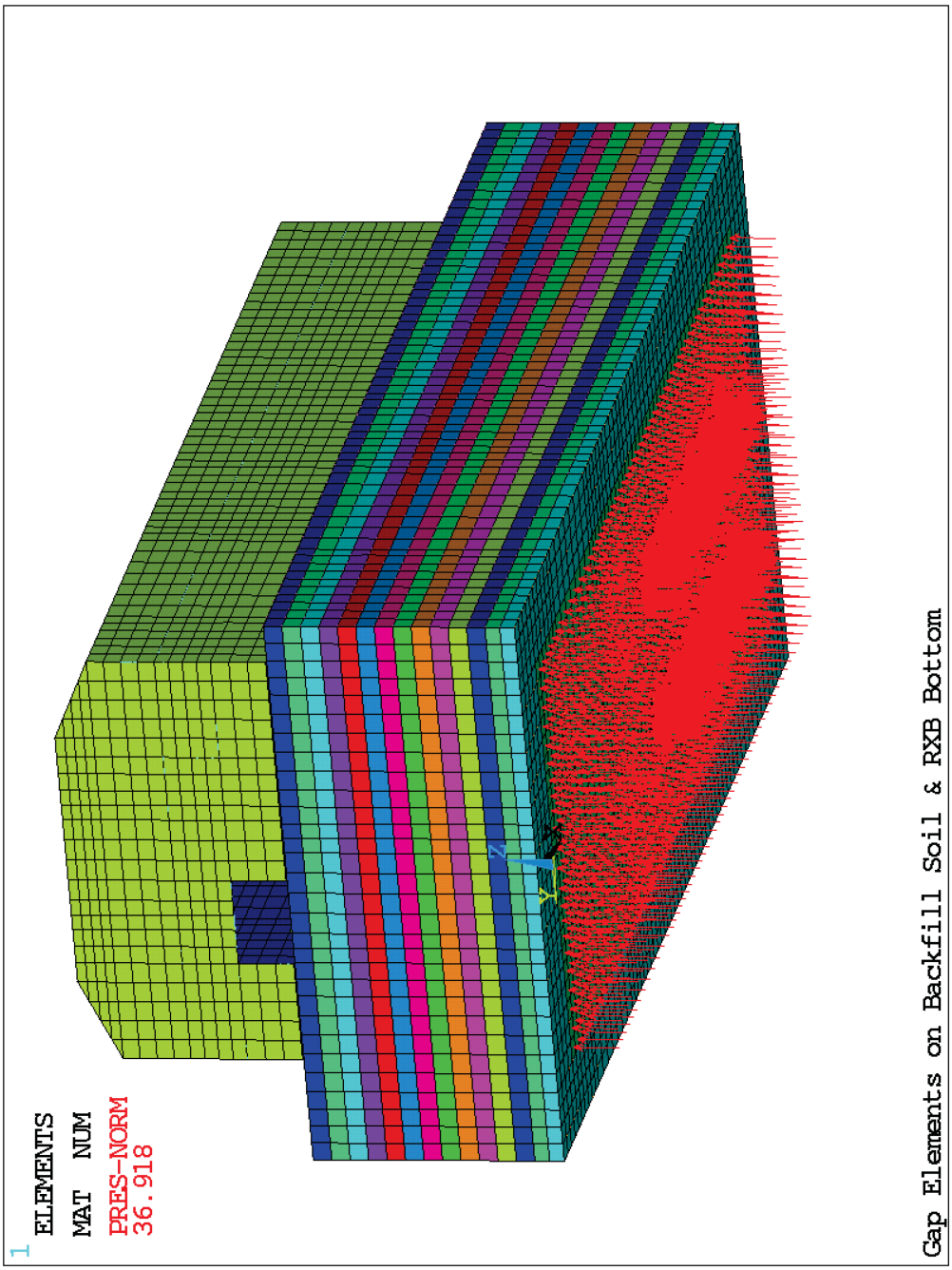

Figure 3.8.5-16: Buoyancy Load on Basemat

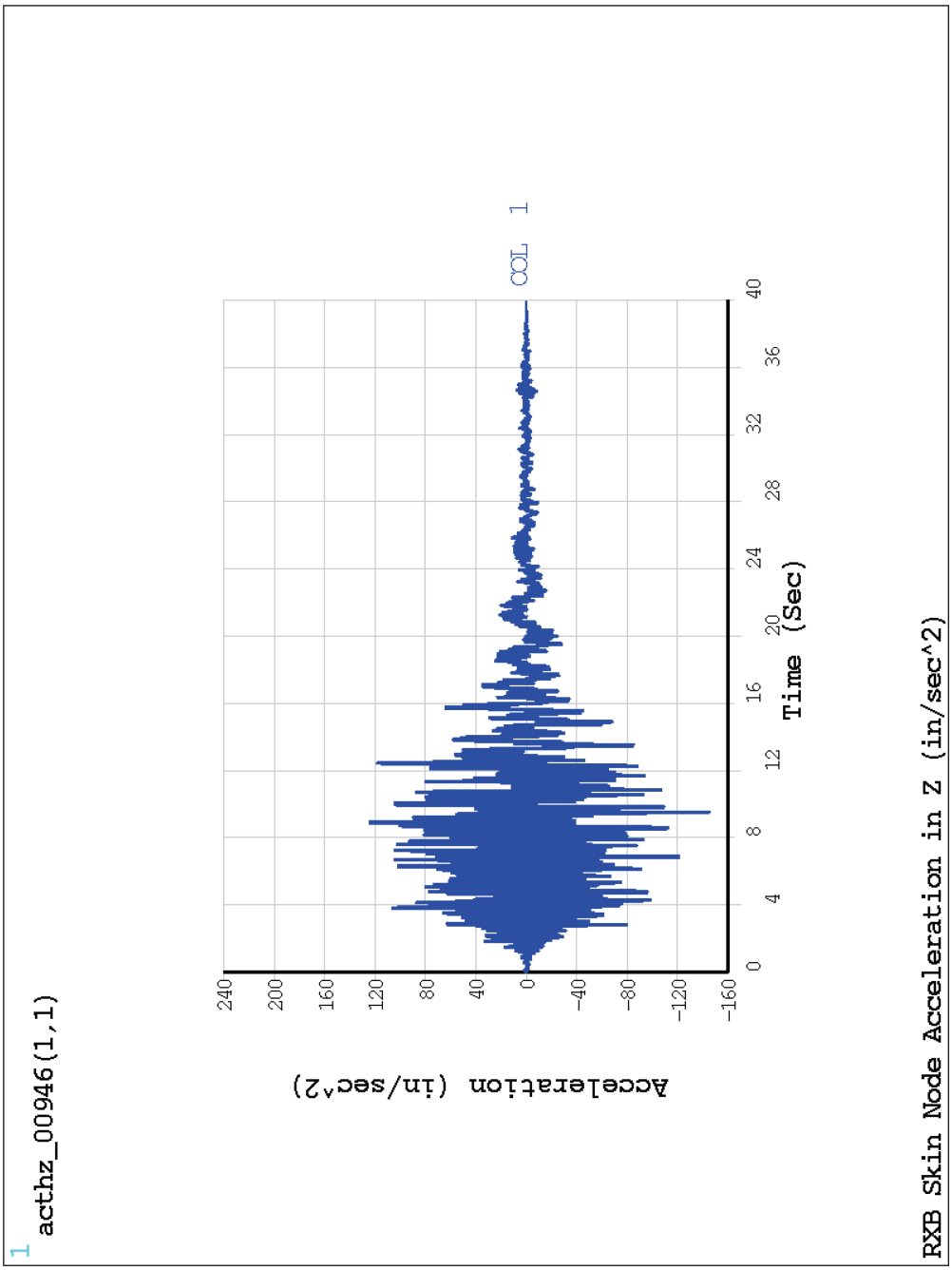

Figure 3.8.5-17: Soil Type 7 - Acceleration Time History - Vertical

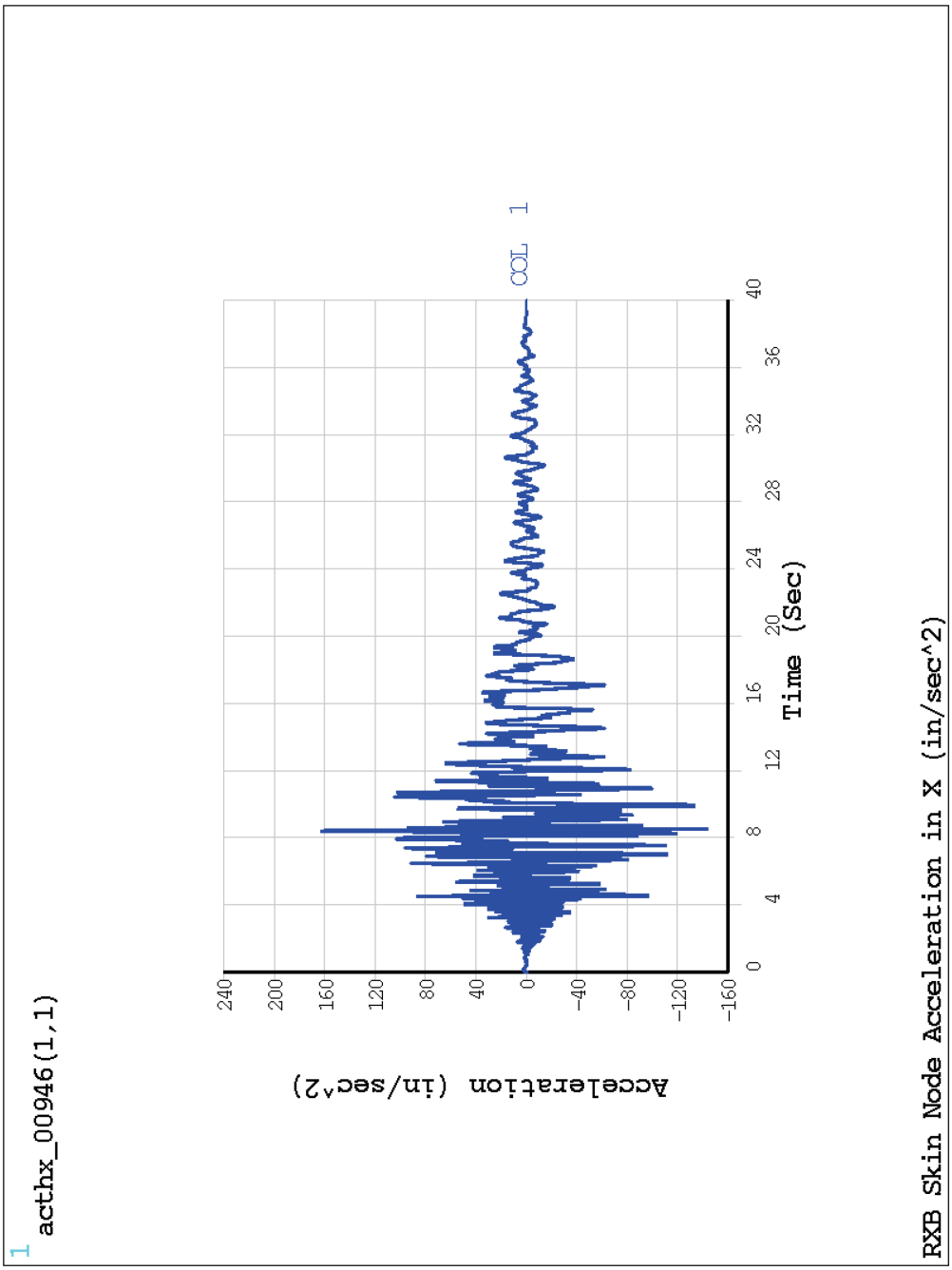

Figure 3.8.5-18: Soil Type 7 - Acceleration Time History - E-W

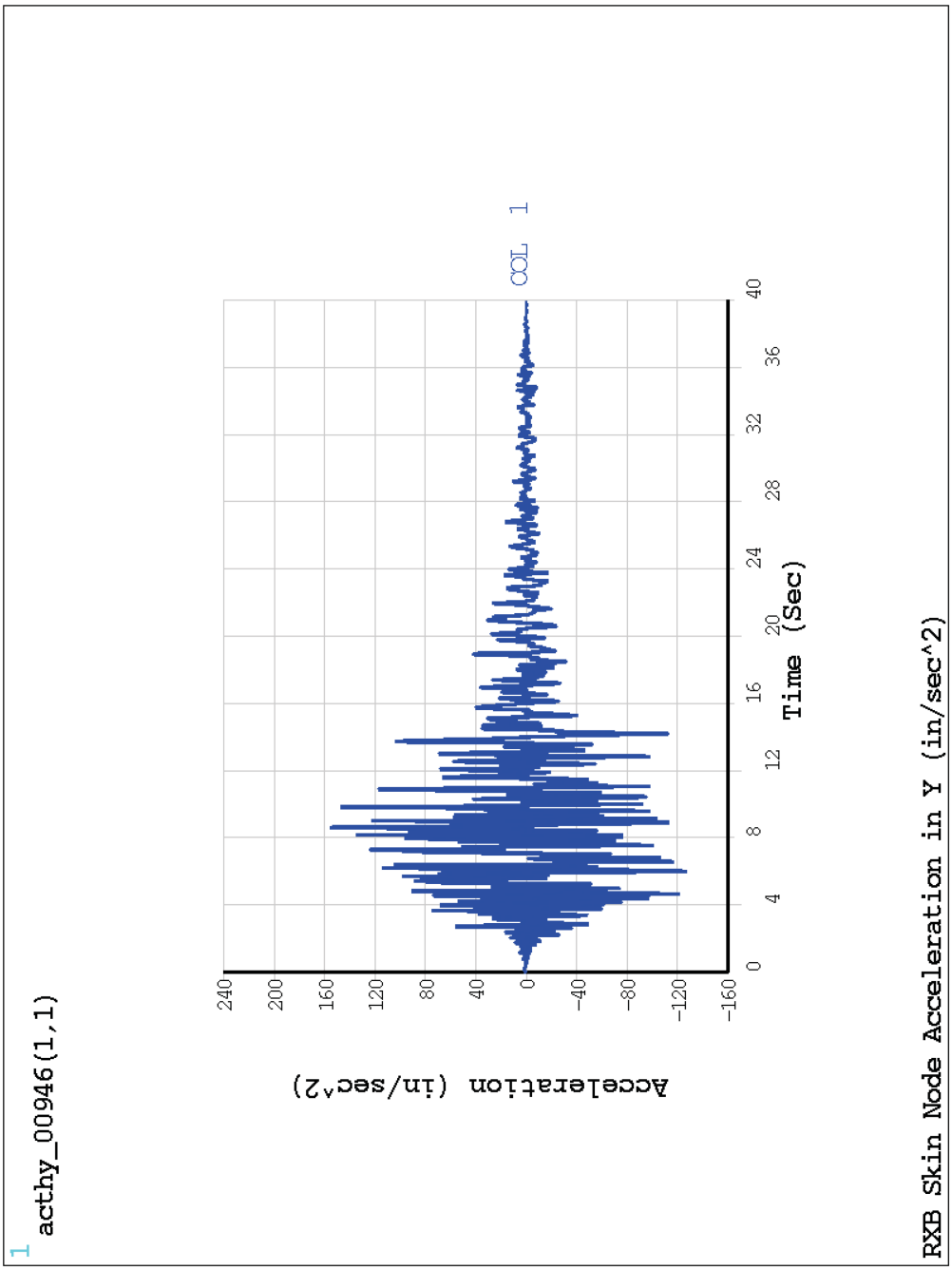

Figure 3.8.5-19: Soil Type 7 - Acceleration Time History - N-S

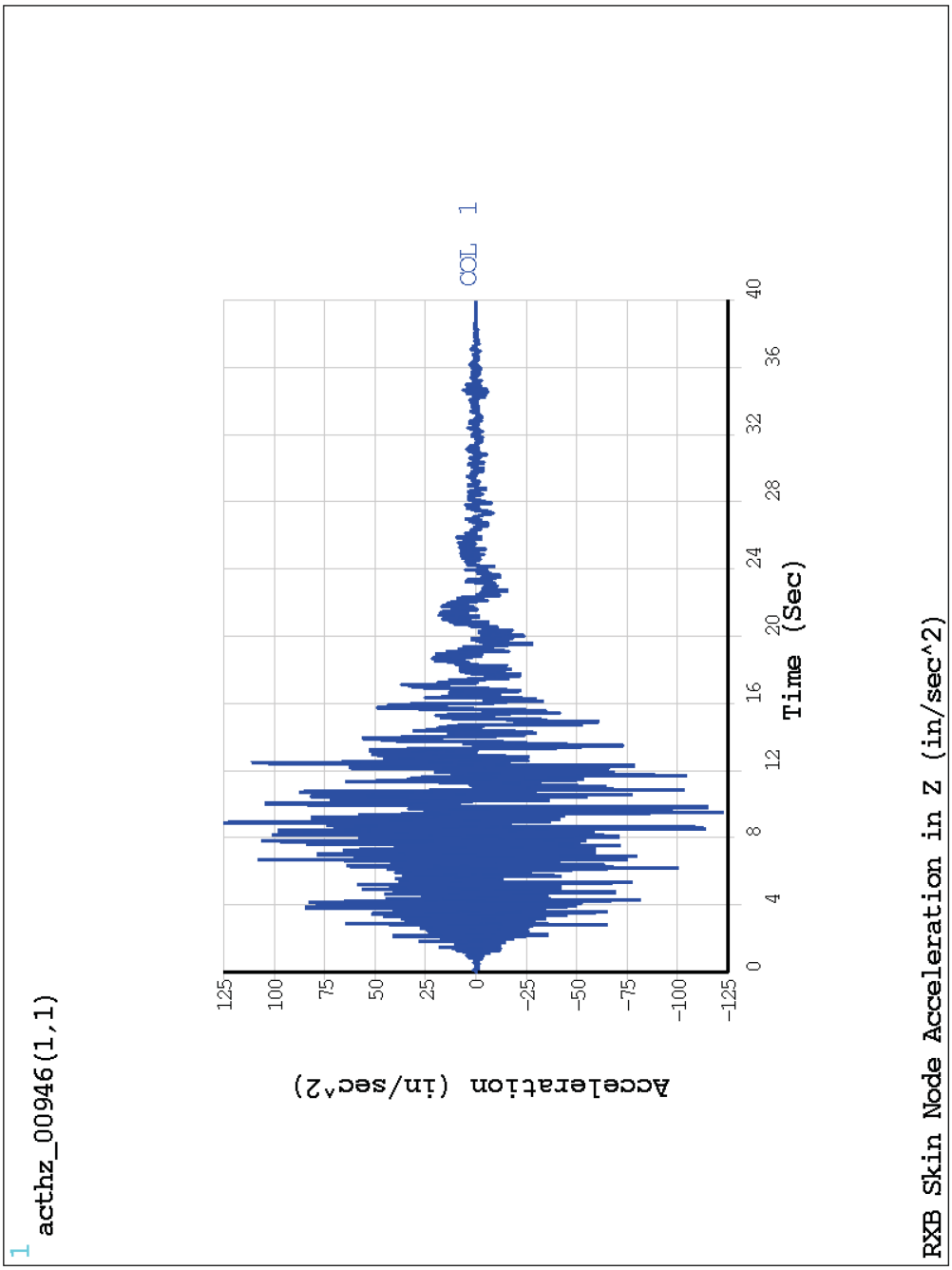

Figure 3.8.5-20: Soil Type 8 - Acceleration Time History - Vertical

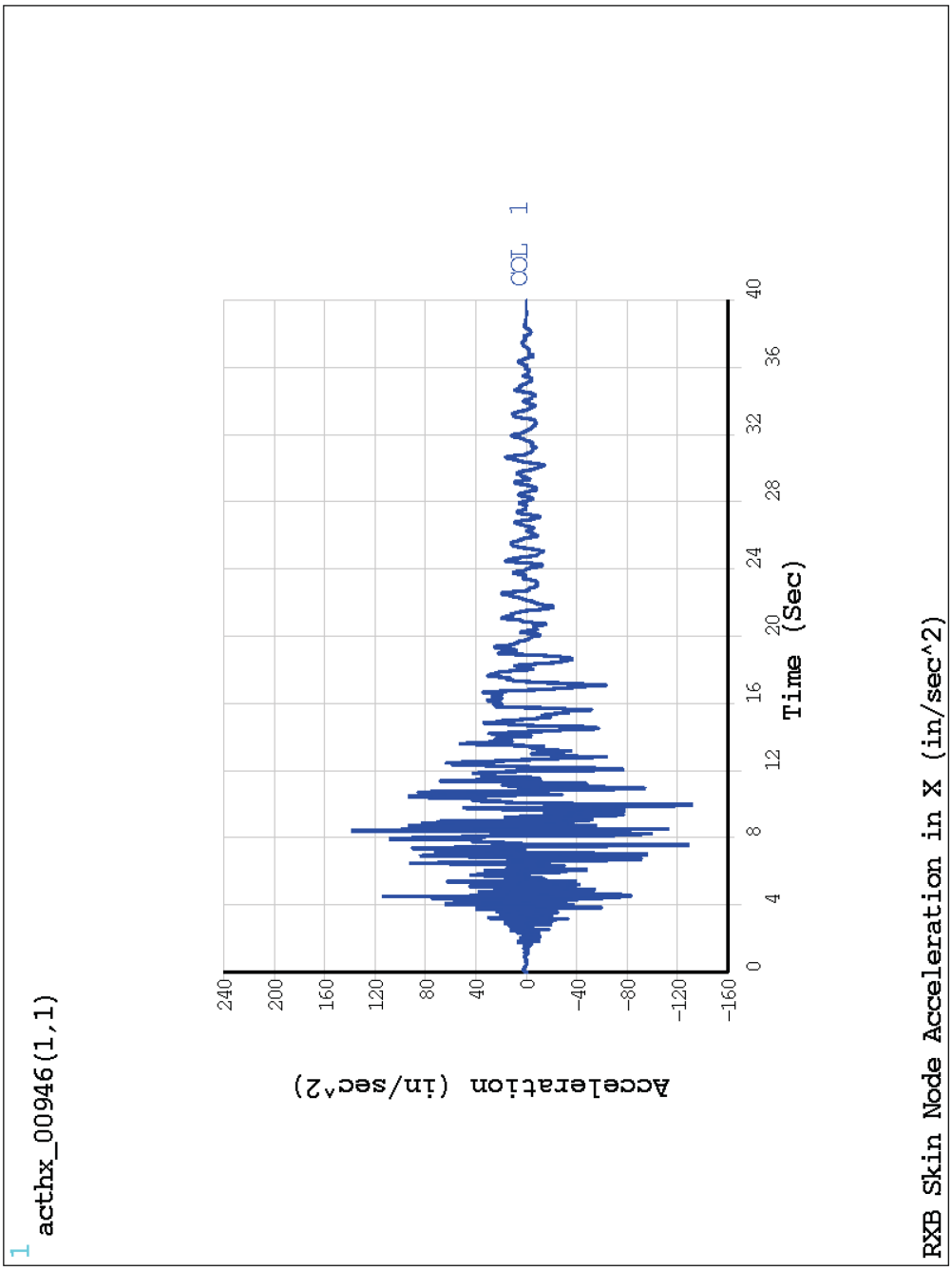

Figure 3.8.5-21: Soil Type 8 - Acceleration Time History - E-W

Figure 3.8.5-22: Soil Type 8 - Acceleration Time History - N-S

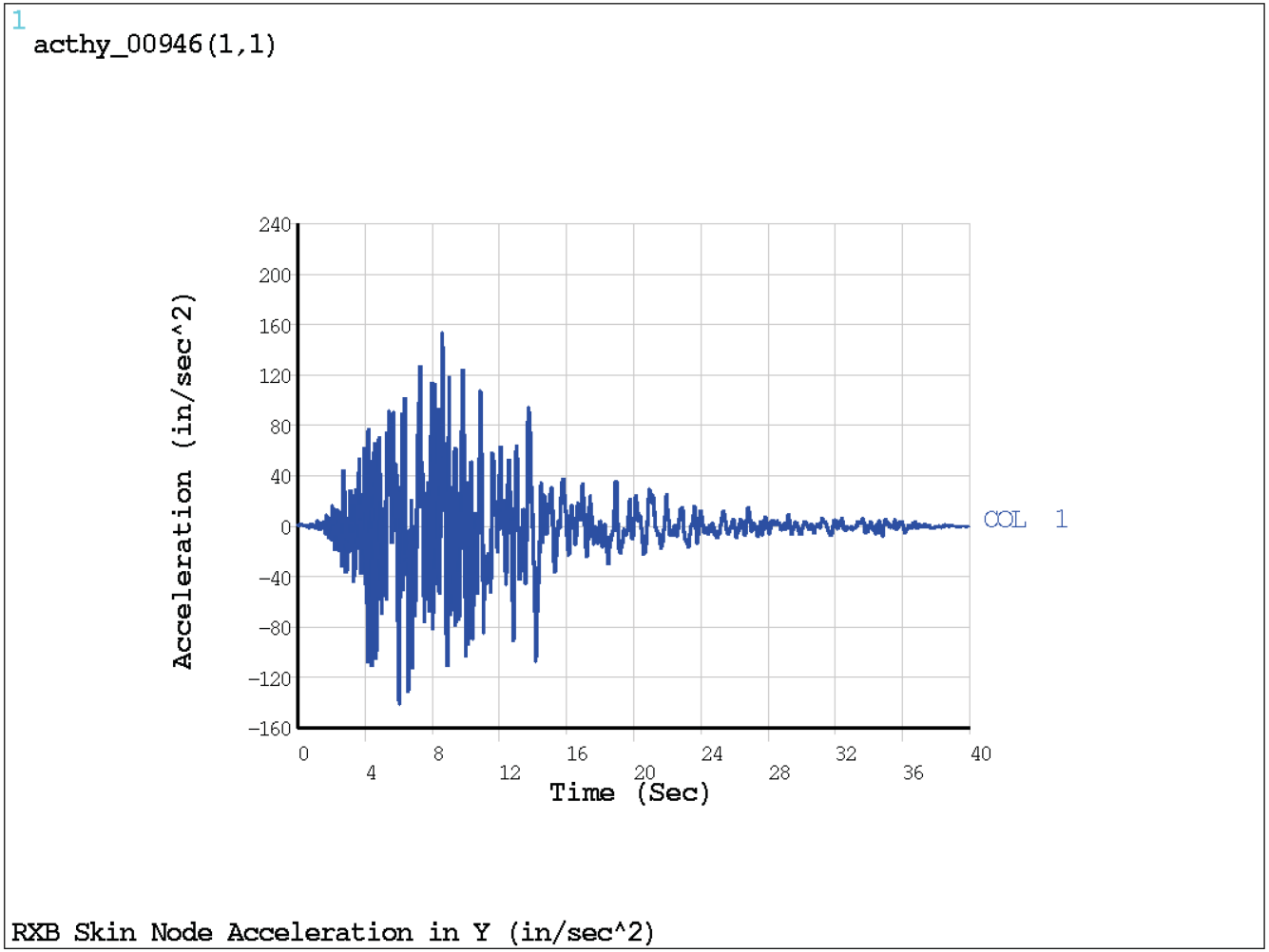

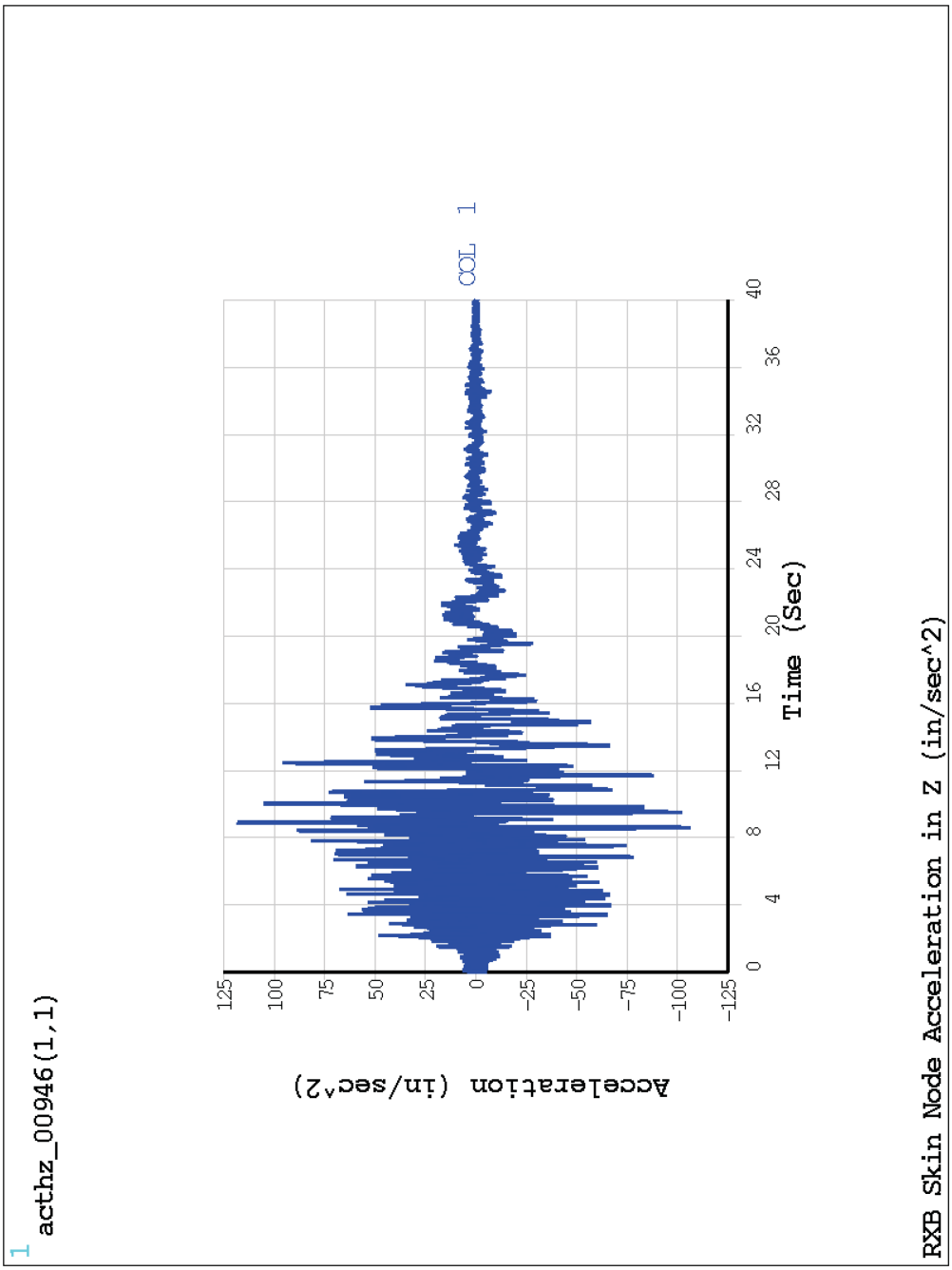

Figure 3.8.5-23: Soil Type 11 - Acceleration Time History - Vertical

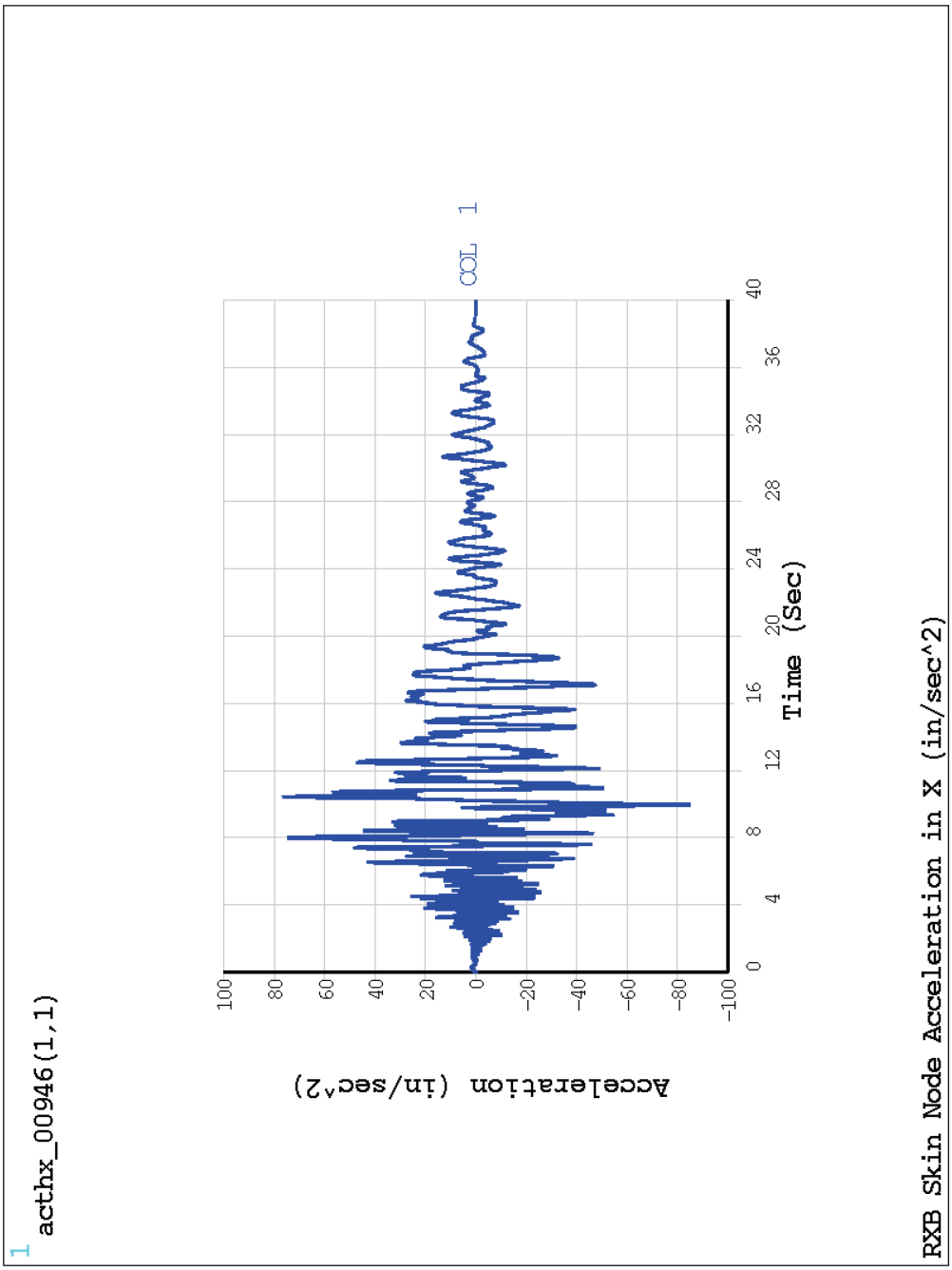

Figure 3.8.5-24: Soil Type 11 - Acceleration Time History - E-W

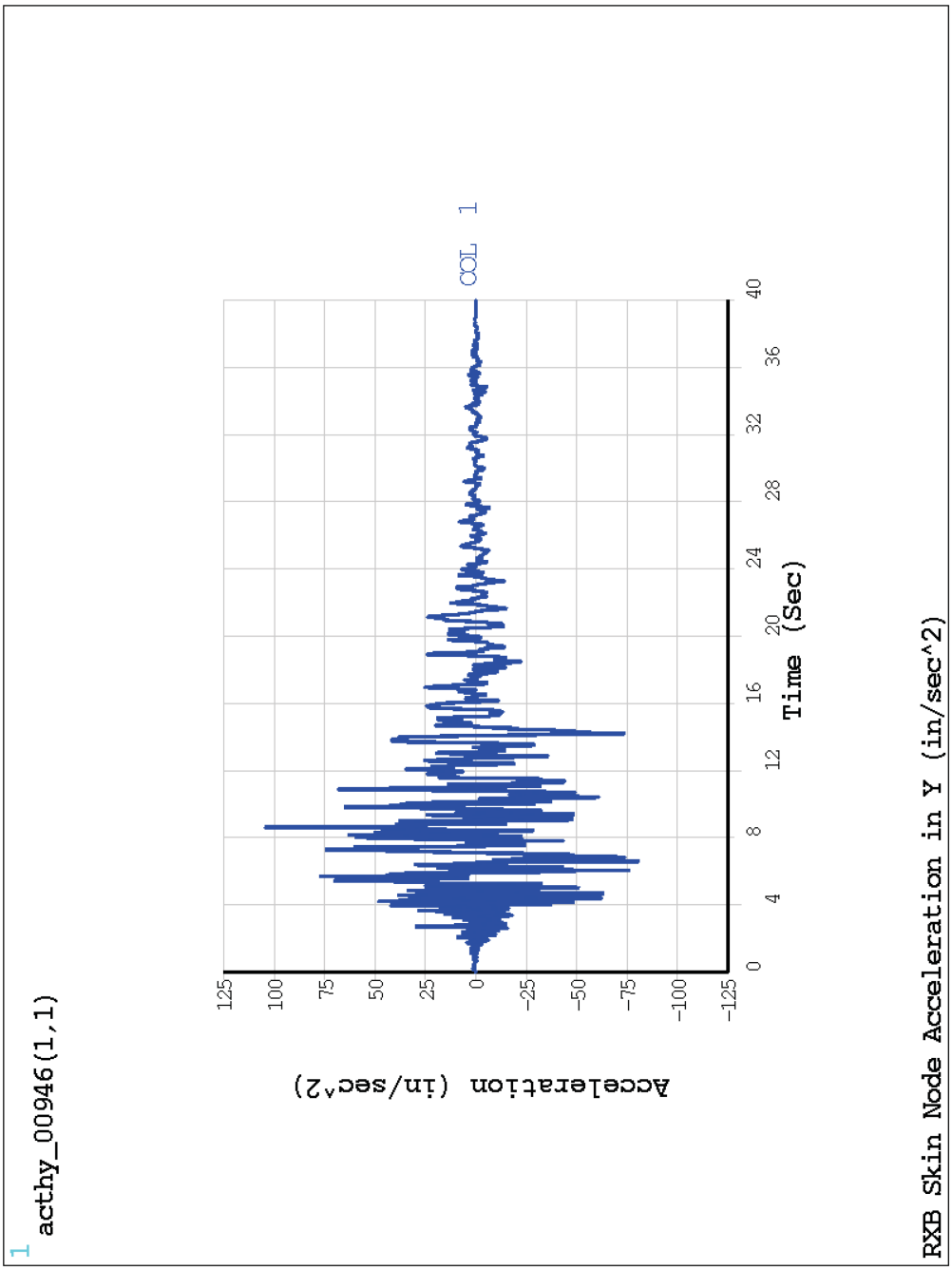

Figure 3.8.5-25: Soil Type 11 - Acceleration Time History - N-S

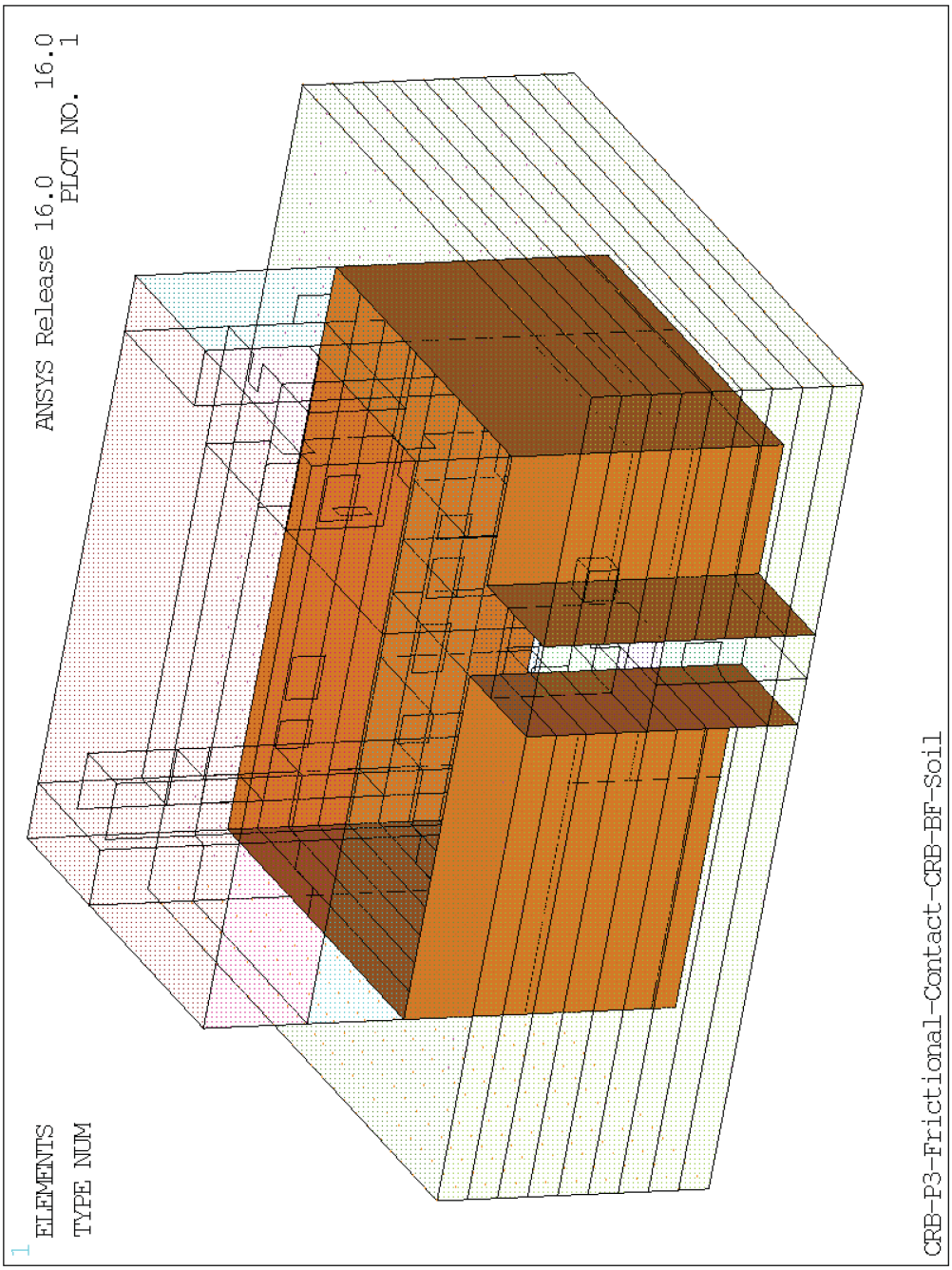

Figure 3.8.5-26: Nonlinear Contact Region between CRB and Soil

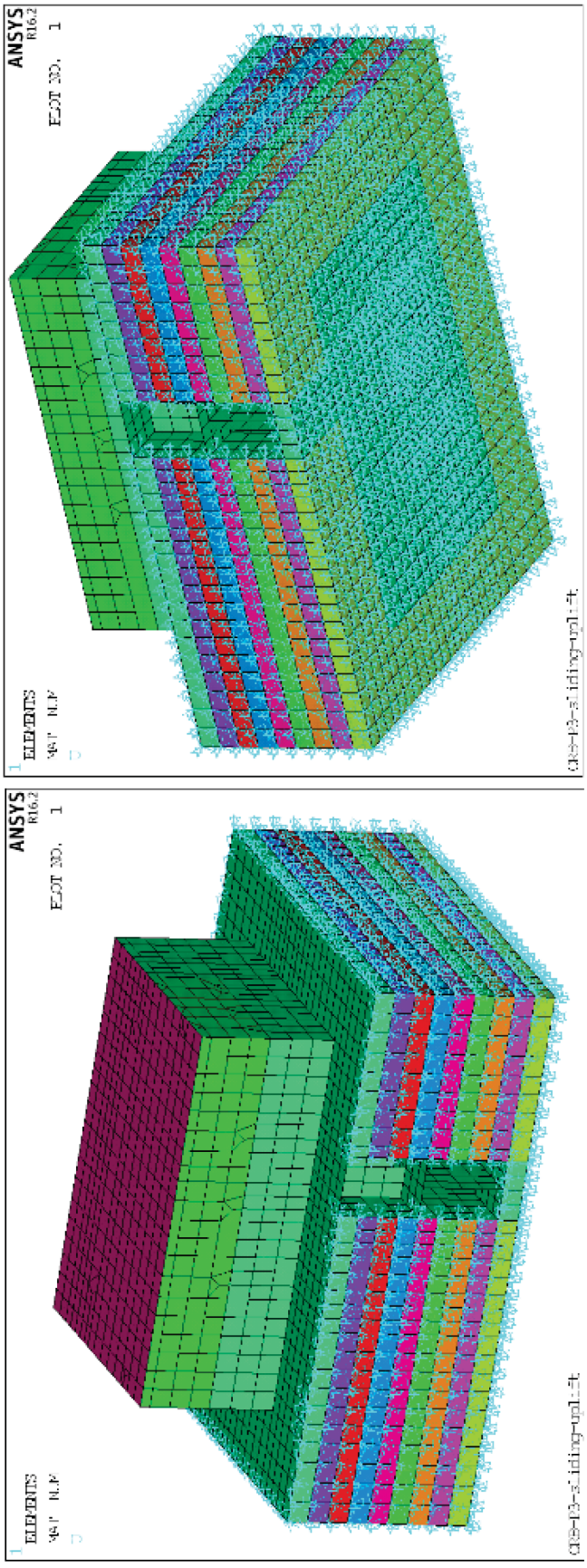

Figure 3.8.5-27: CRB Time Histories from SASSI Applied to ANSYS Model Boundary

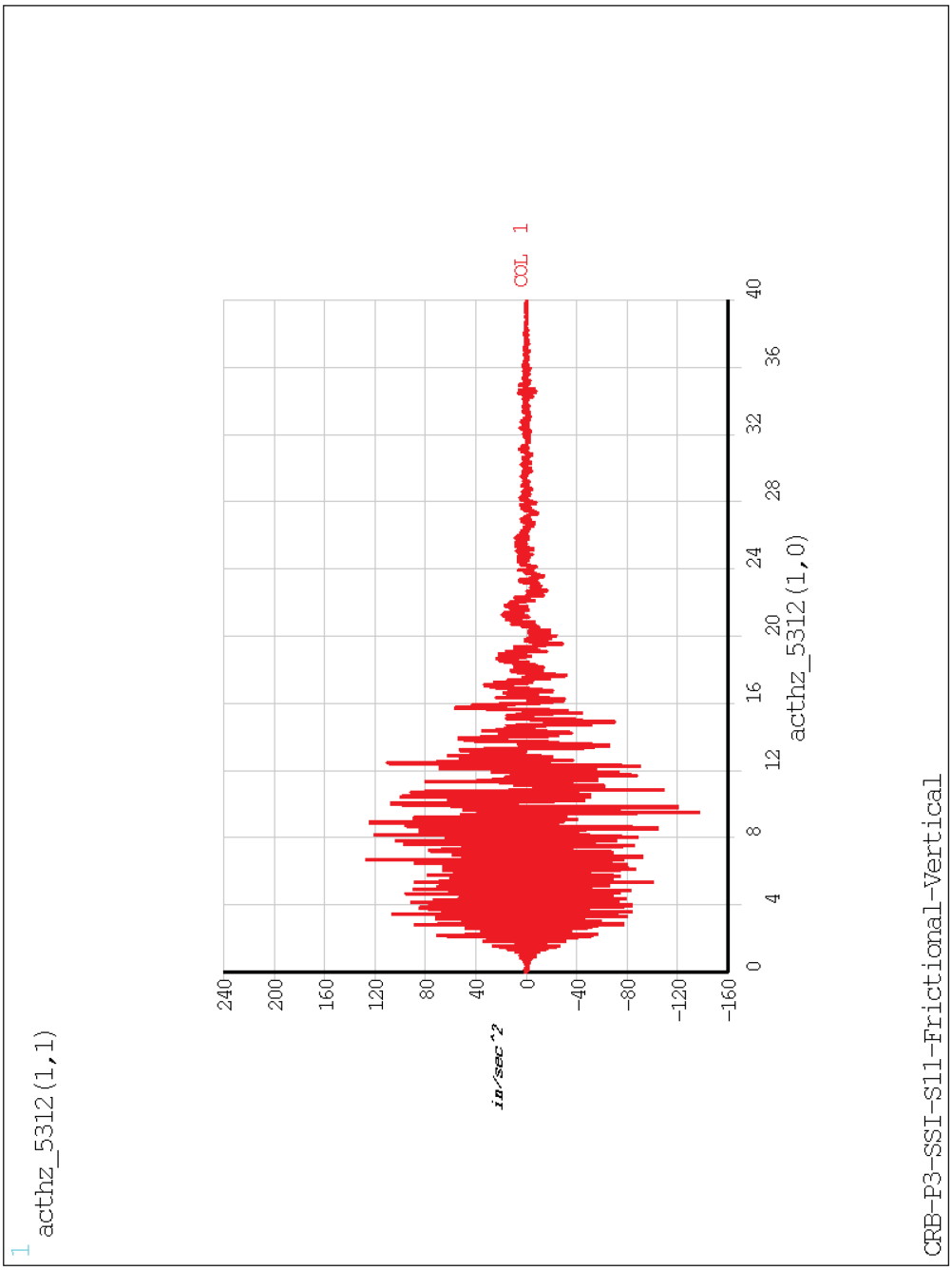

Figure 3.8.5-28: Soil Type 11, Capitola Input - Acceleration Time History - Vertical

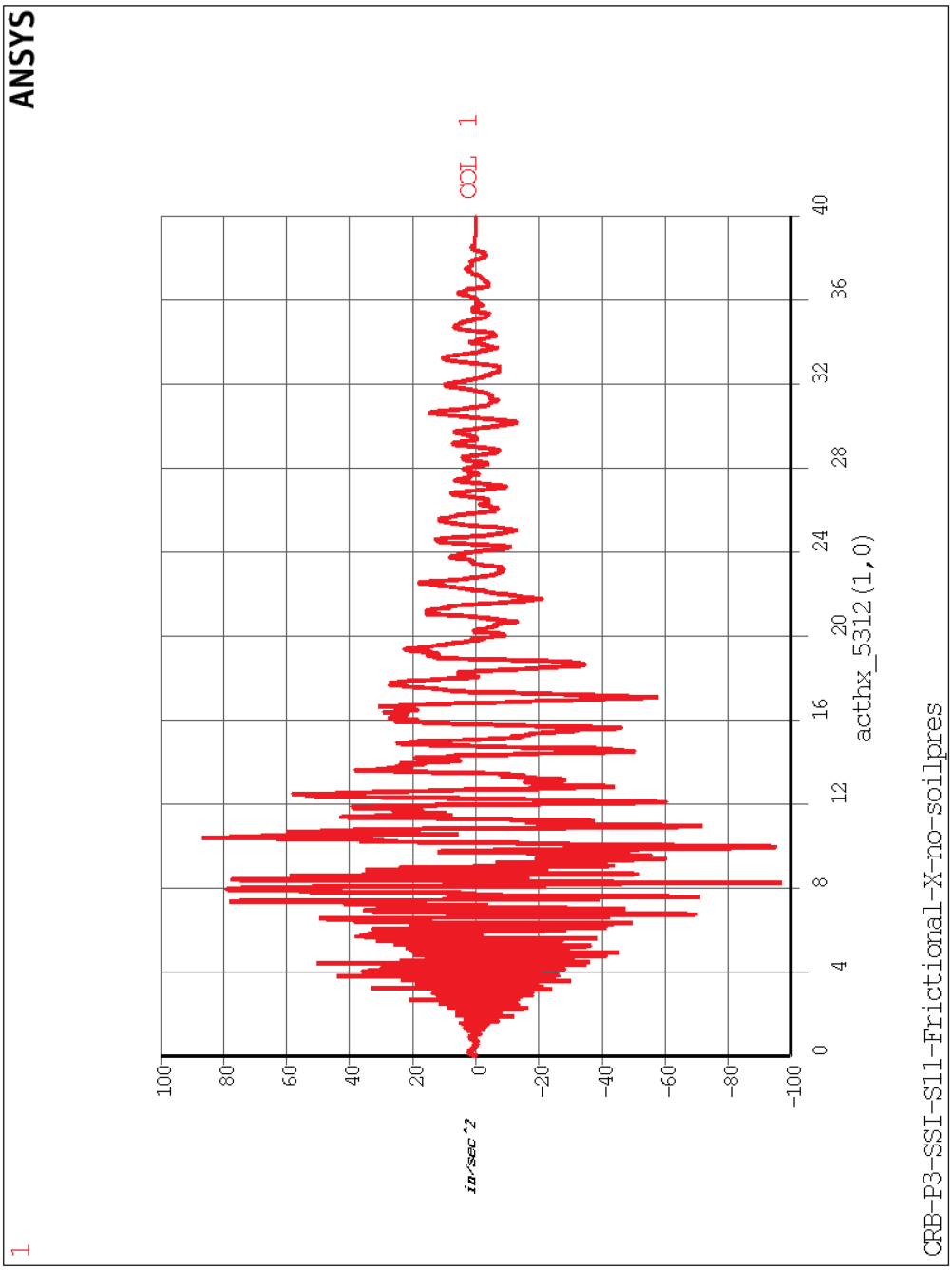

Figure 3.8.5-29: Soil Type 11, Capitola Input - Acceleration Time History - E-W

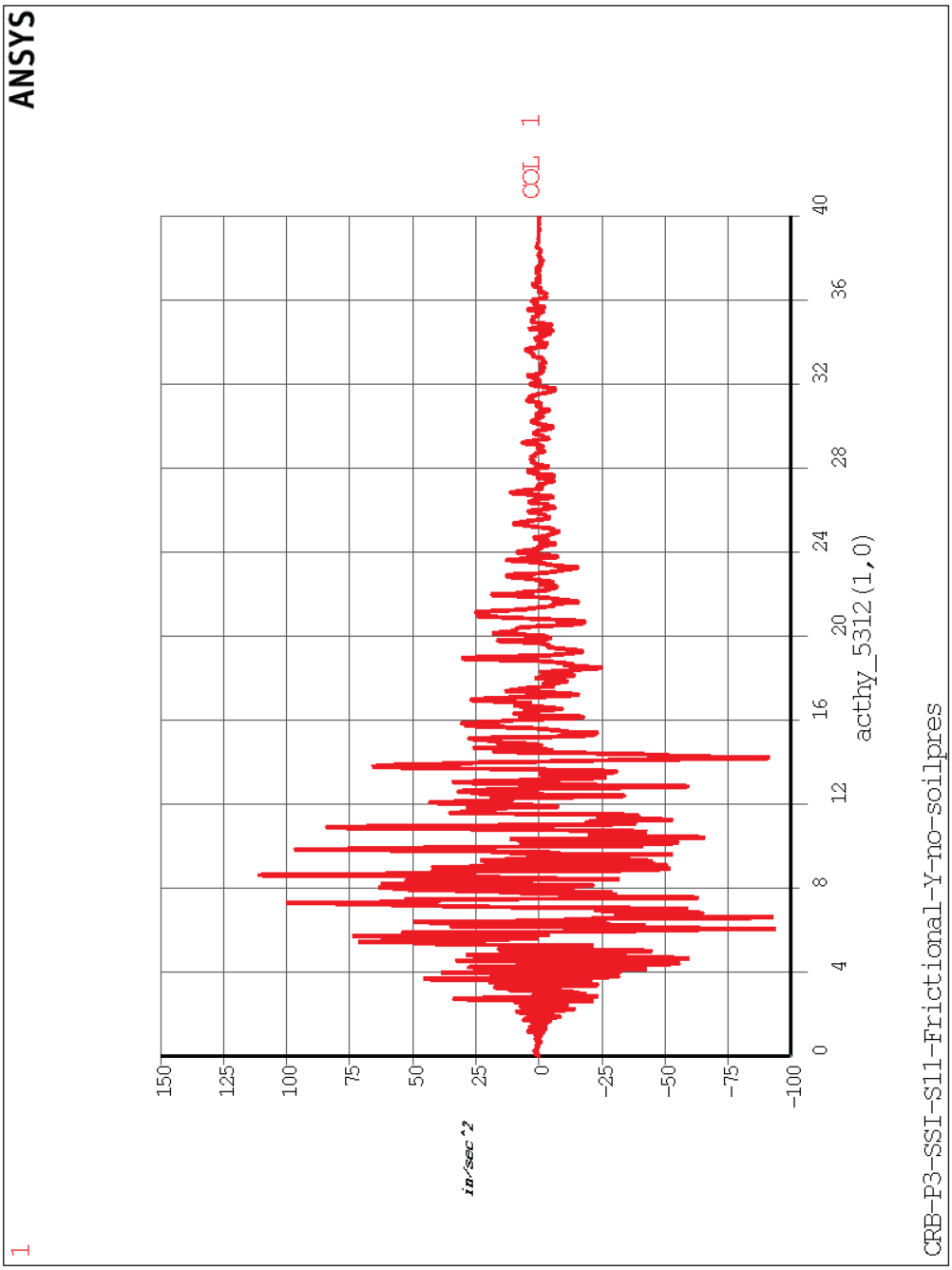

Figure 3.8.5-30: Soil Type 11, Capitola Input - Acceleration Time History - N-S

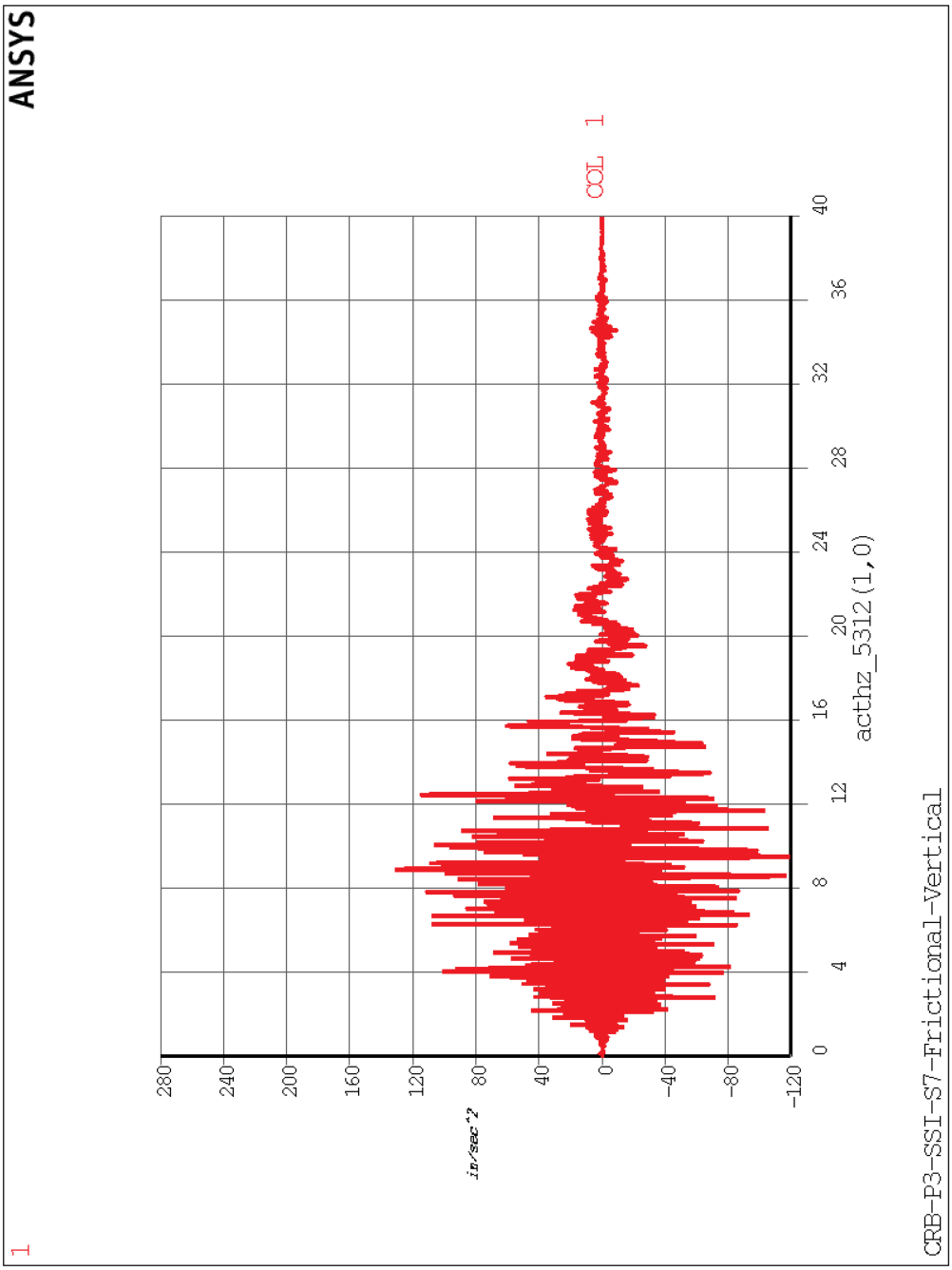

Figure 3.8.5-31: Soil Type 7, Capitola Input - Acceleration Time History - Vertical

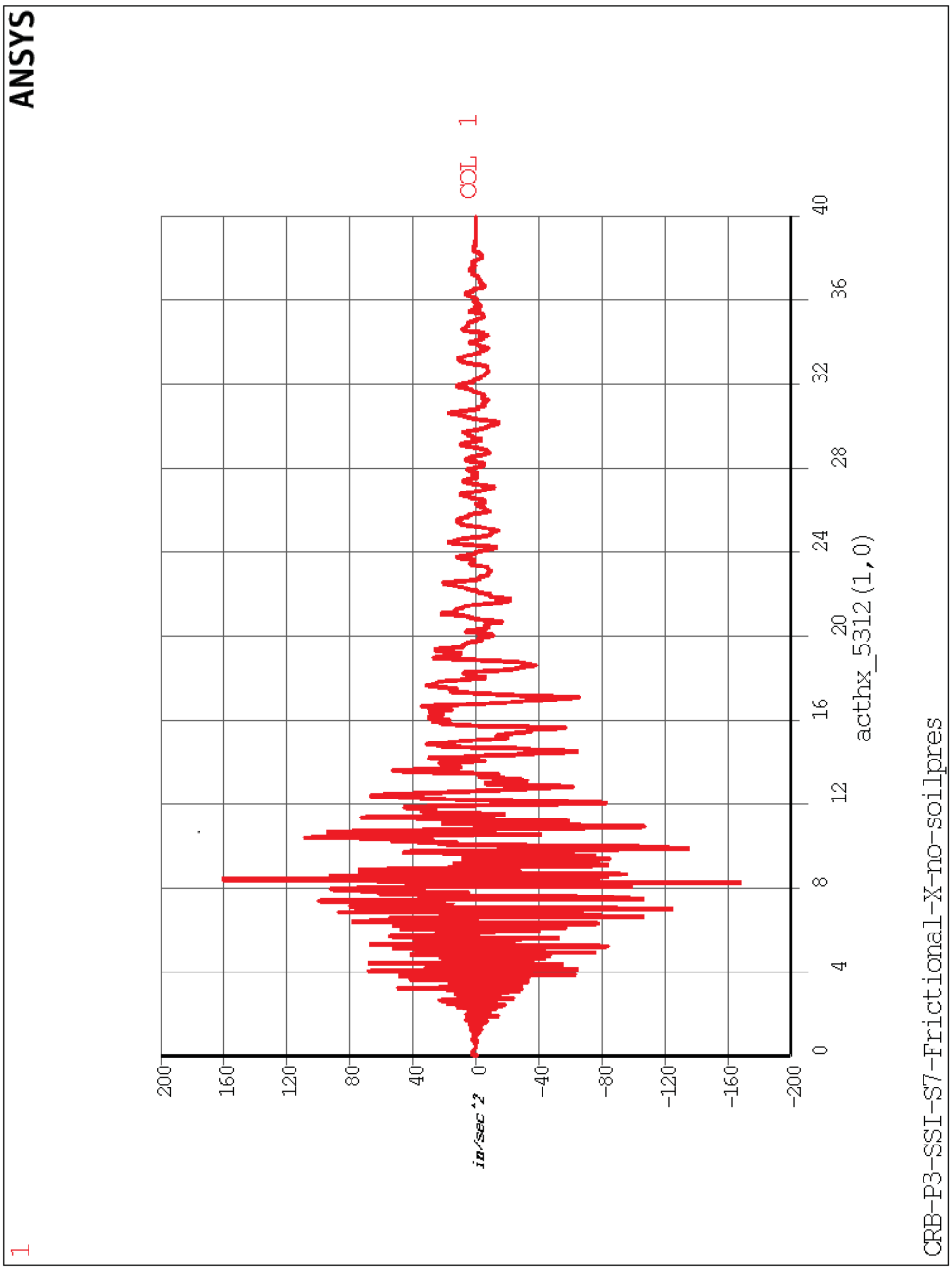

Figure 3.8.5-32: Soil Type 7, Capitola Input - Acceleration Time History - E-W

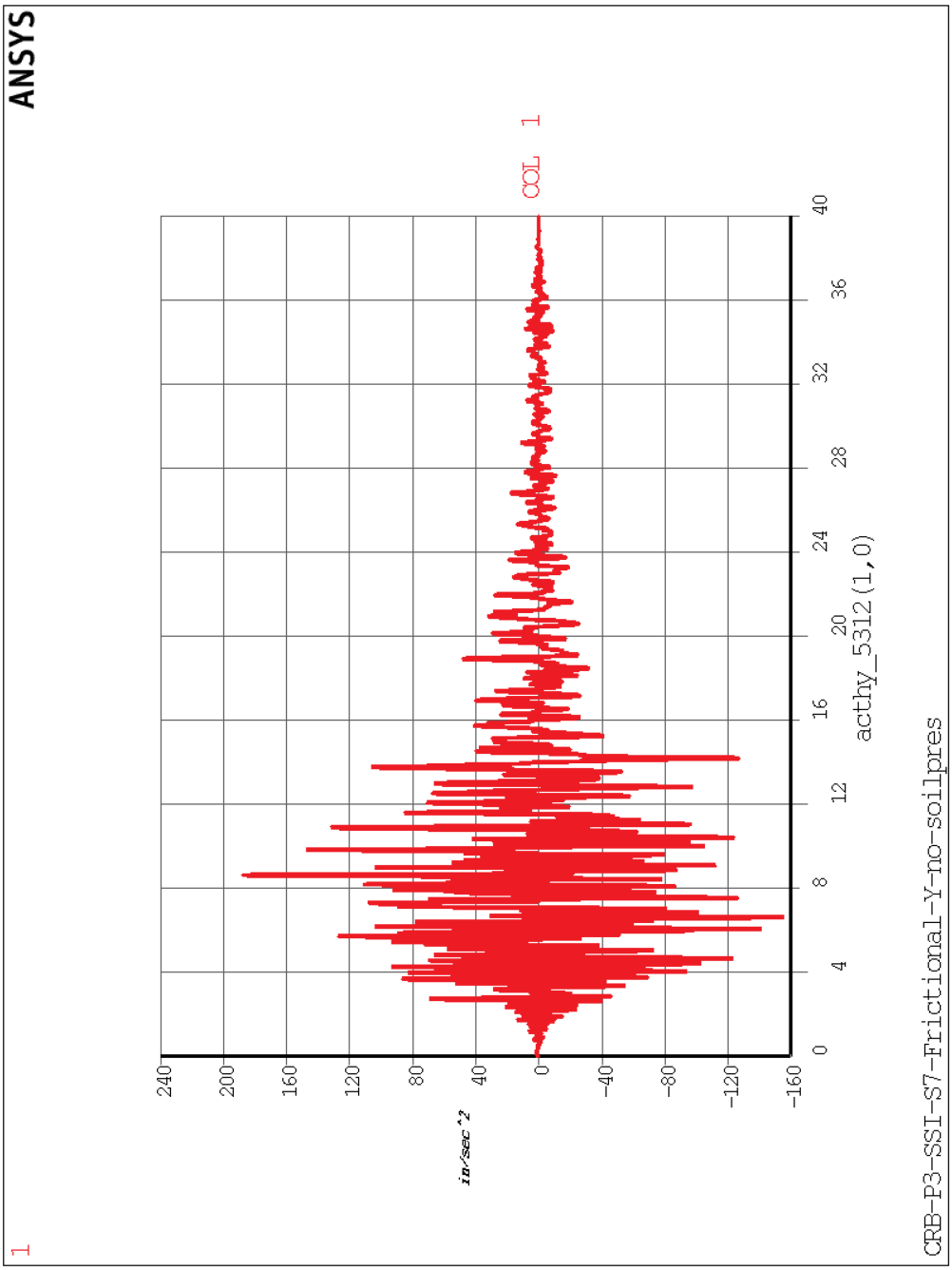

Figure 3.8.5-33: Soil Type 7, Capitola Input - Acceleration Time History - N-S

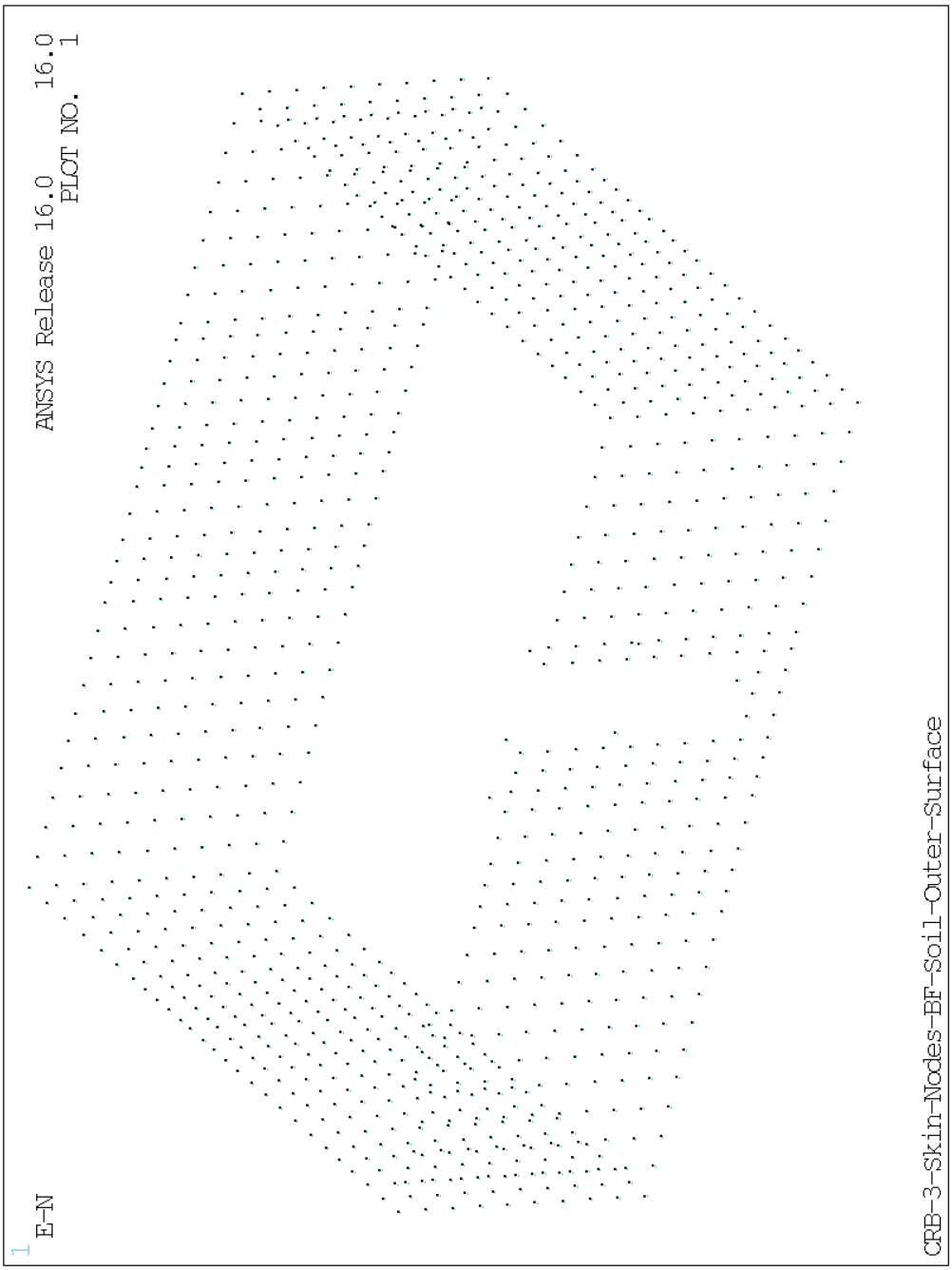

Figure 3.8.5-34: CRB Skin Nodes on Backfill Outer Boundaries for Applying SASSI Time Histories

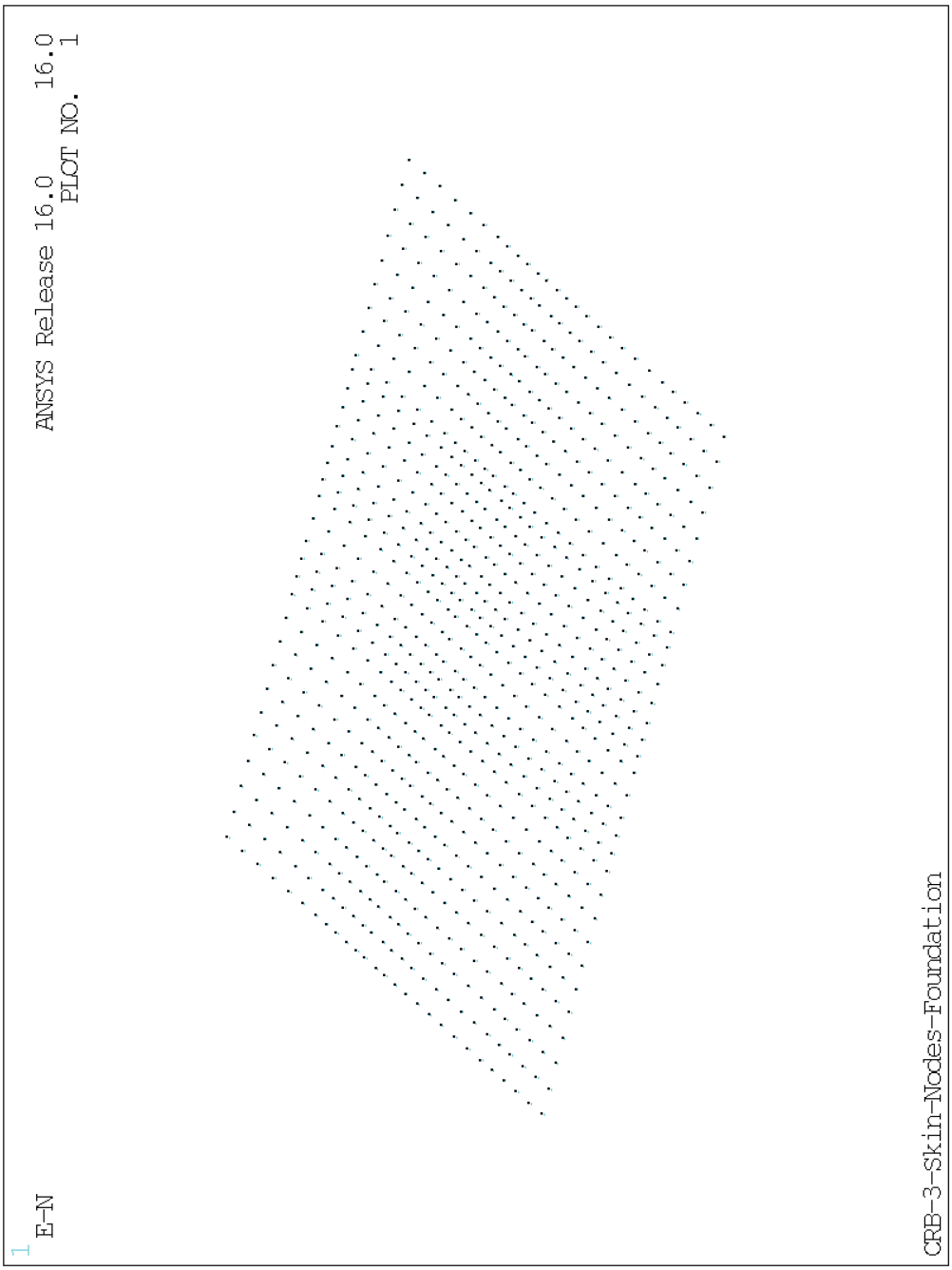

Figure 3.8.5-35: CRB Foundation Bottom Skin Nodes for Applying SASSI Time Histories

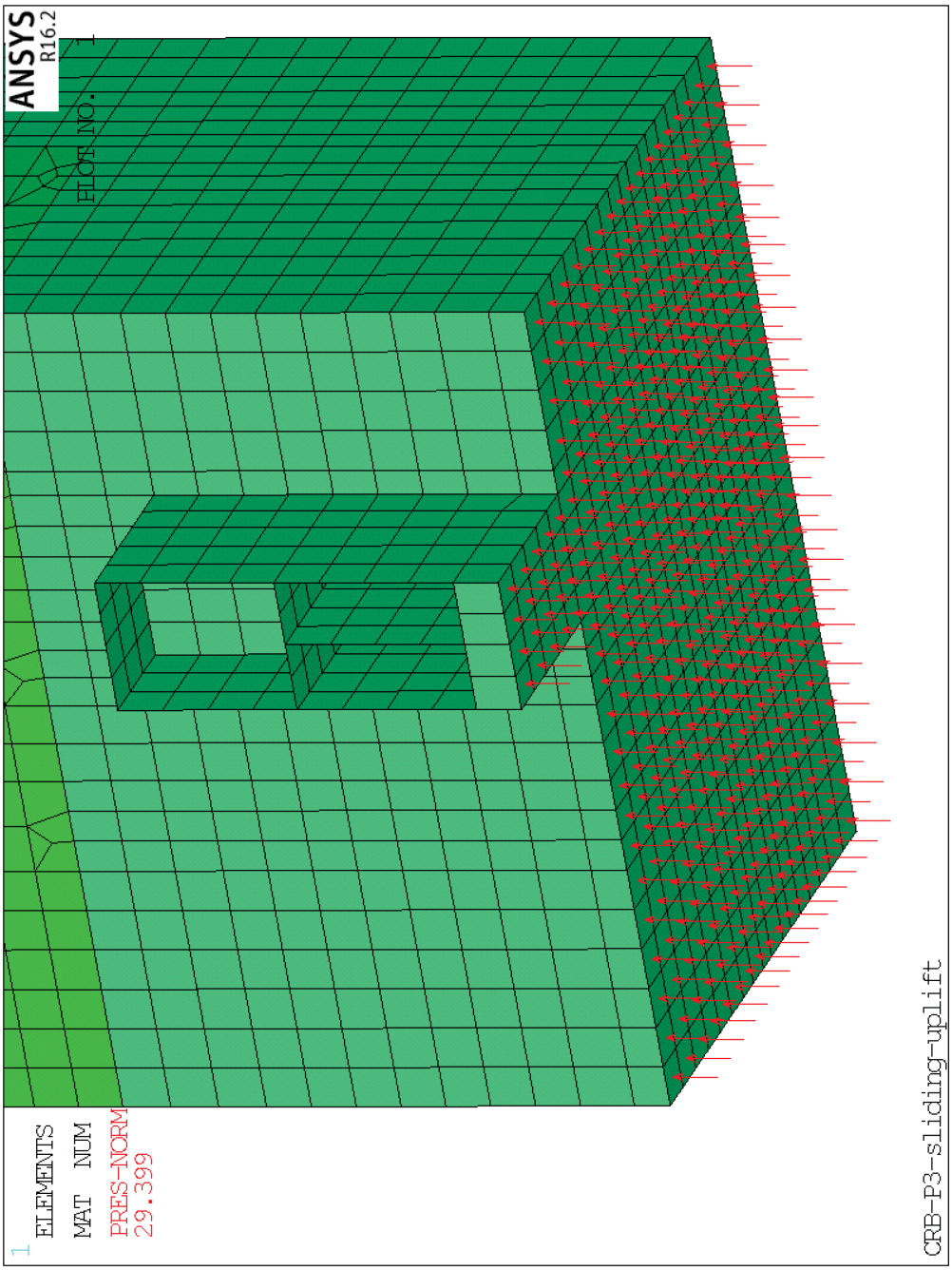

Figure 3.8.5-36: Buoyancy Load on Basemat

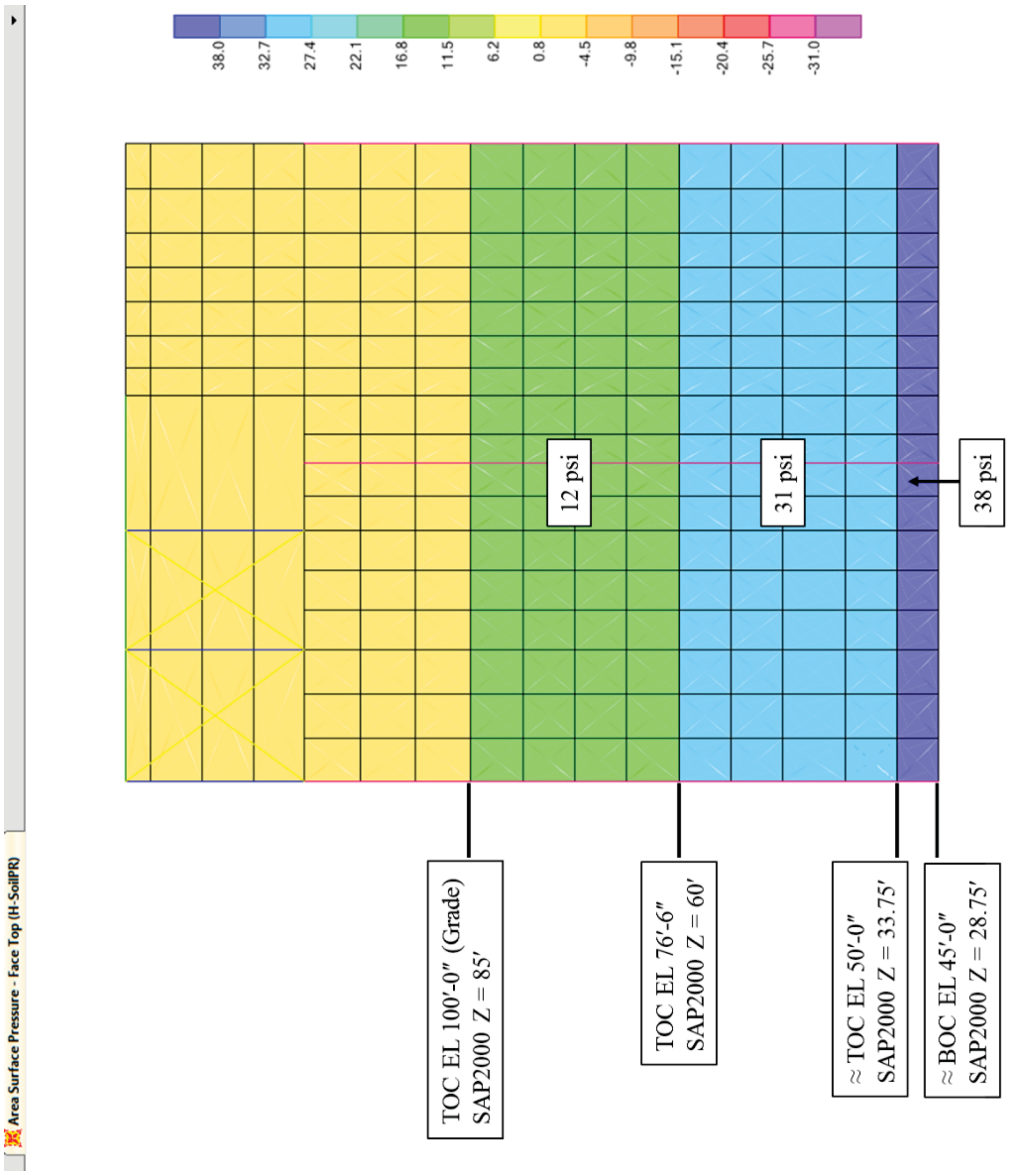

Figure 3.8.5-37: Static Soil Pressure on CRB Outer Walls

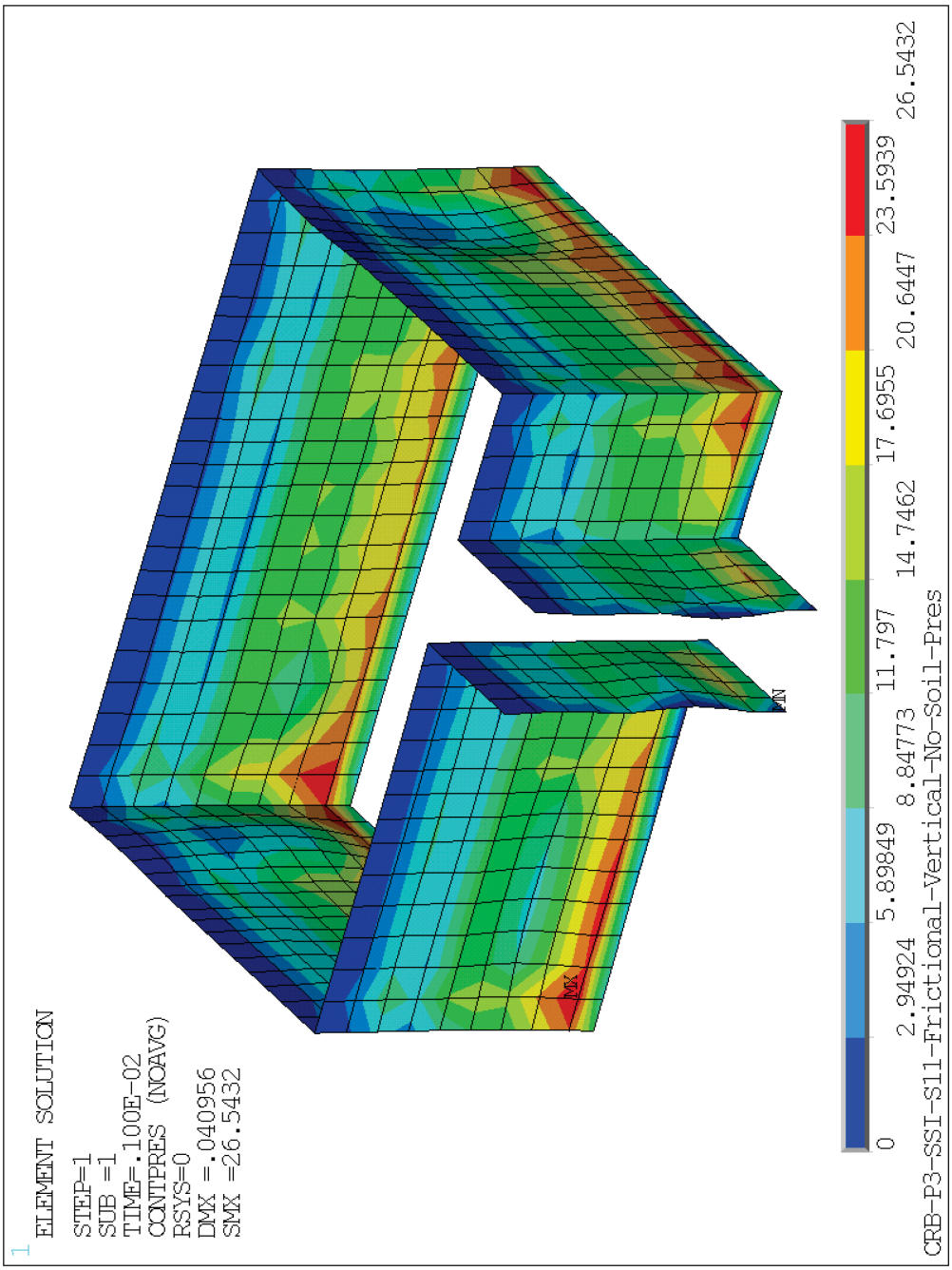

Figure 3.8.5-38: CRB Static Soil Pressure from Poisson's Ratio Effect - Soil Type 11

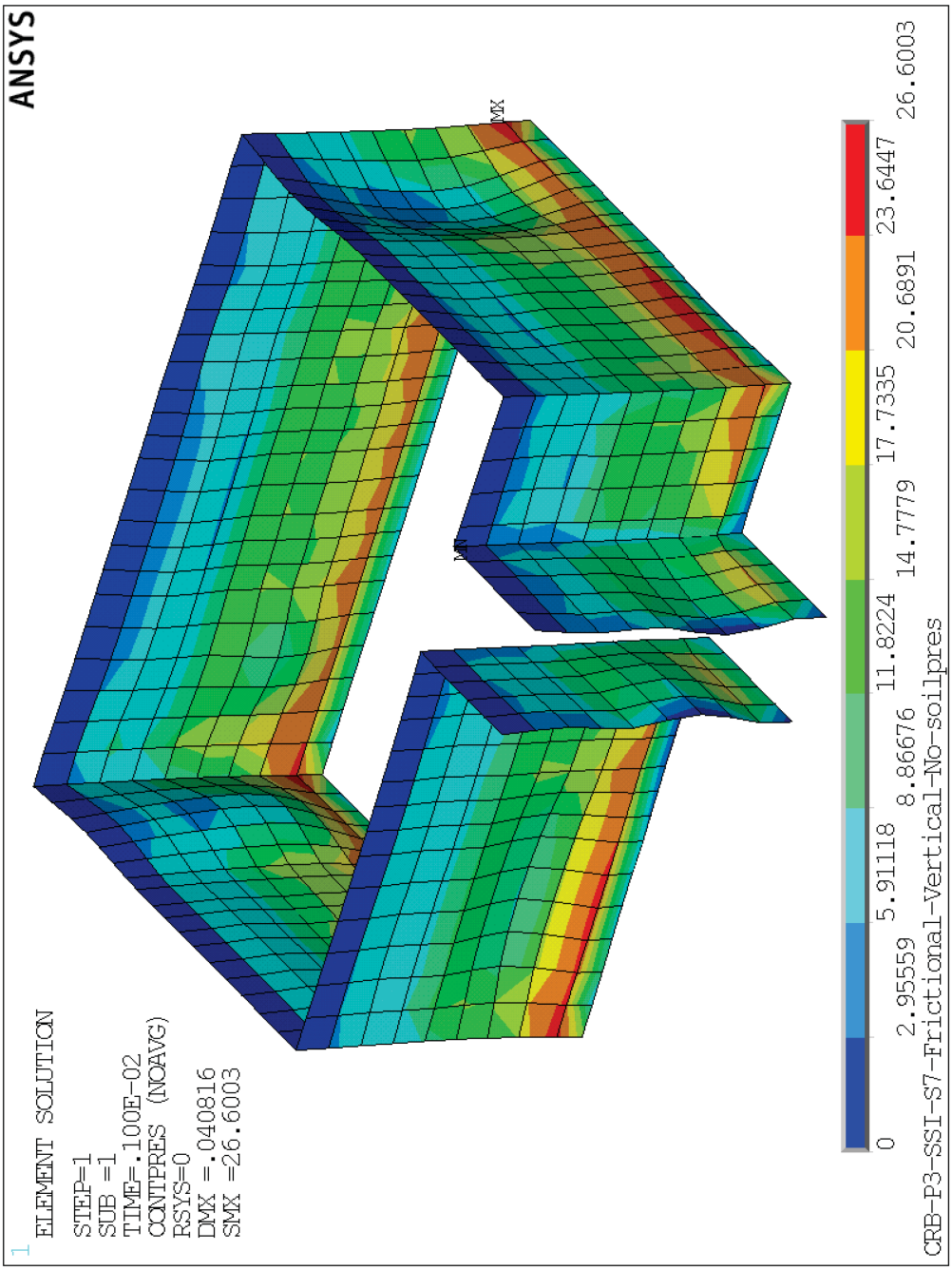

Figure 3.8.5-39: CRB Static Soil Pressure from Poisson's Ratio Effect - Soil Type 7

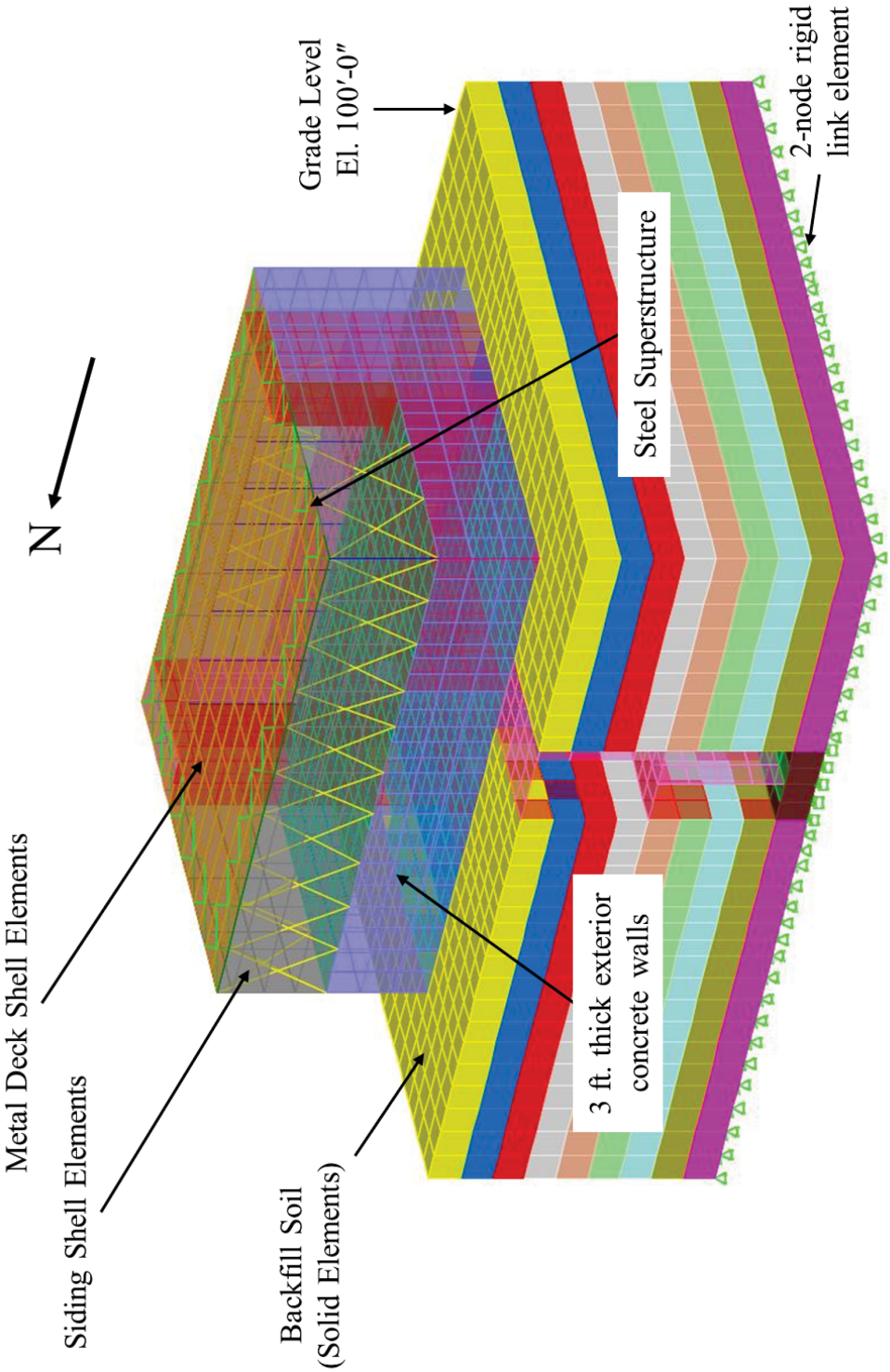

Figure 3.8.5-40: CRB SAP2000 Model with Backfill Soil

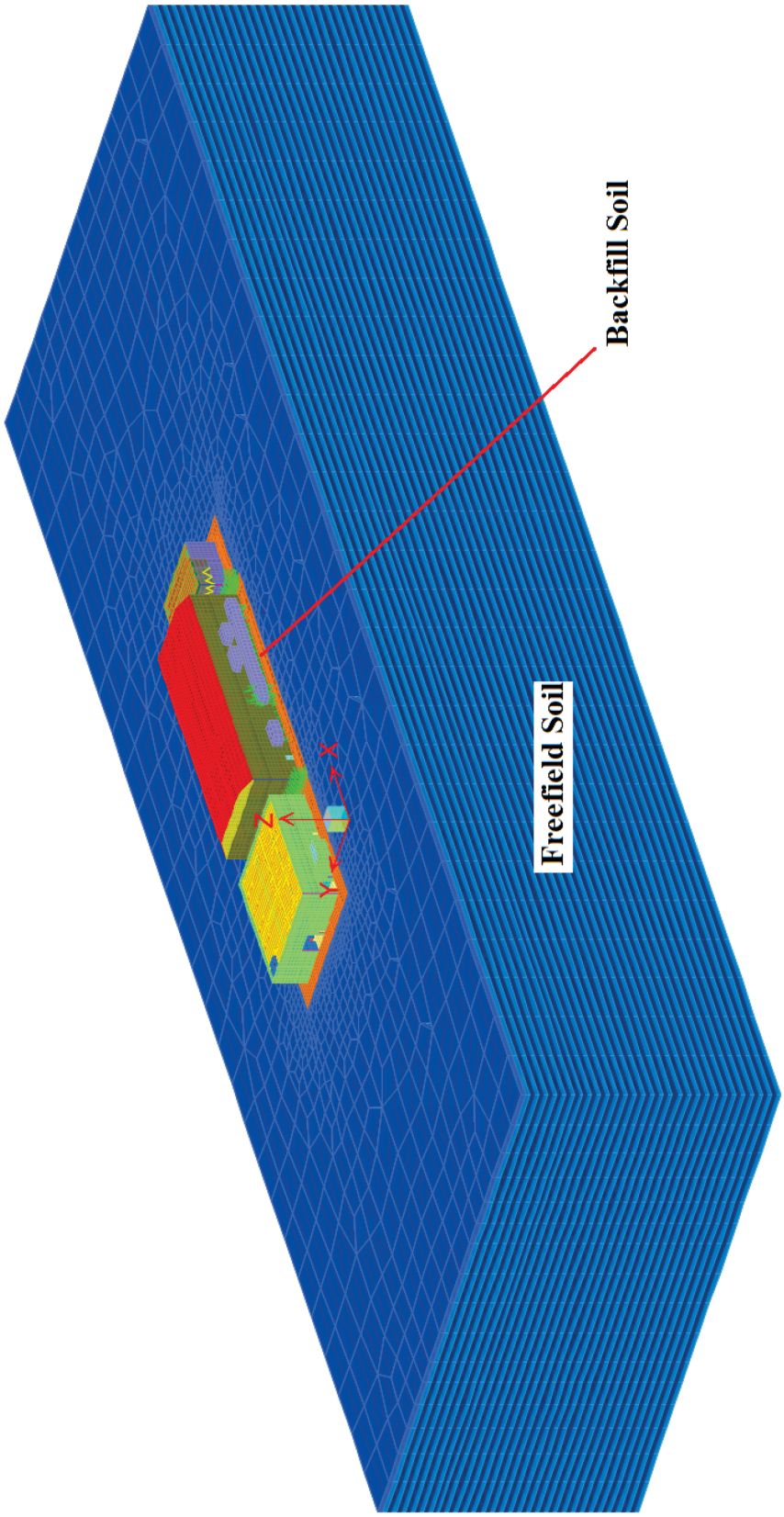

Figure 3.8.5-41: SAP2000 Model for Settlement

Figure 3.8.5-42: Total Cracked Base Vertical Reaction Time History due to Capitola for Soil Type 7

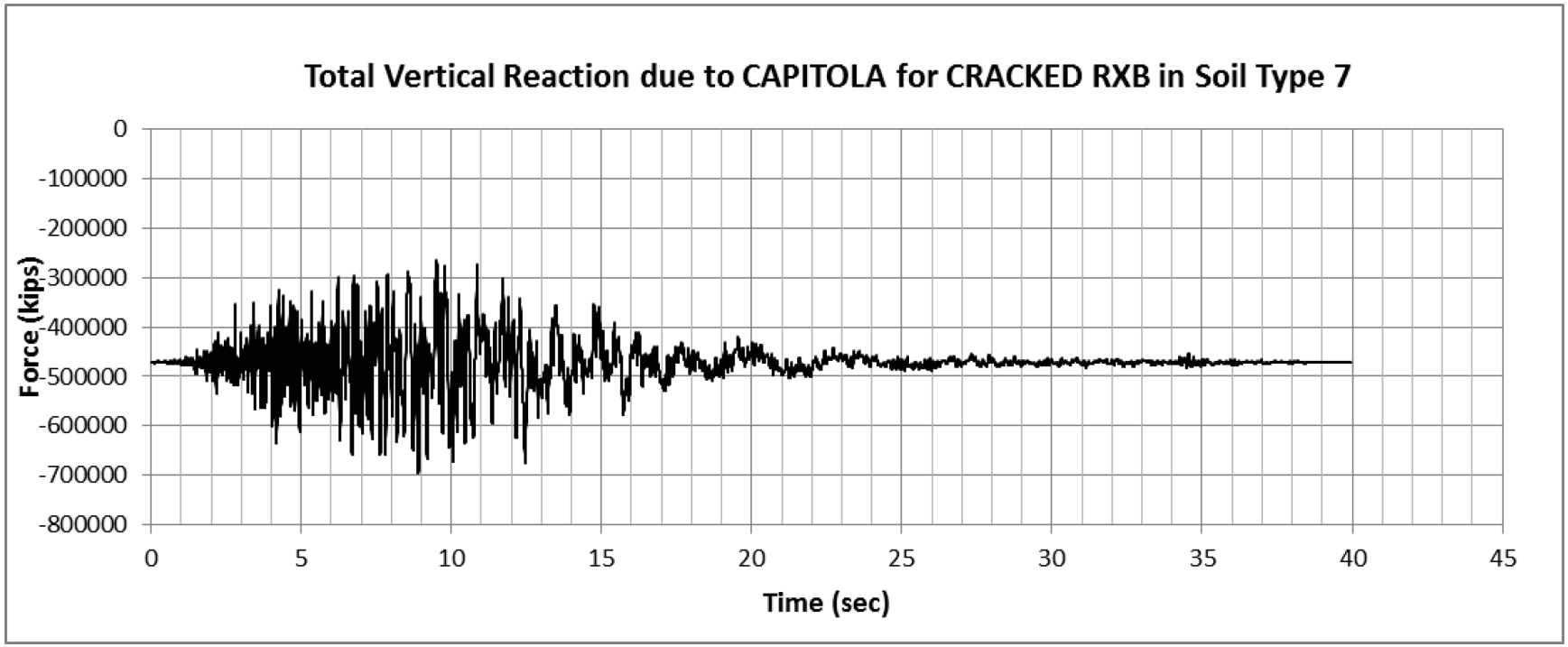

Figure 3.8.5-43: Total Uncracked Base Vertical Reaction Time History due to Capitola for Soil Type 7

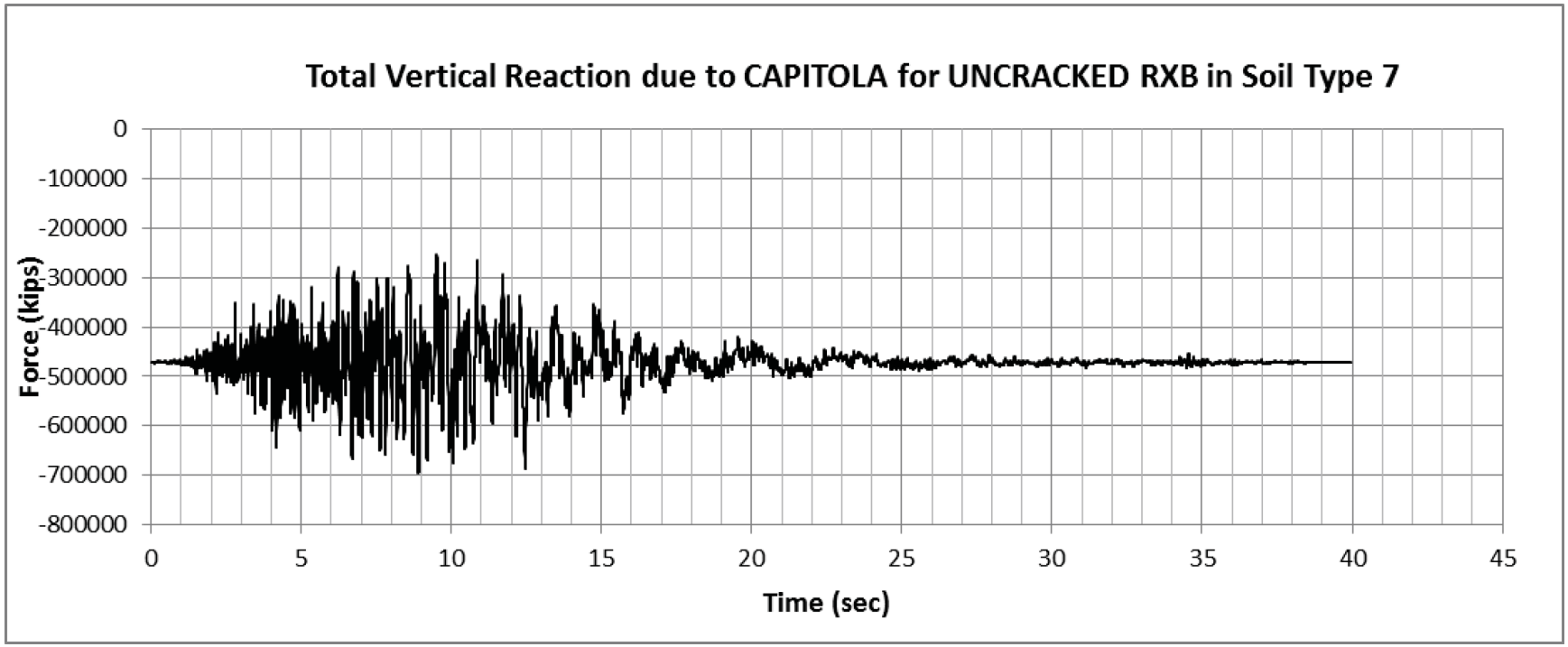

Figure 3.8.5-44: Total Cracked Base Vertical Reaction Time History due to Capitola for Soil Type 8

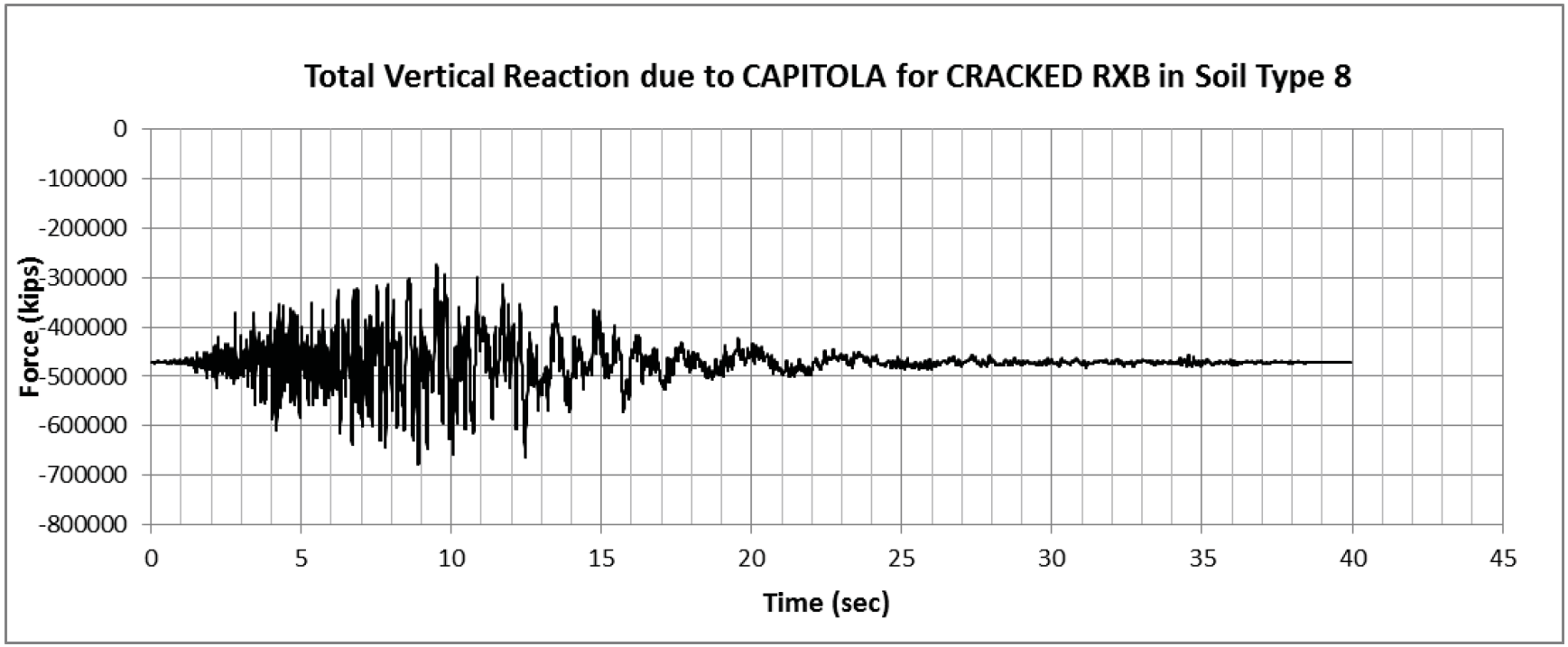

Figure 3.8.5-45: Total Cracked Base Vertical Reaction Time History due to Capitola for Soil Type 11

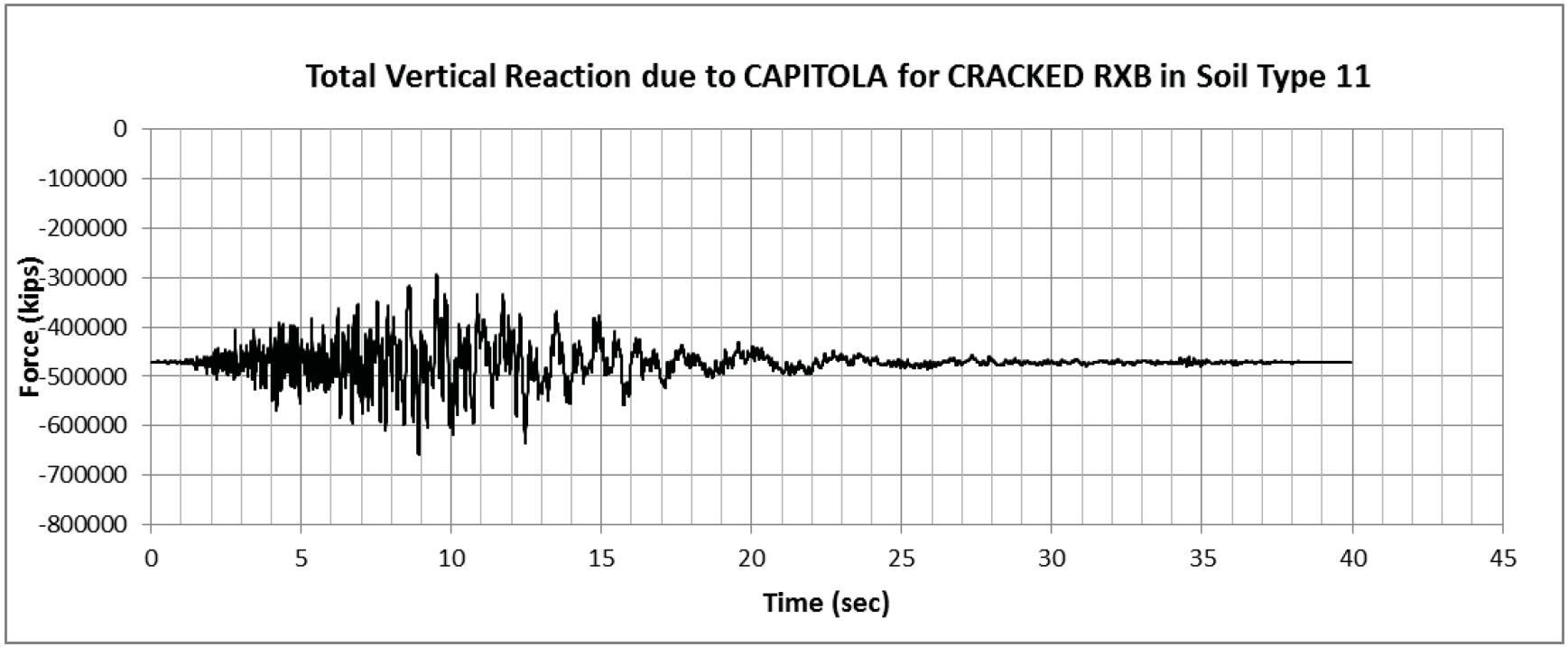

Figure 3.8.5-46: Total Cracked Base Vertical Reaction Time History due to Lucerne for Soil Type 7

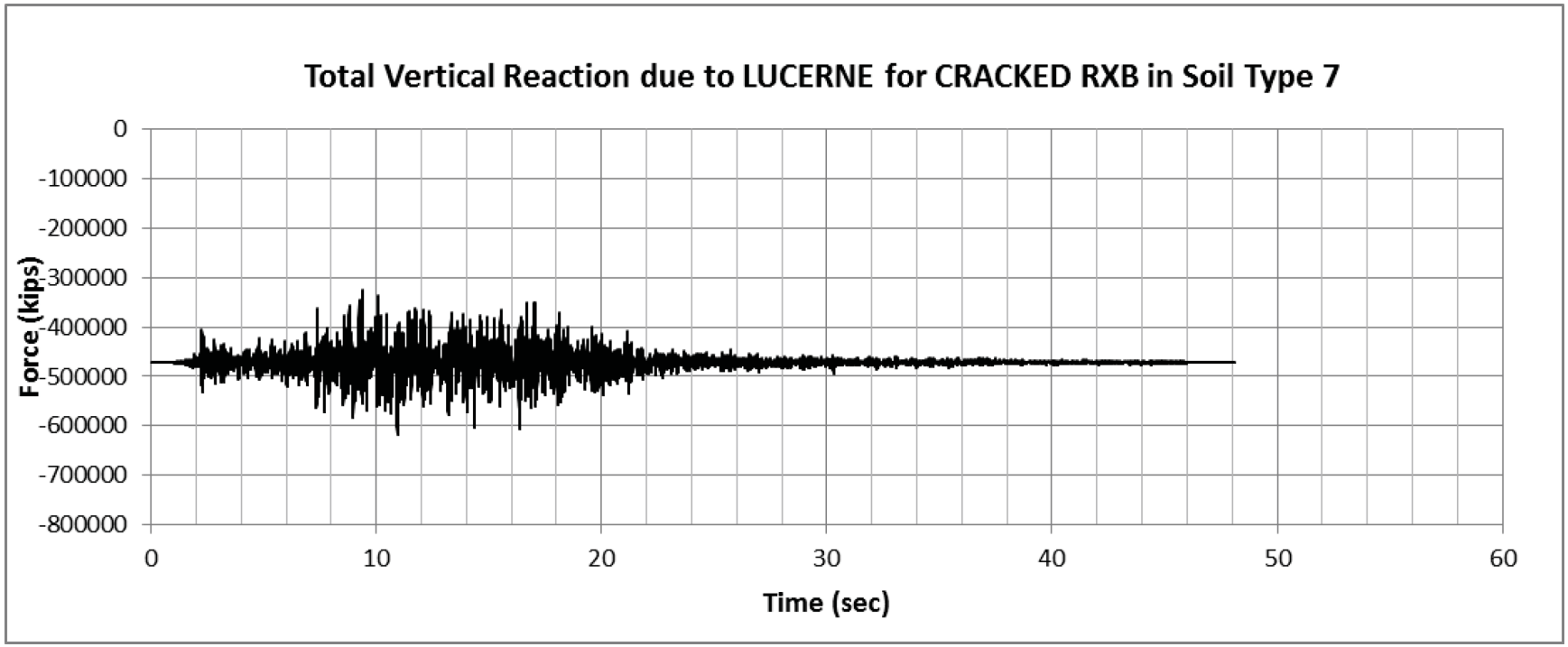

Figure 3.8.5-47: Total Cracked Base Vertical Reaction Time History due to Lucerne for Soil Type 9

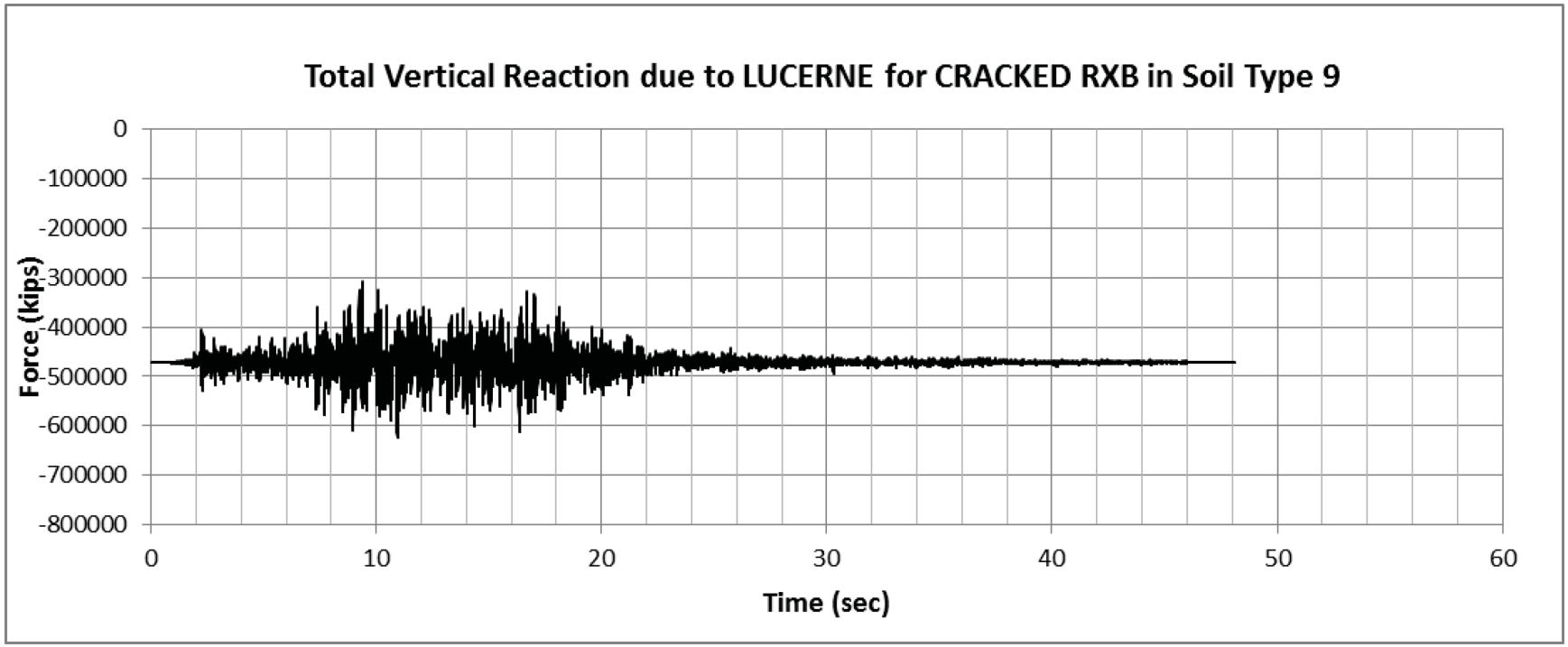

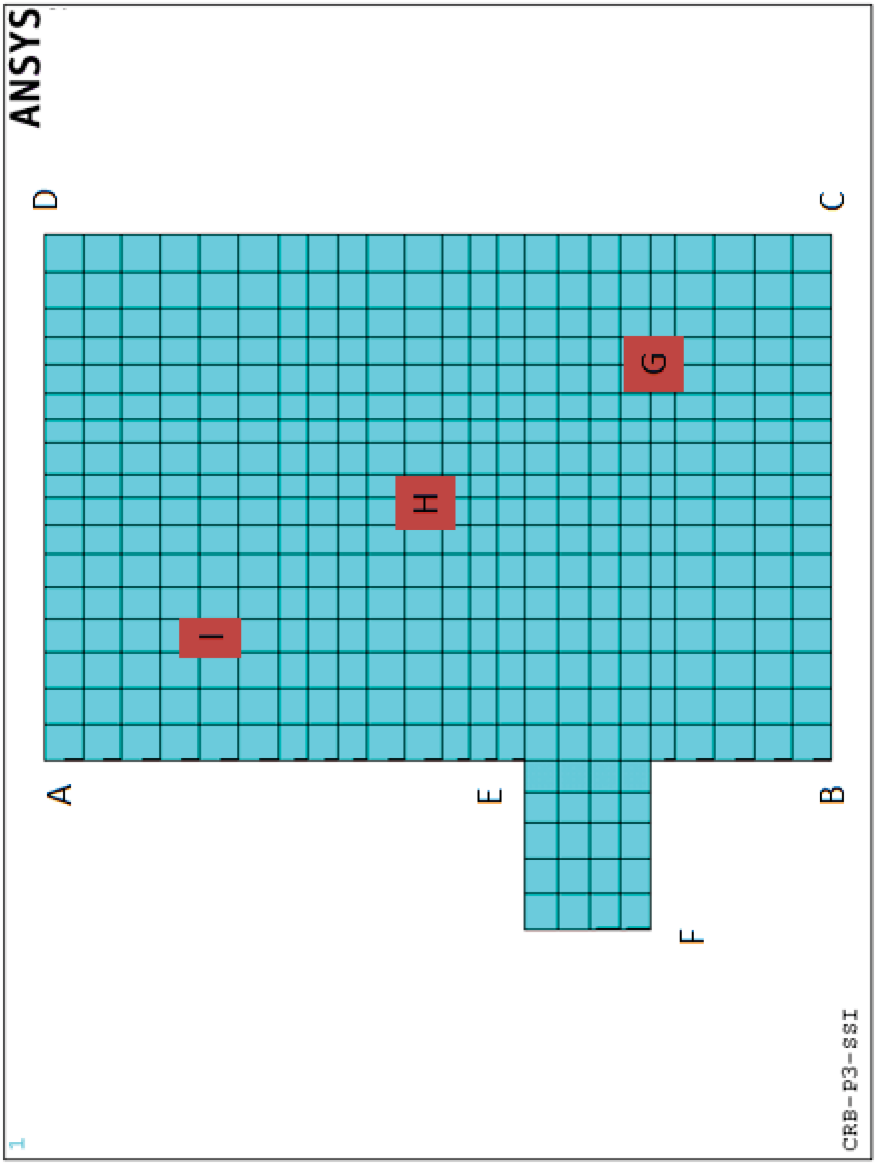

Figure 3.8.5-48: CRB Foundation Time History Location Designations

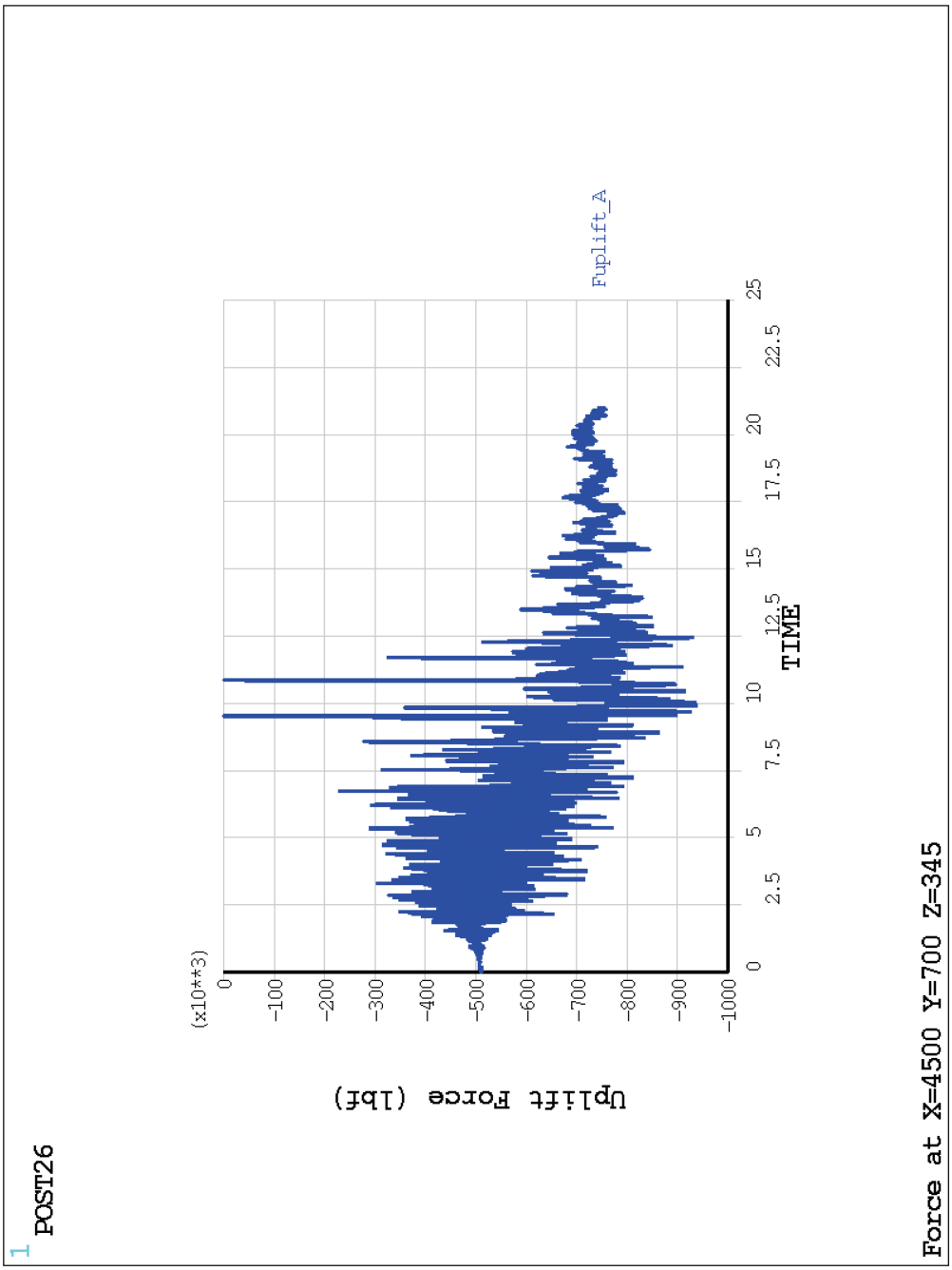

Figure 3.8.5-49: Reaction Force at Location A (S11 - Vertical Excitation)

Figure 3.8.5-50: Relative Displacement (Uplift) at Location A (S11 - Vertical Excitation)

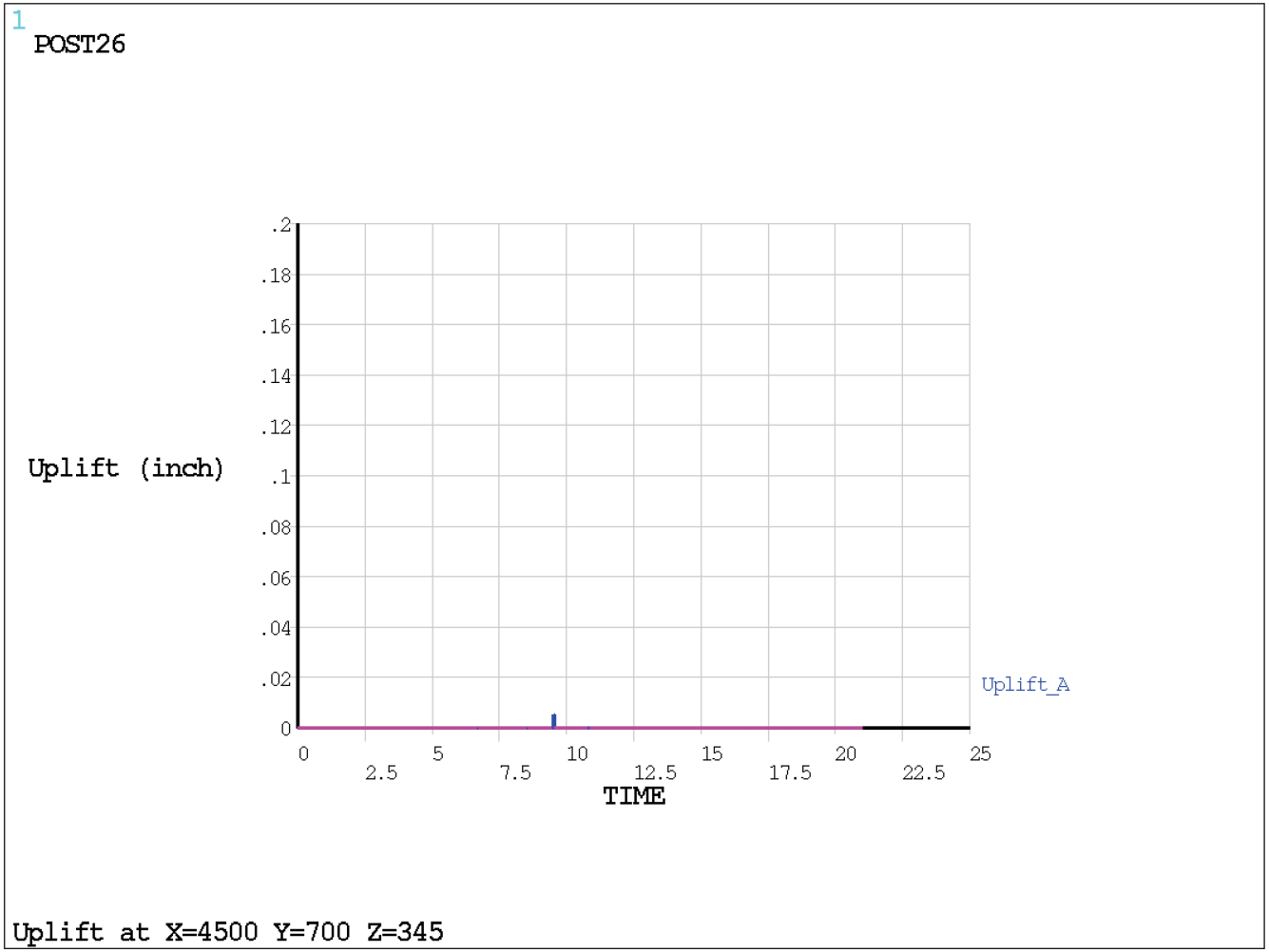

Figure 3.8.5-51: Lateral Relative Displacements (Sliding) at Location A (S11 - Vertical Excitation)

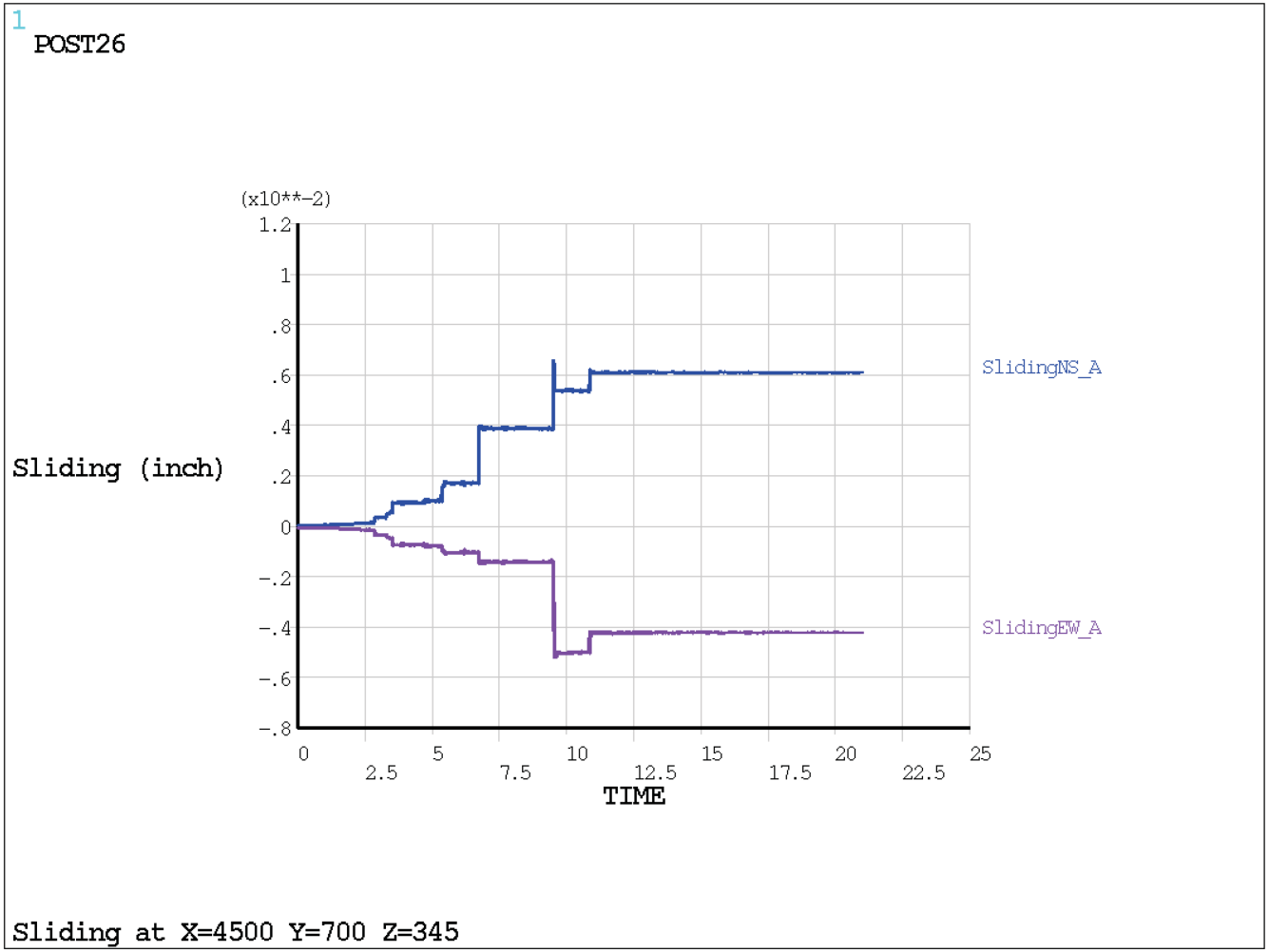

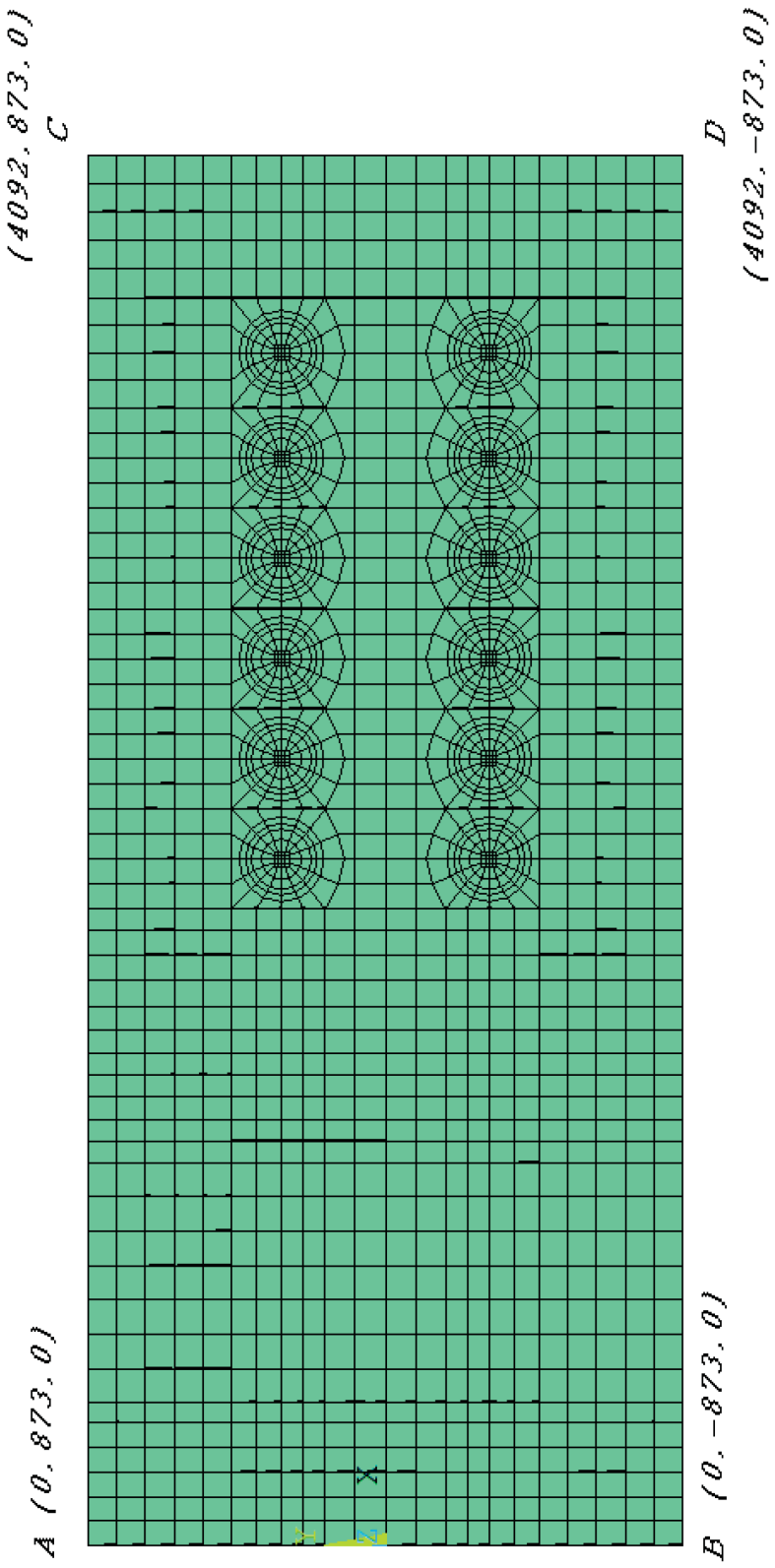

Figure 3.8.5-52: RXB Foundation Time History Location Designations

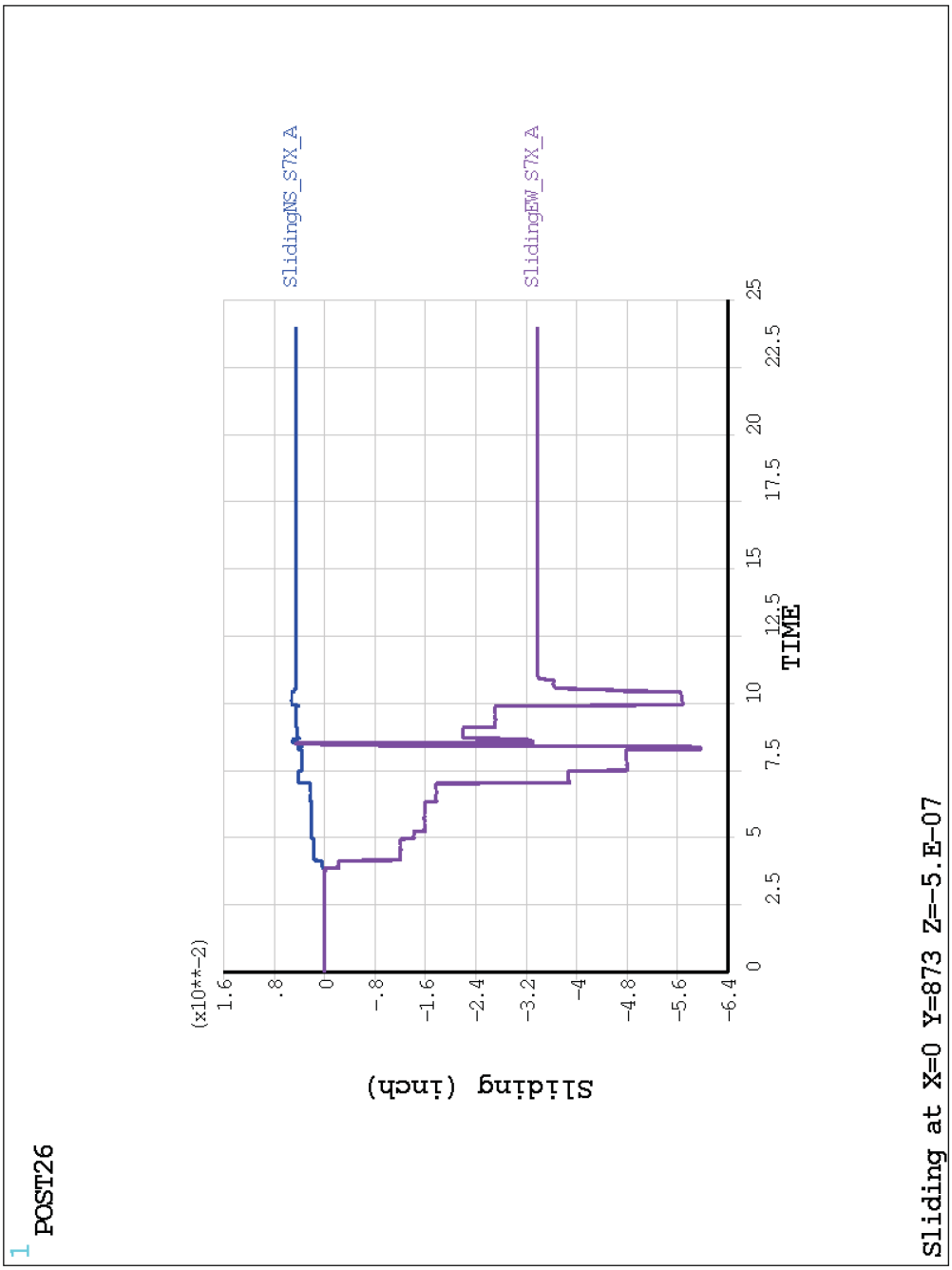

Figure 3.8.5-53: Lateral Relative Displacements (Sliding) at Location A (S7 - E-W Excitation)

Figure 3.8.5-54: Lateral Relative Displacements (Sliding) at Location B (S7 – E-W Excitation)

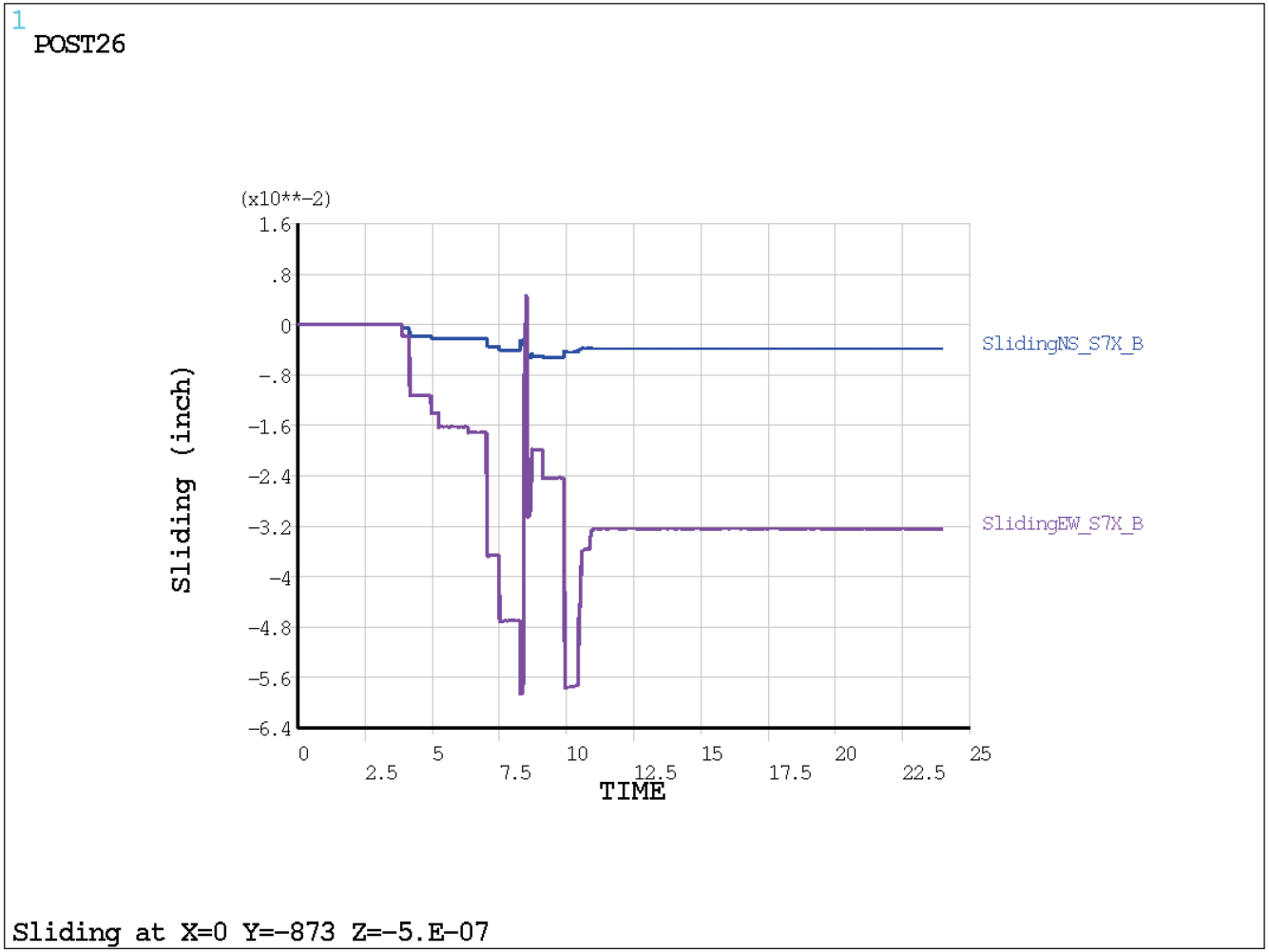

Figure 3.8.5-55: Lateral Relative Displacements (Sliding) at Location C (S7 - E-W Excitation)

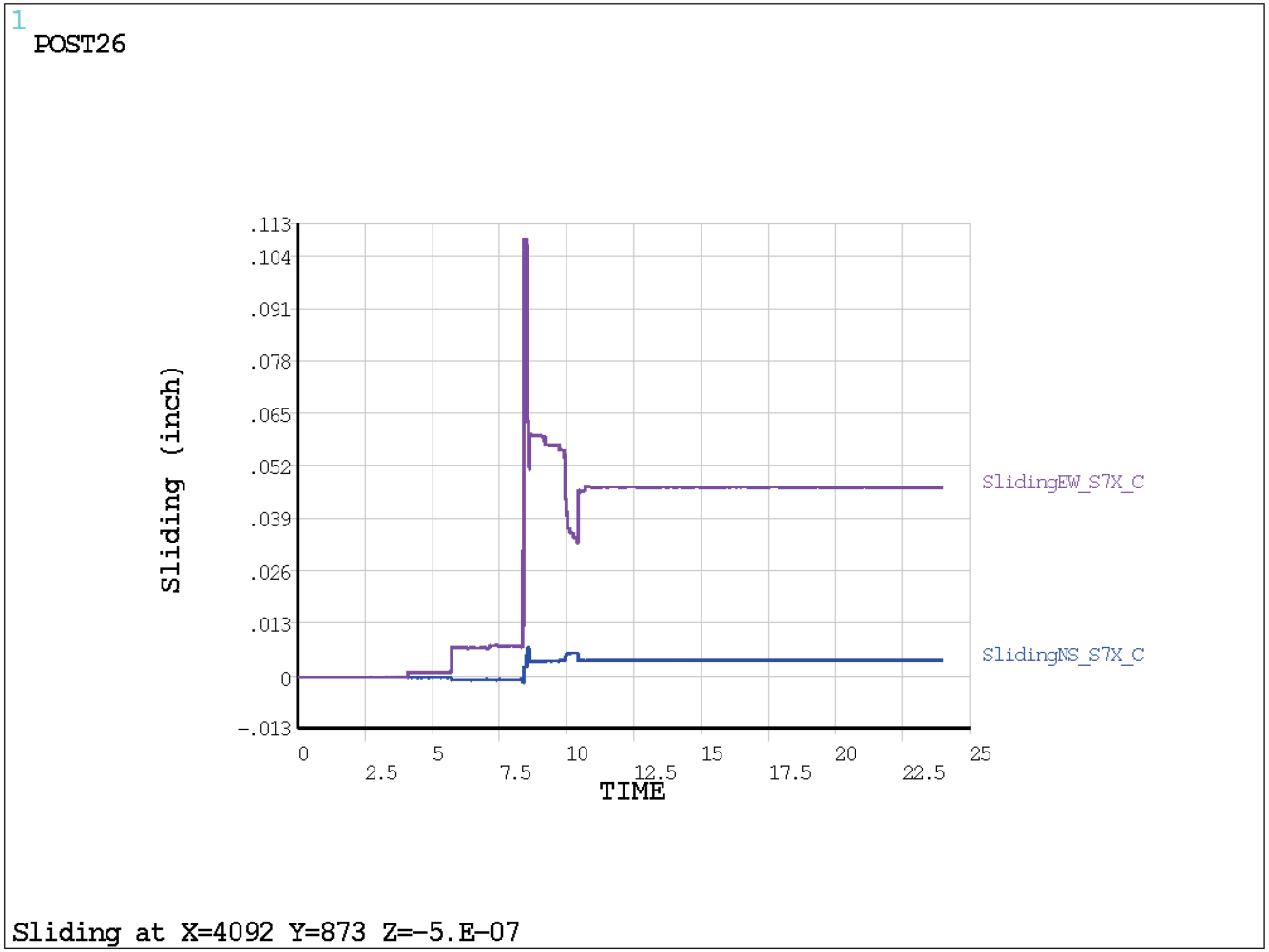

Figure 3.8.5-56: Lateral Relative Displacements (Sliding) at Location D (S7 - E-W Excitation)

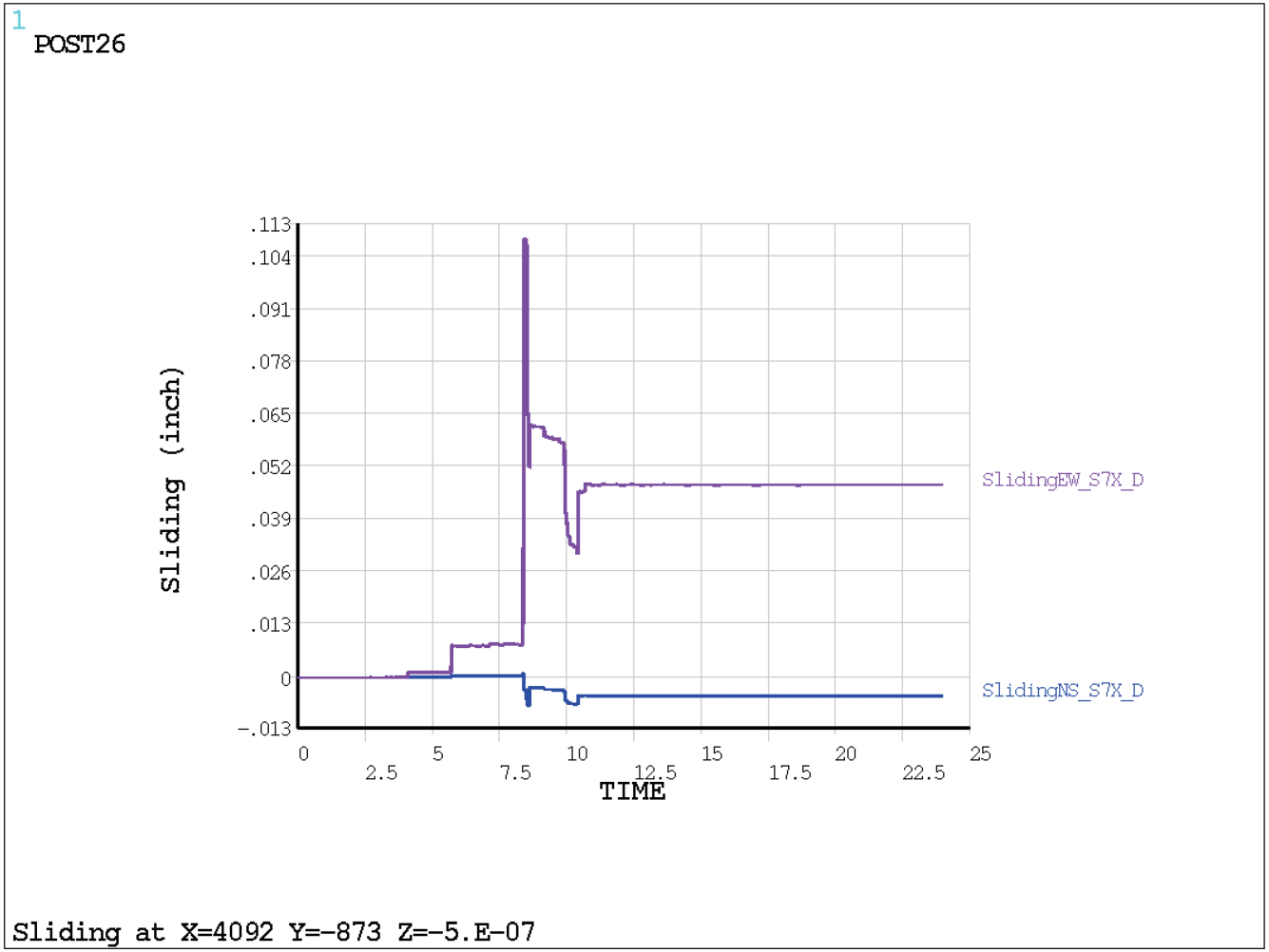

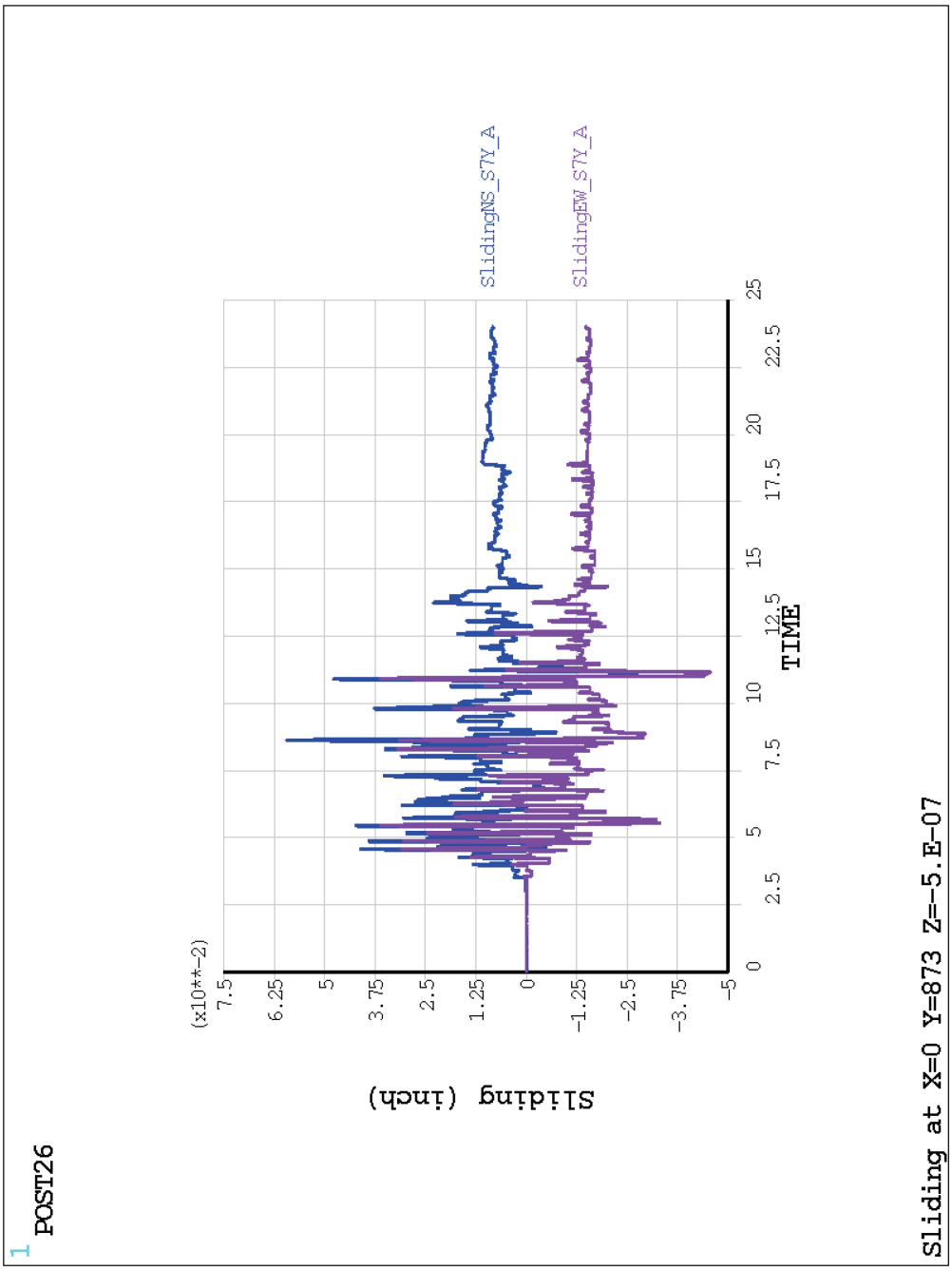

Figure 3.8.5-57: Lateral Relative Displacements (Sliding) at Location A (S7 - N-S Excitation)

Figure 3.8.5-58: Lateral Relative Displacements (Sliding) at Location B (S7 - N-S Excitation)

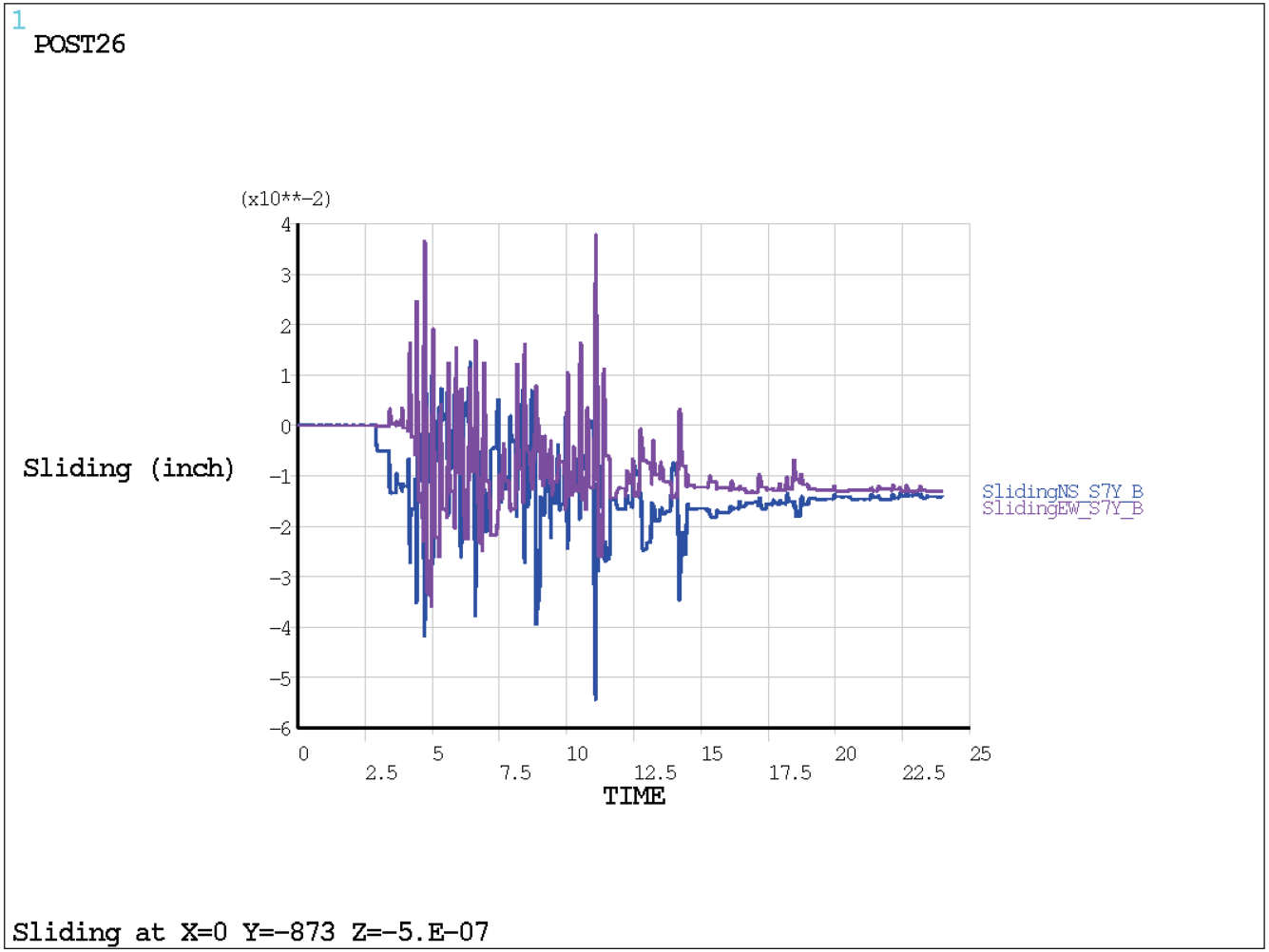

Figure 3.8.5-59: Lateral Relative Displacements (Sliding) at Location C (S7 - N-S Excitation)

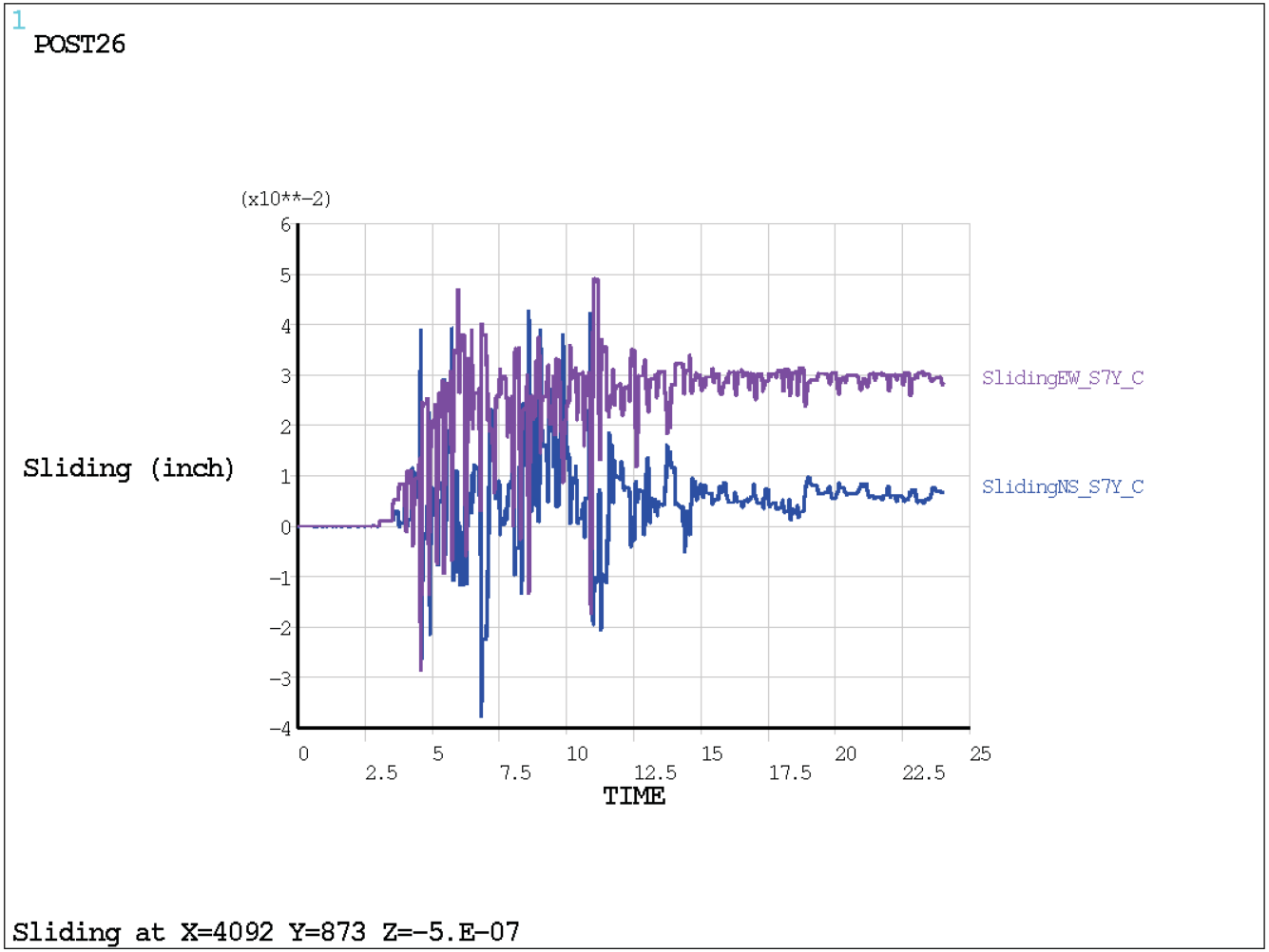

Figure 3.8.5-60: Lateral Relative Displacements (Sliding) at Location D (S7 - N-S Excitation)

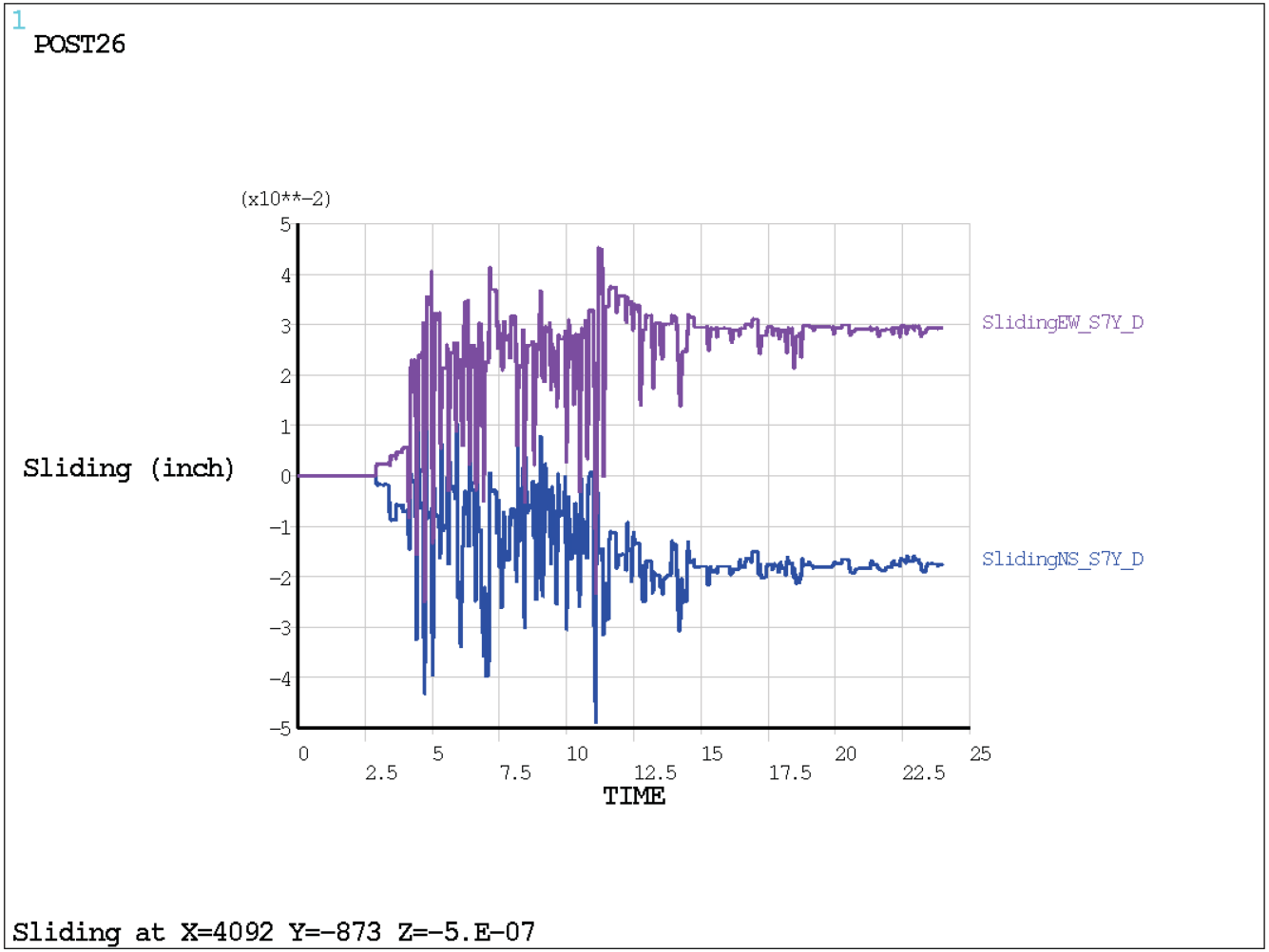

Figure 3.8.5-61: Lateral Relative Displacements (Sliding) at Location A (S11 - E-W Excitation)

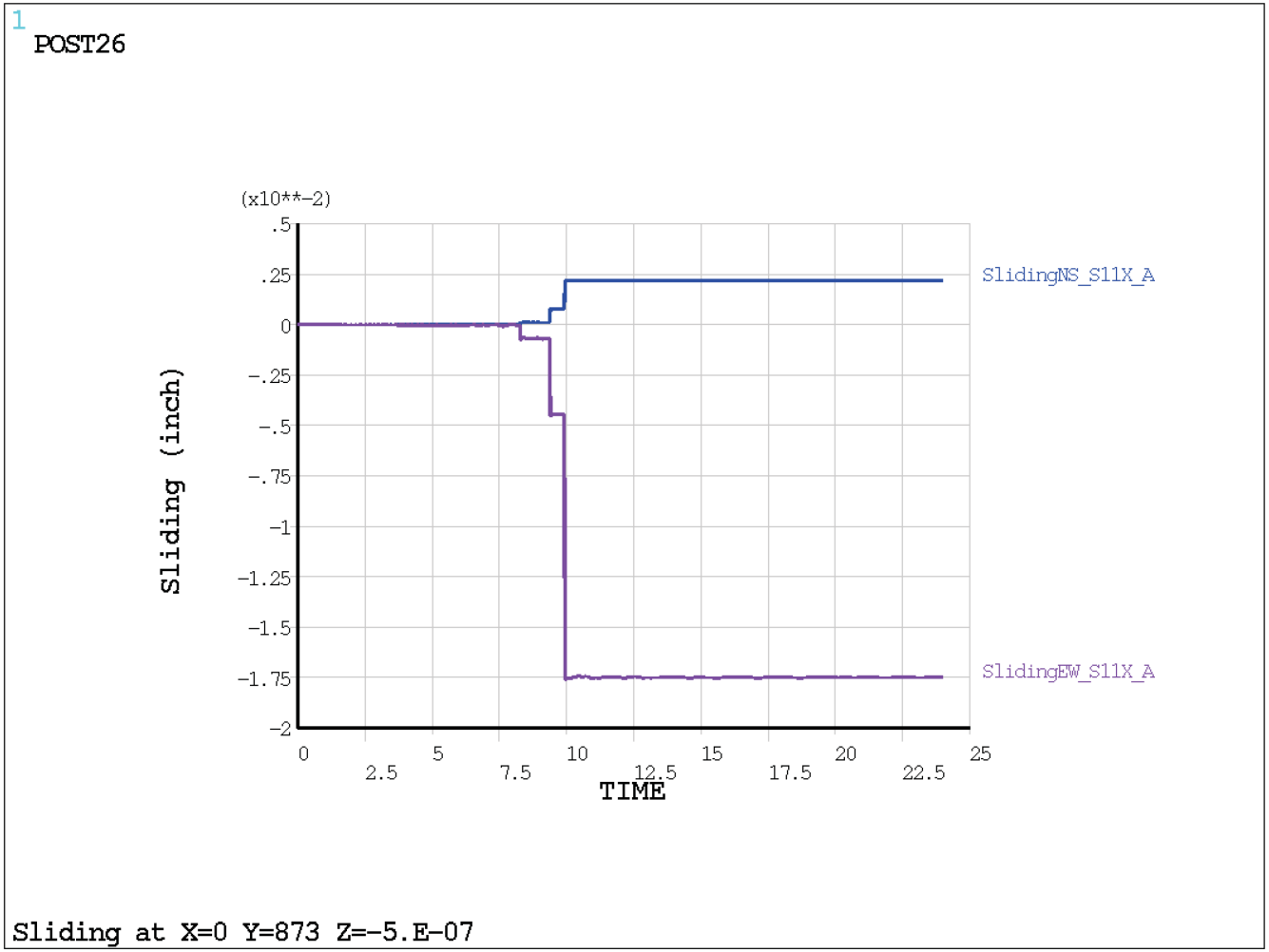

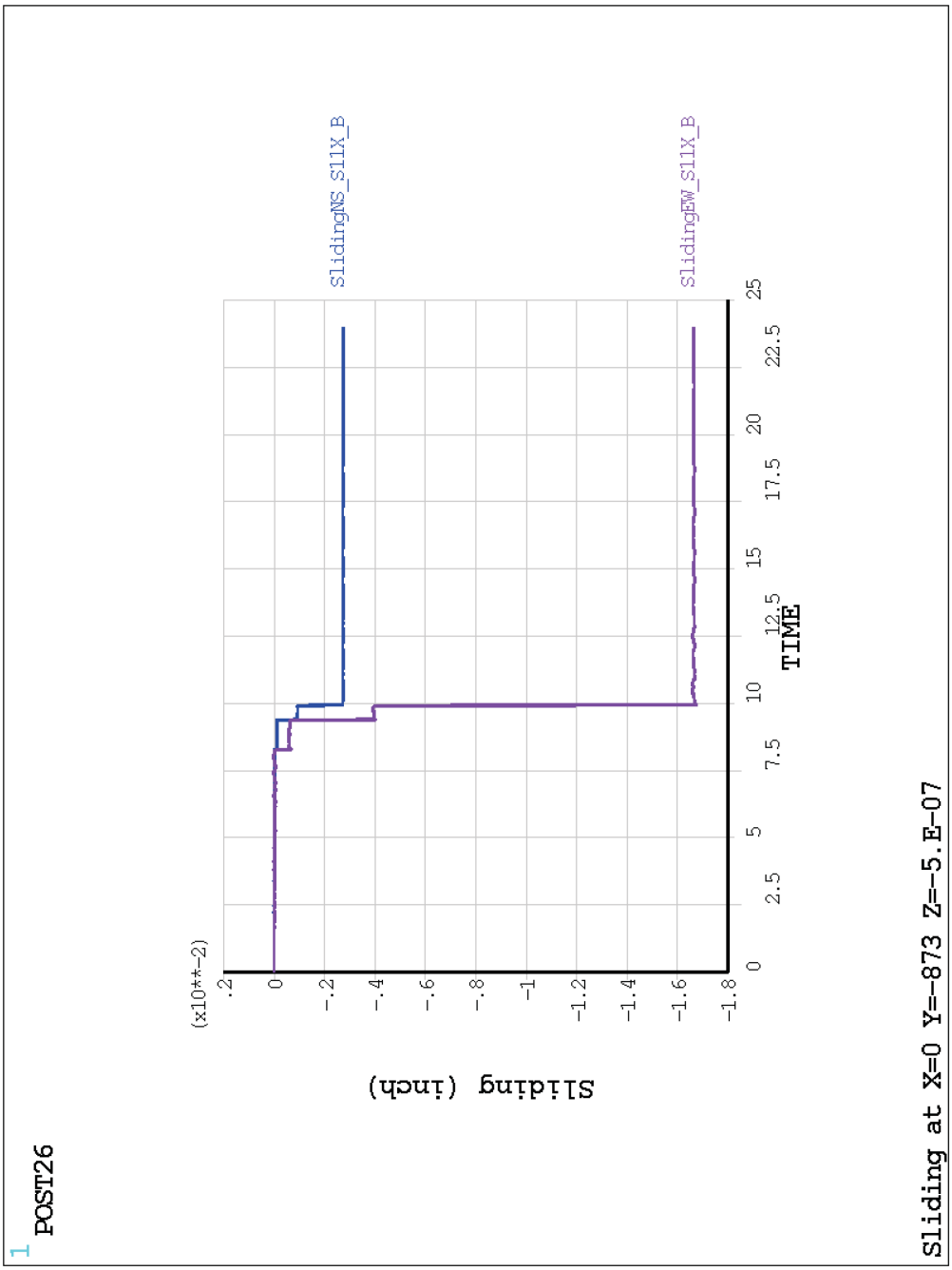

Figure 3.8.5-62: Lateral Relative Displacements (Sliding) at Location B (S11 - E-W Excitation)

Figure 3.8.5-63: Lateral Relative Displacements (Sliding) at Location C (S11 - E-W Excitation)

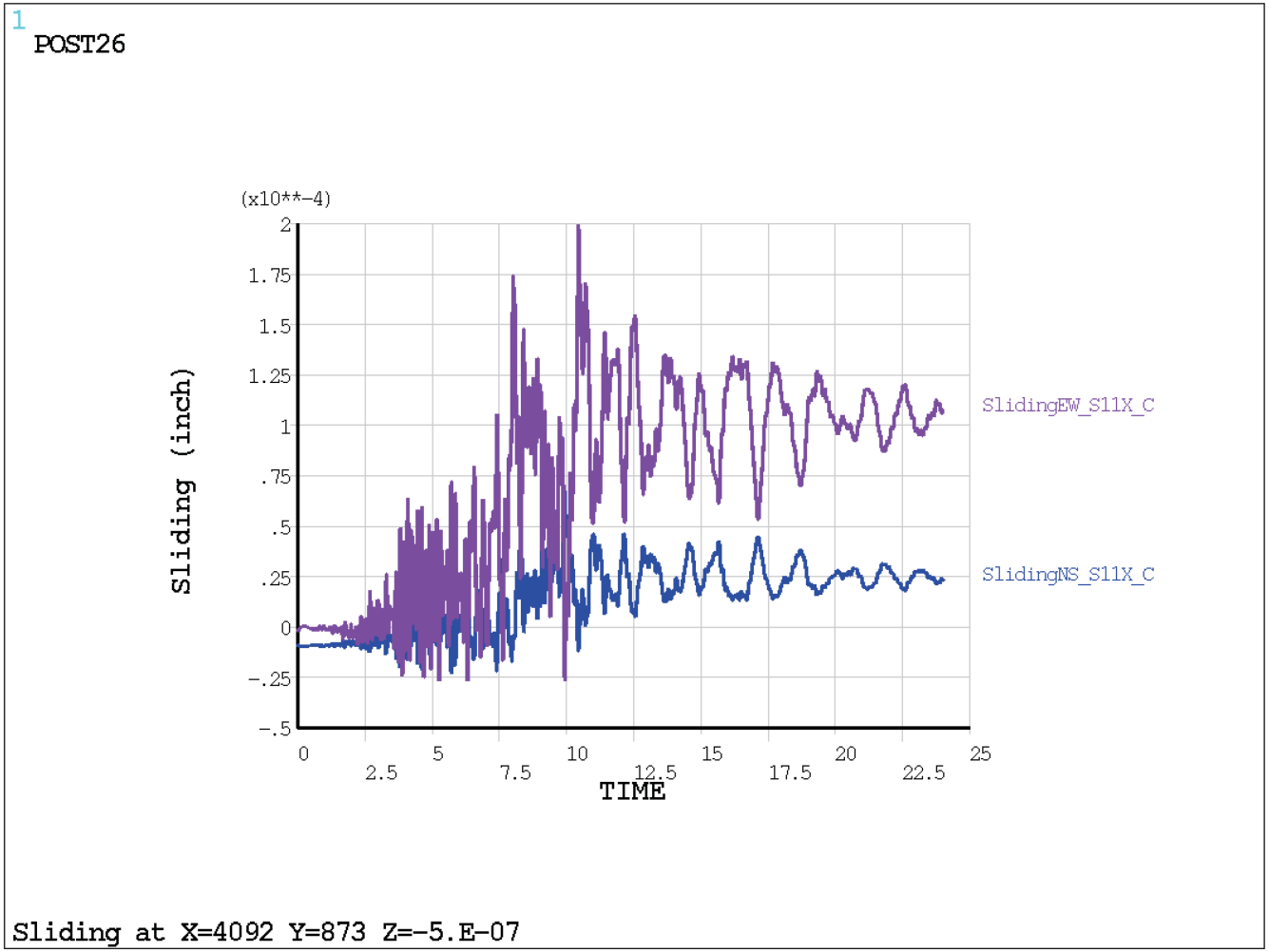

Figure 3.8.5-64: Lateral Relative Displacements (Sliding) at Location D (S11 - E-W Excitation)

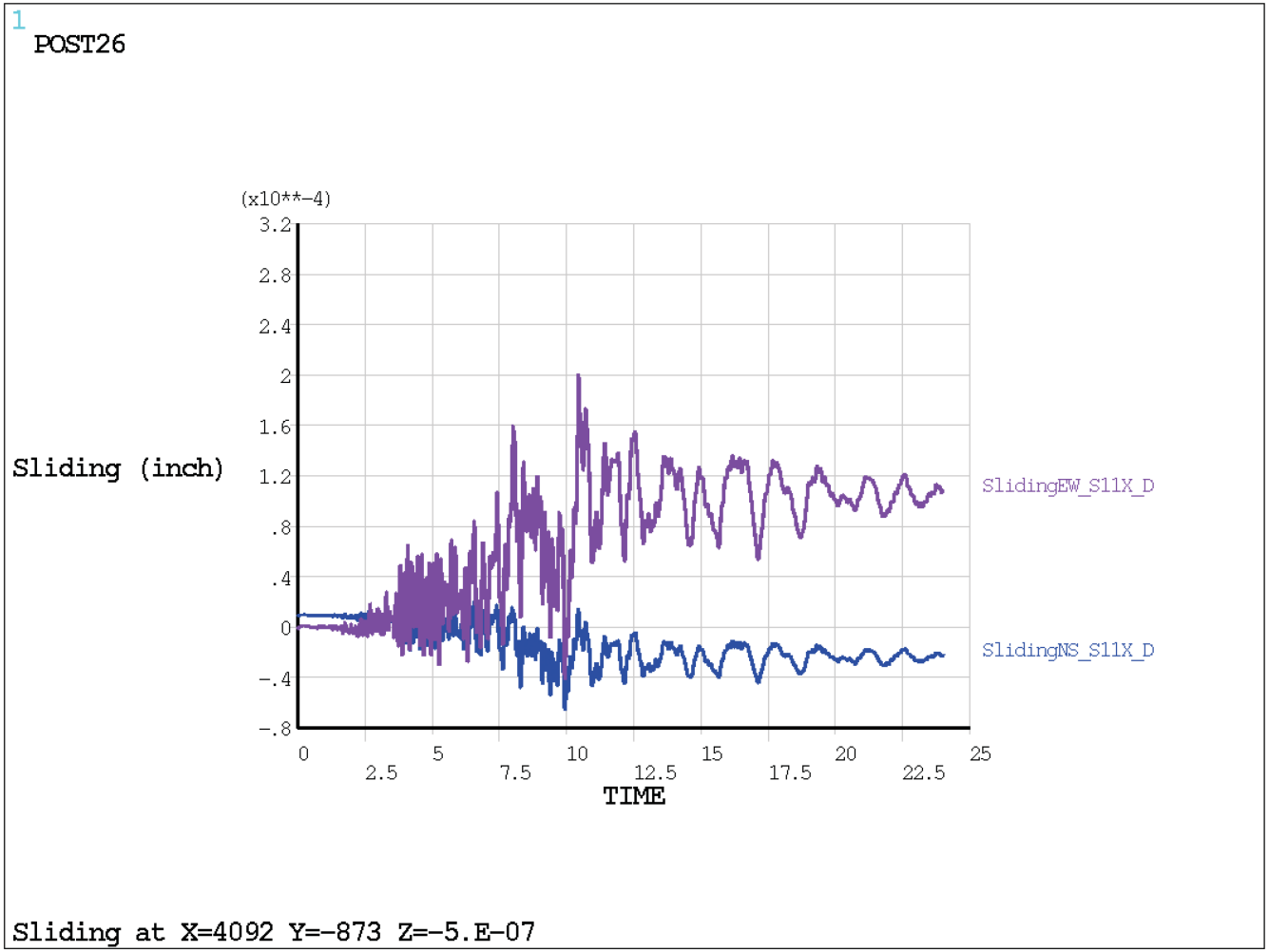

Figure 3.8.5-65: Lateral Relative Displacements (Sliding) at Location A (S11 - N-S Excitation)

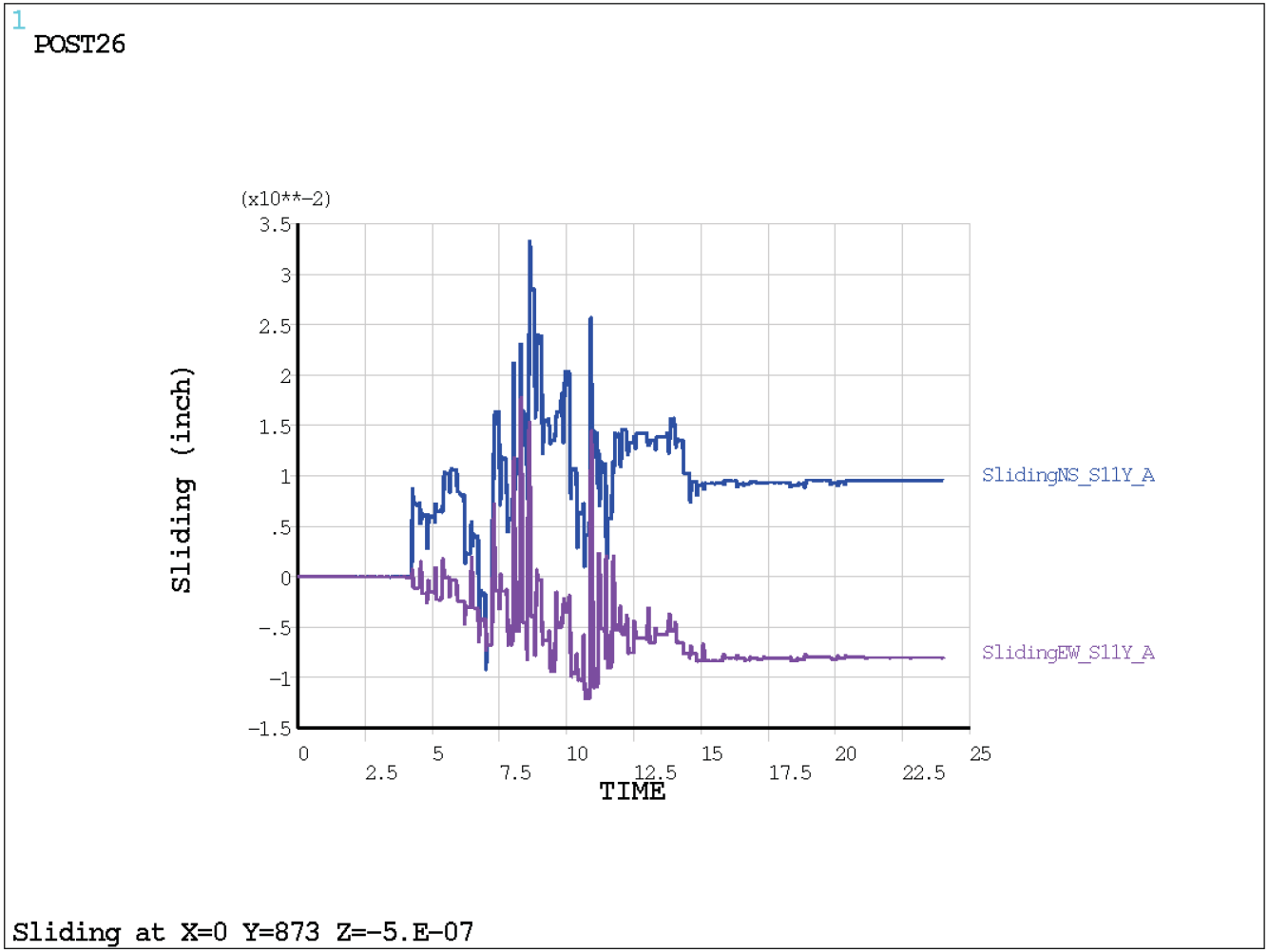

Figure 3.8.5-66: Lateral Relative Displacements (Sliding) at Location B (S11 - N-S Excitation)

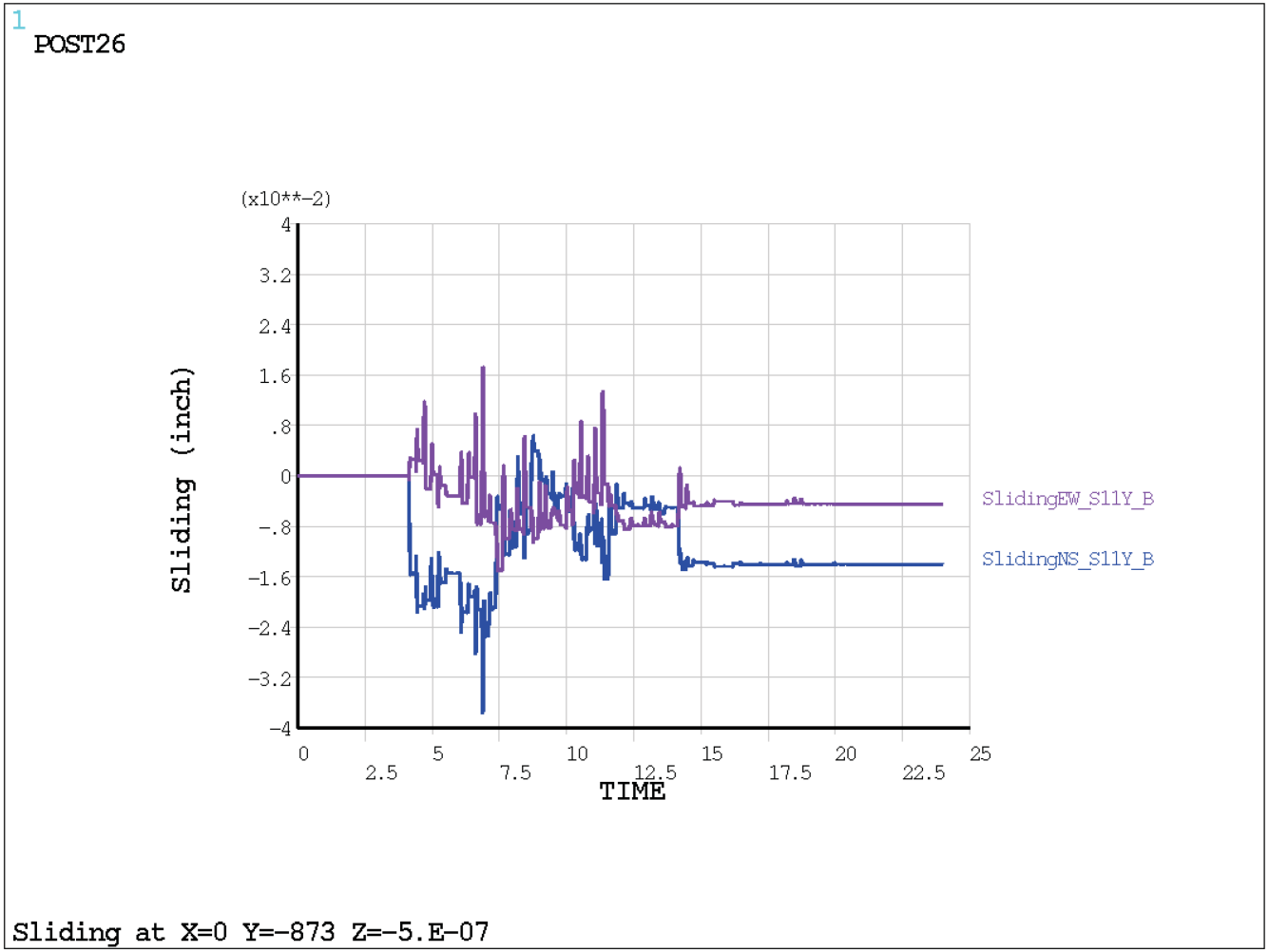

Figure 3.8.5-67: Lateral Relative Displacements (Sliding) at Location C (S11 - N-S Excitation)

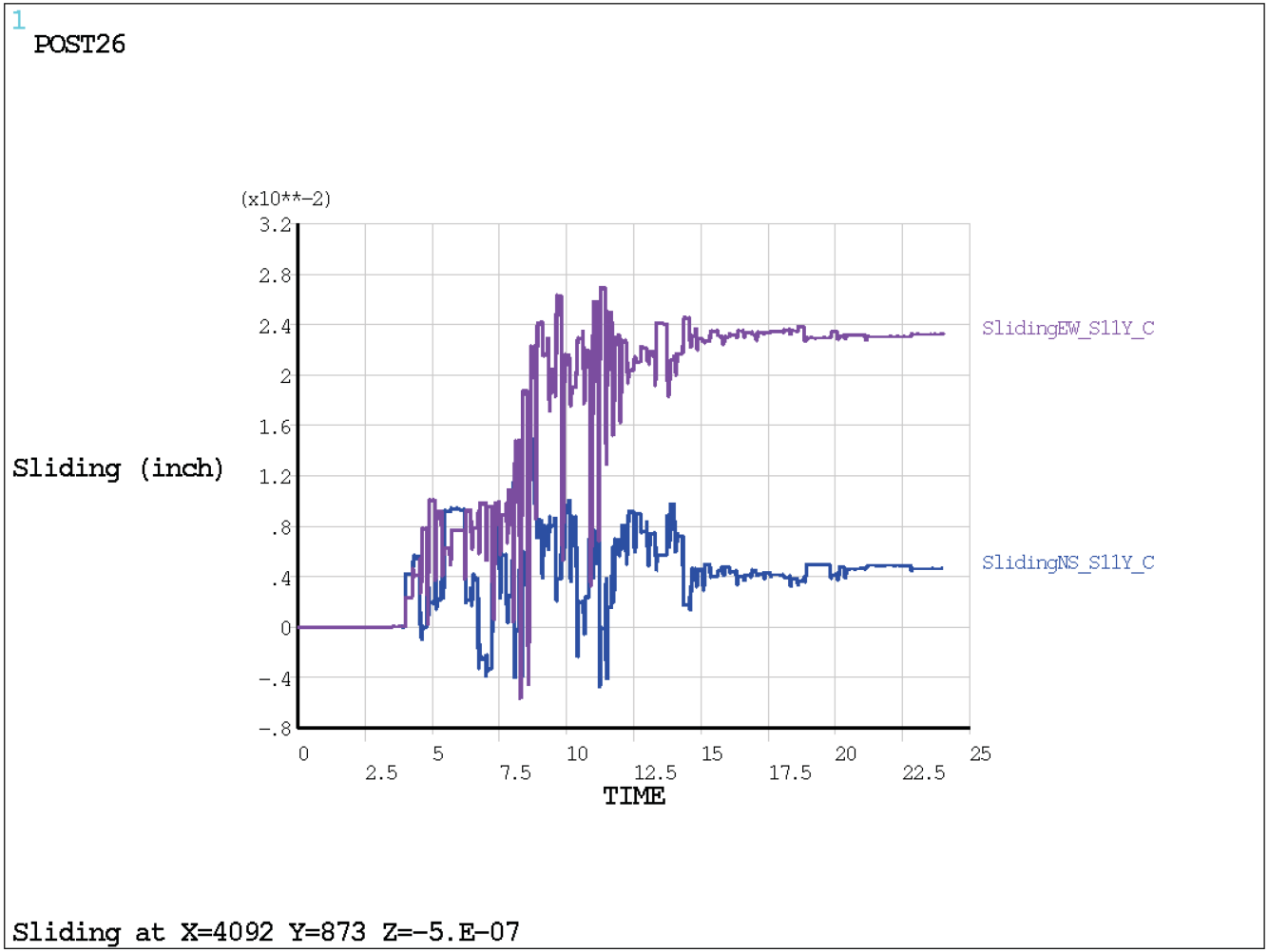

Figure 3.8.5-68: Lateral Relative Displacements (Sliding) at Location D (S11 - N-S Excitation)

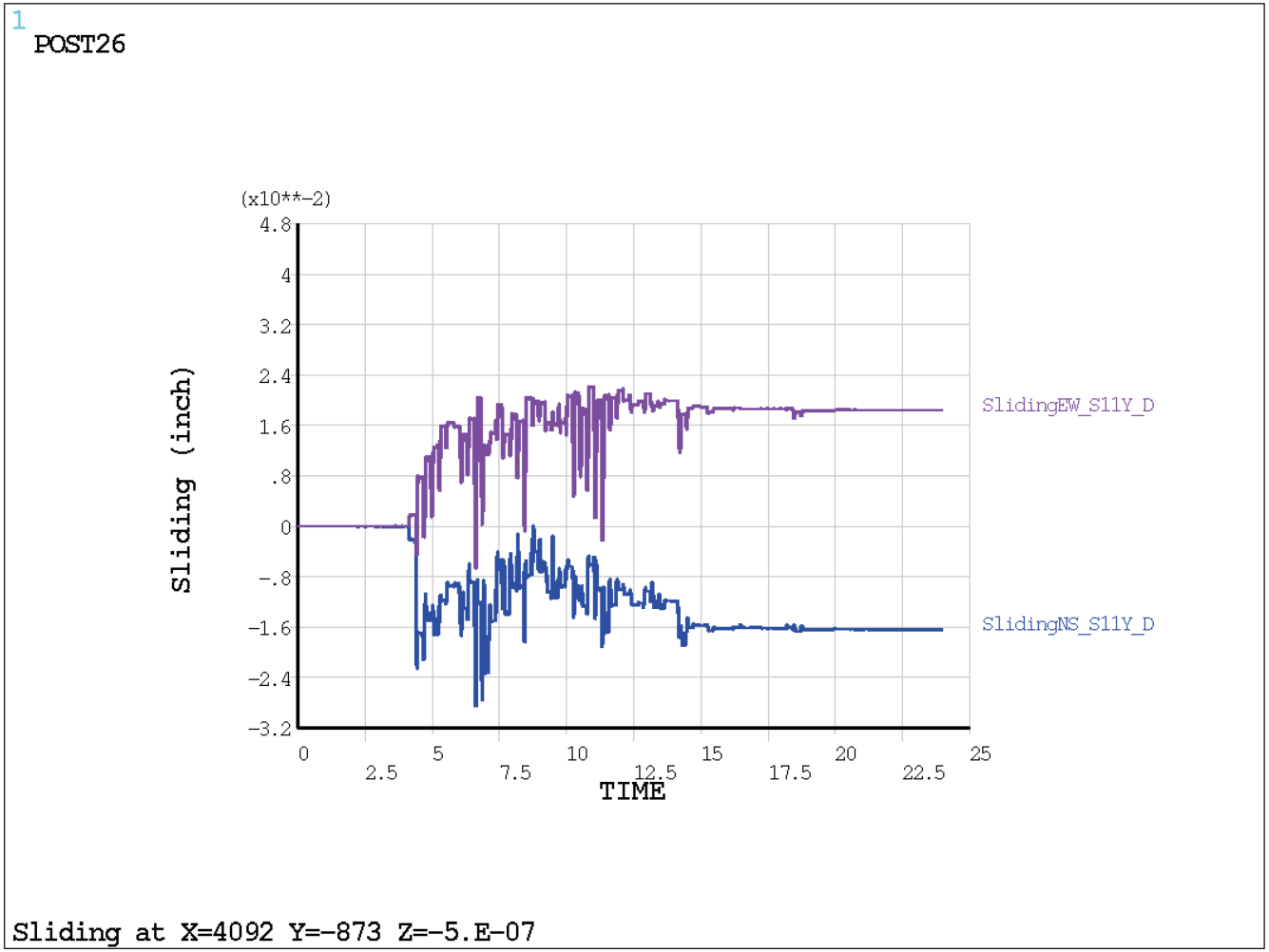

Figure 3.8.5-69: Lateral Relative Displacements (Sliding) at Location A (S8 - E-W Excitation)

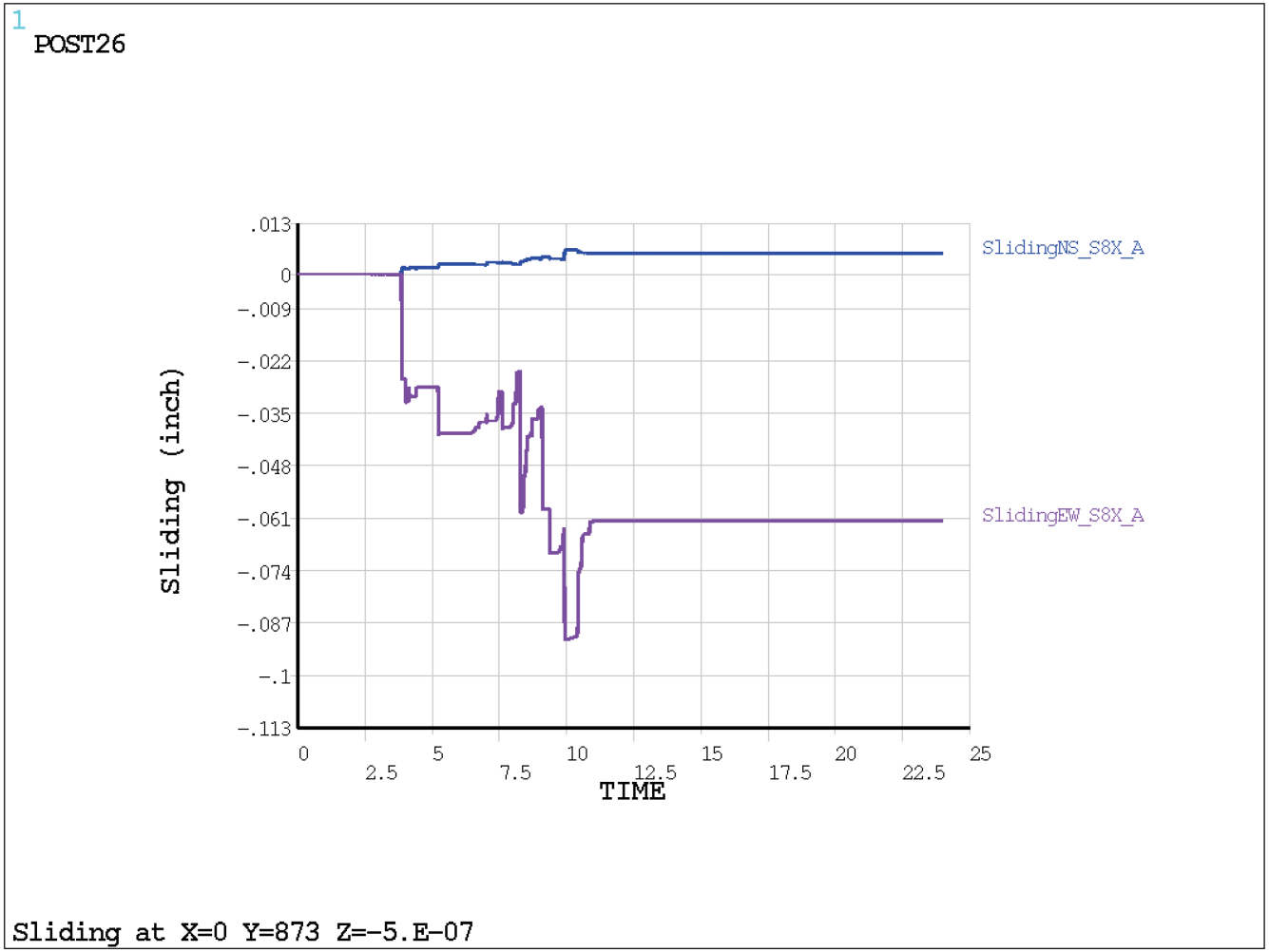

Figure 3.8.5-70: Lateral Relative Displacements (Sliding) at Location B (S8 - E-W Excitation)

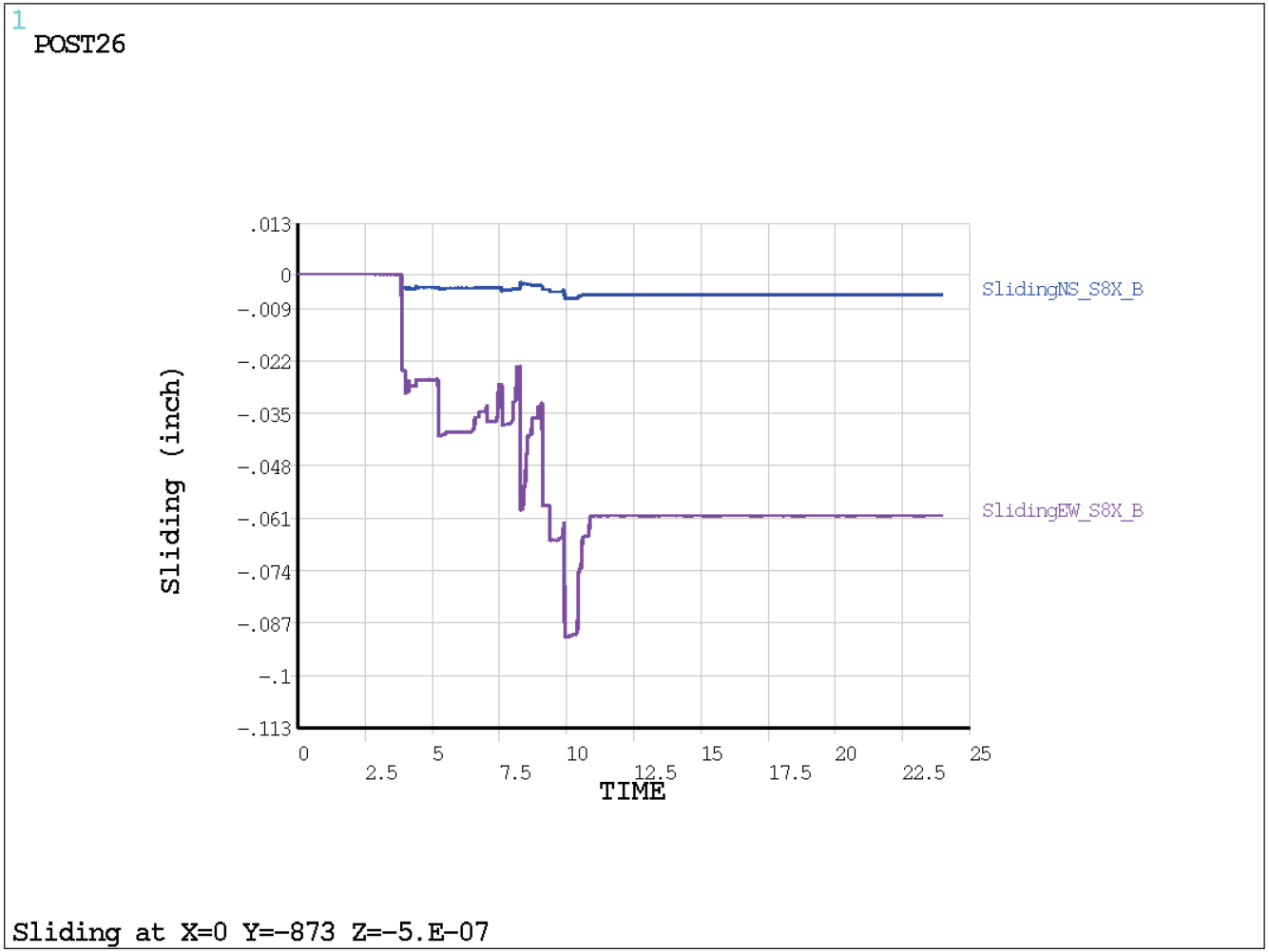

Figure 3.8.5-71: Lateral Relative Displacements (Sliding) at Location C (S8 - E-W Excitation)

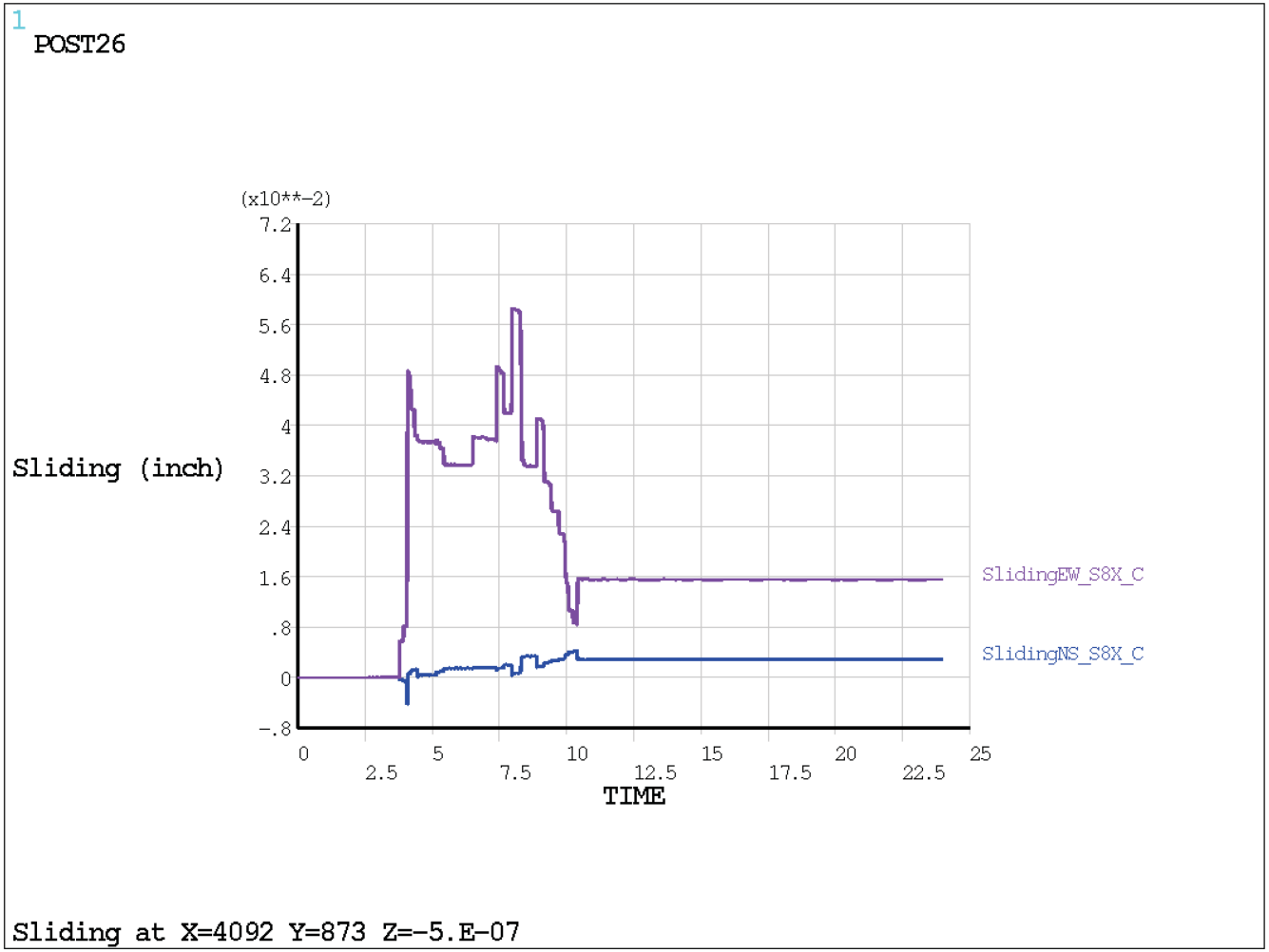

Figure 3.8.5-72: Lateral Relative Displacements (Sliding) at Location D (S8 - E-W Excitation)

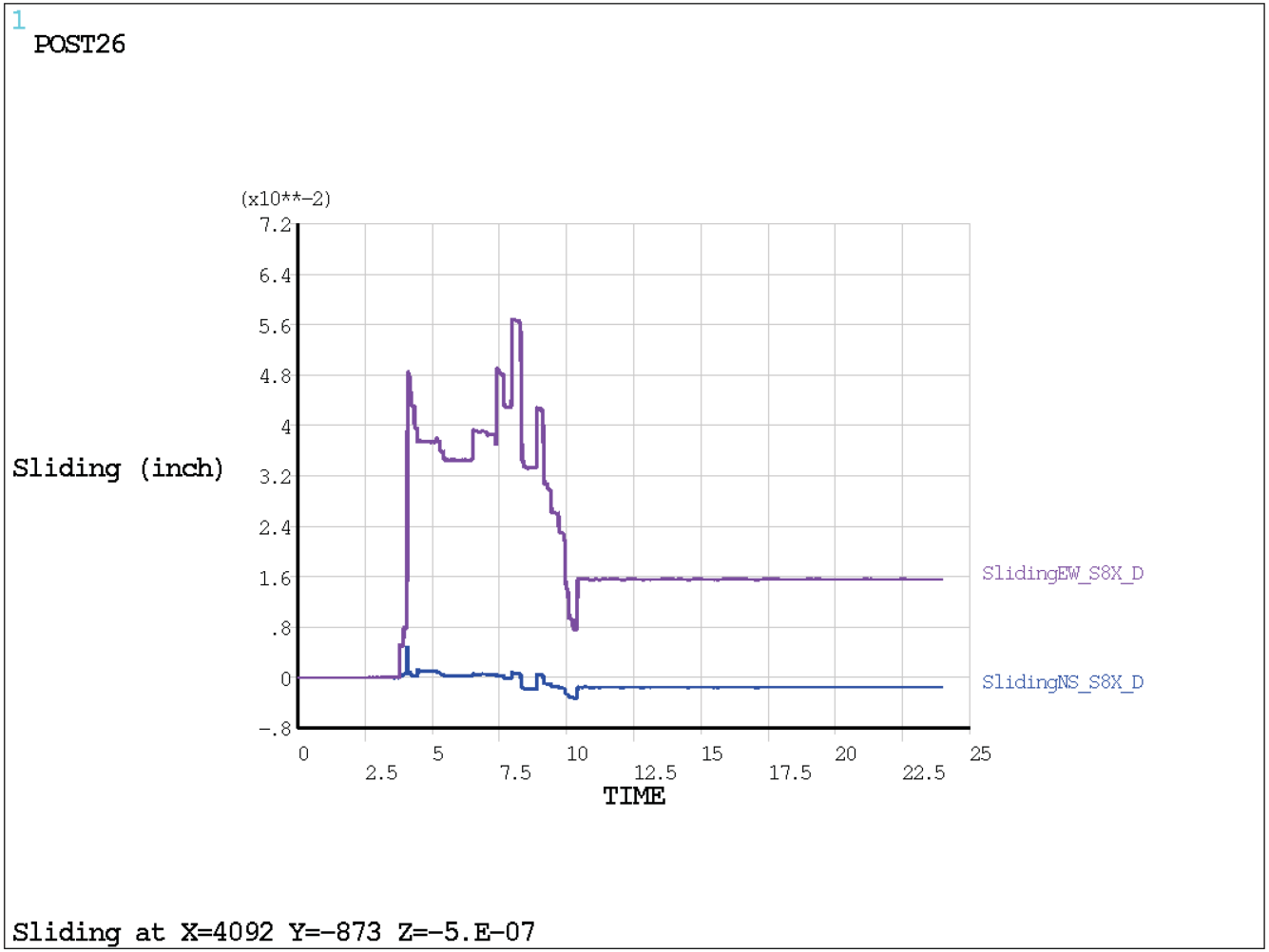

Figure 3.8.5-73: Lateral Relative Displacements (Sliding) at Location A (S8 - N-S Excitation)

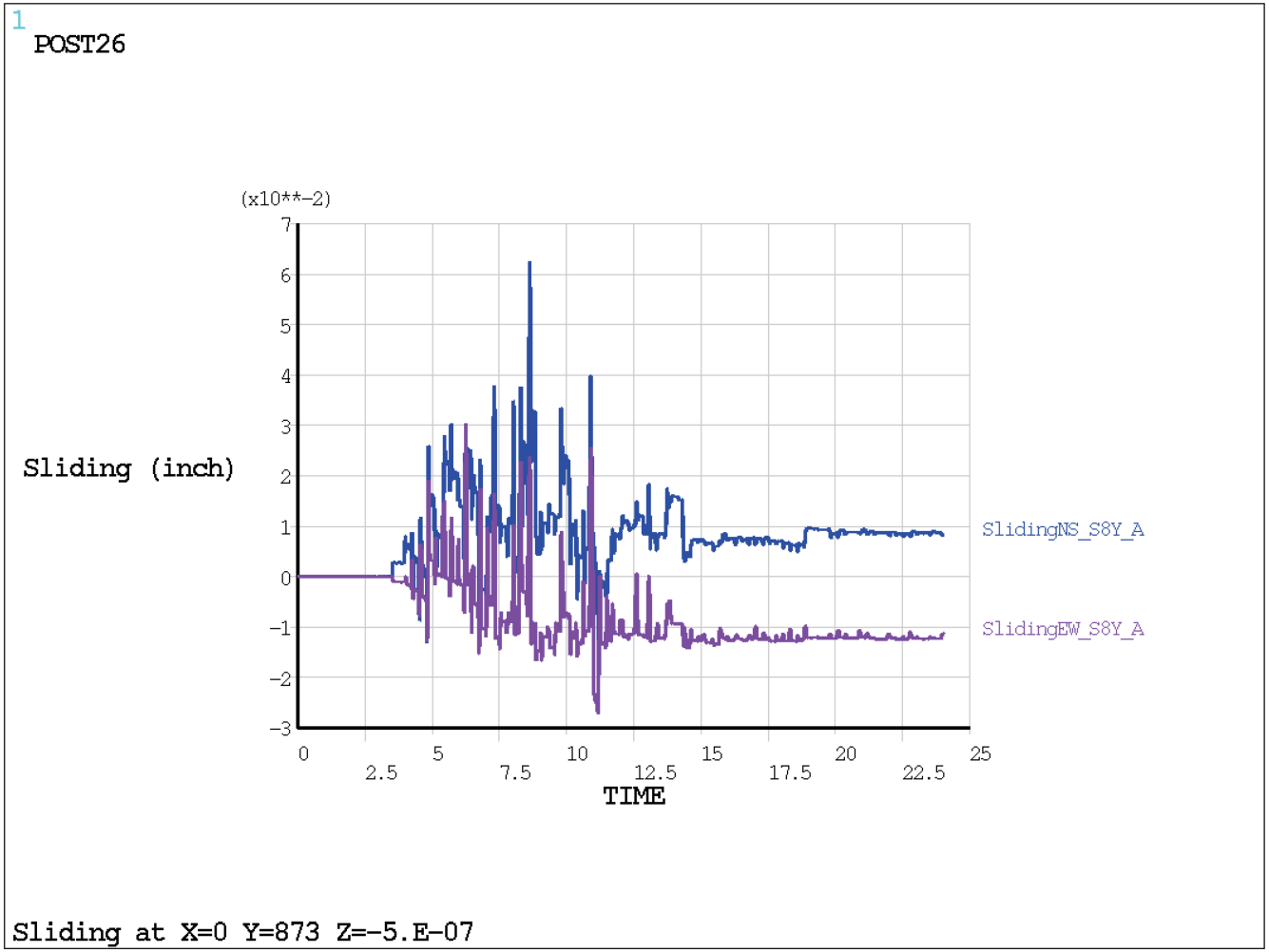

Figure 3.8.5-74: Lateral Relative Displacements (Sliding) at Location B (S8 - N-S Excitation)

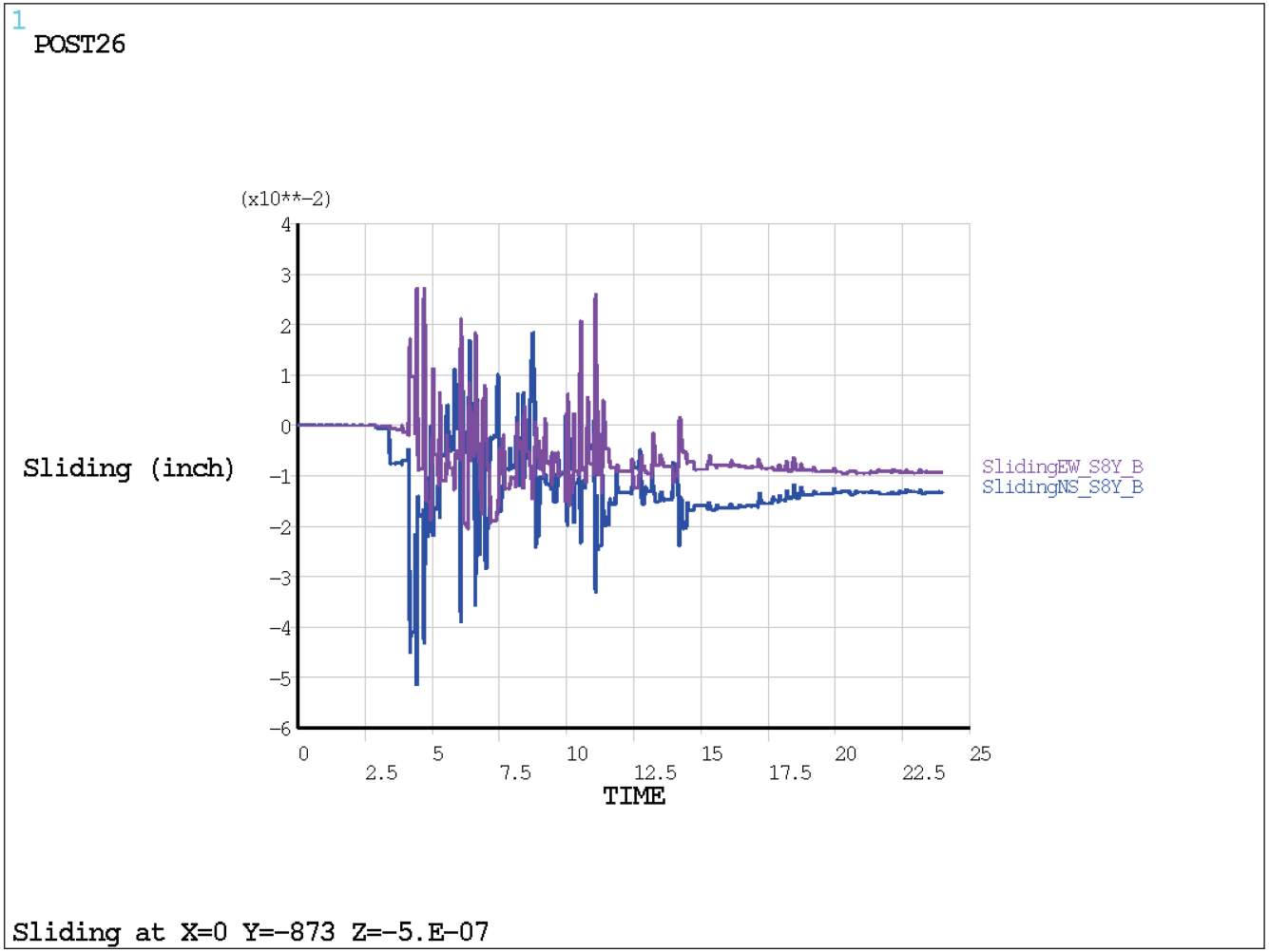

Figure 3.8.5-75: Lateral Relative Displacements (Sliding) at Location C (S8 - N-S Excitation)

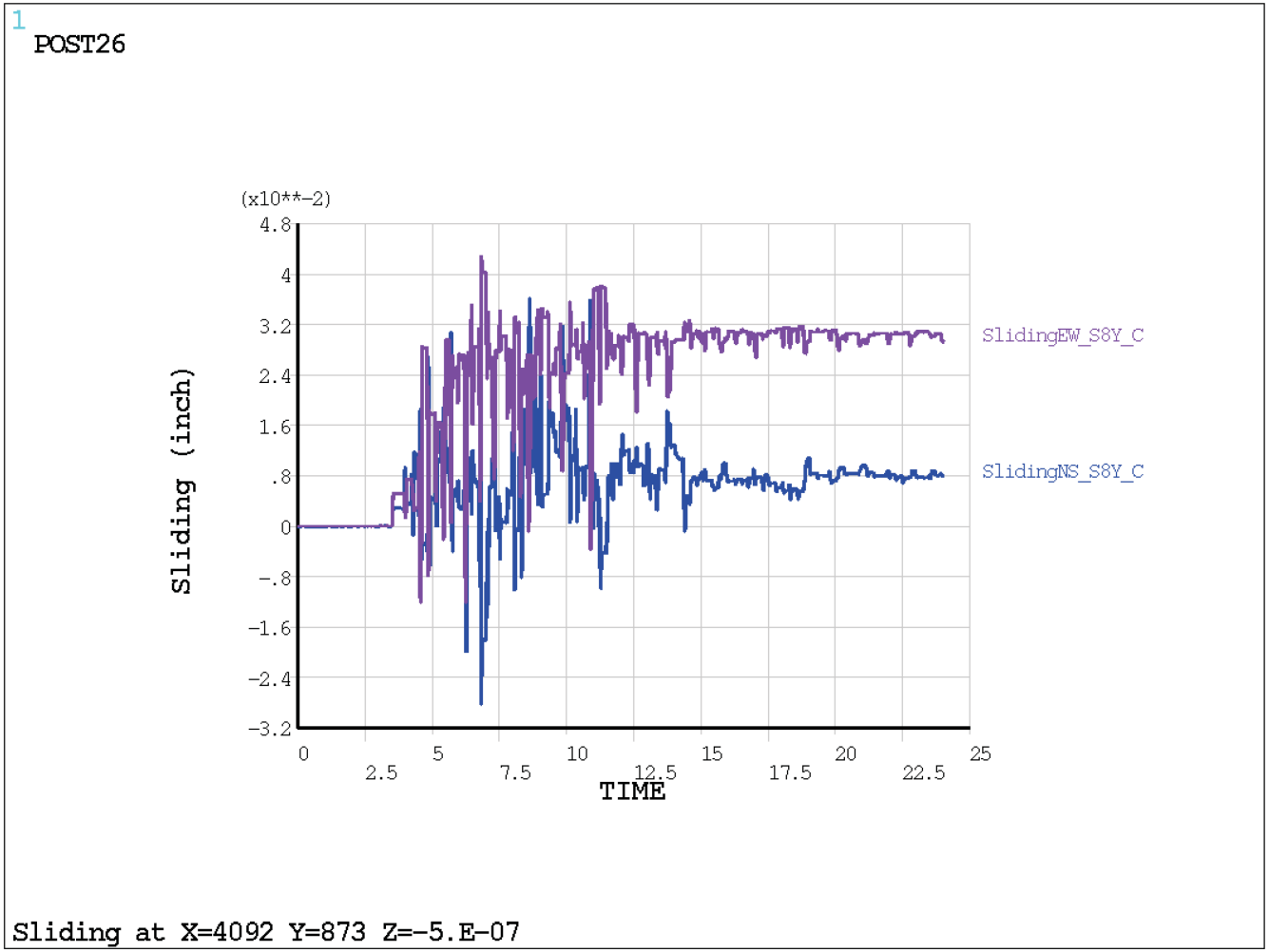

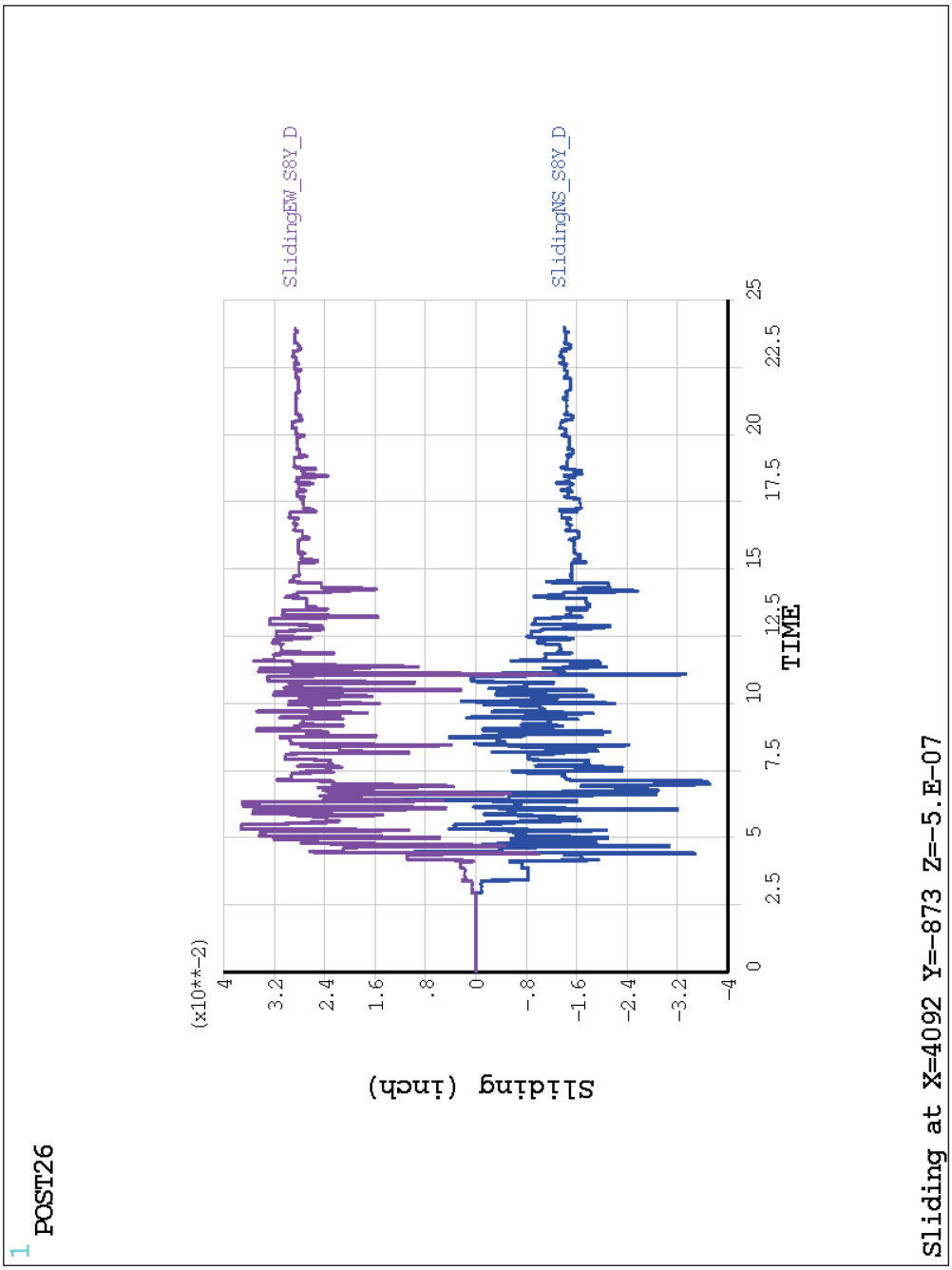

Figure 3.8.5-76: Lateral Relative Displacements (Sliding) at Location D (S8 - N-S Excitation)

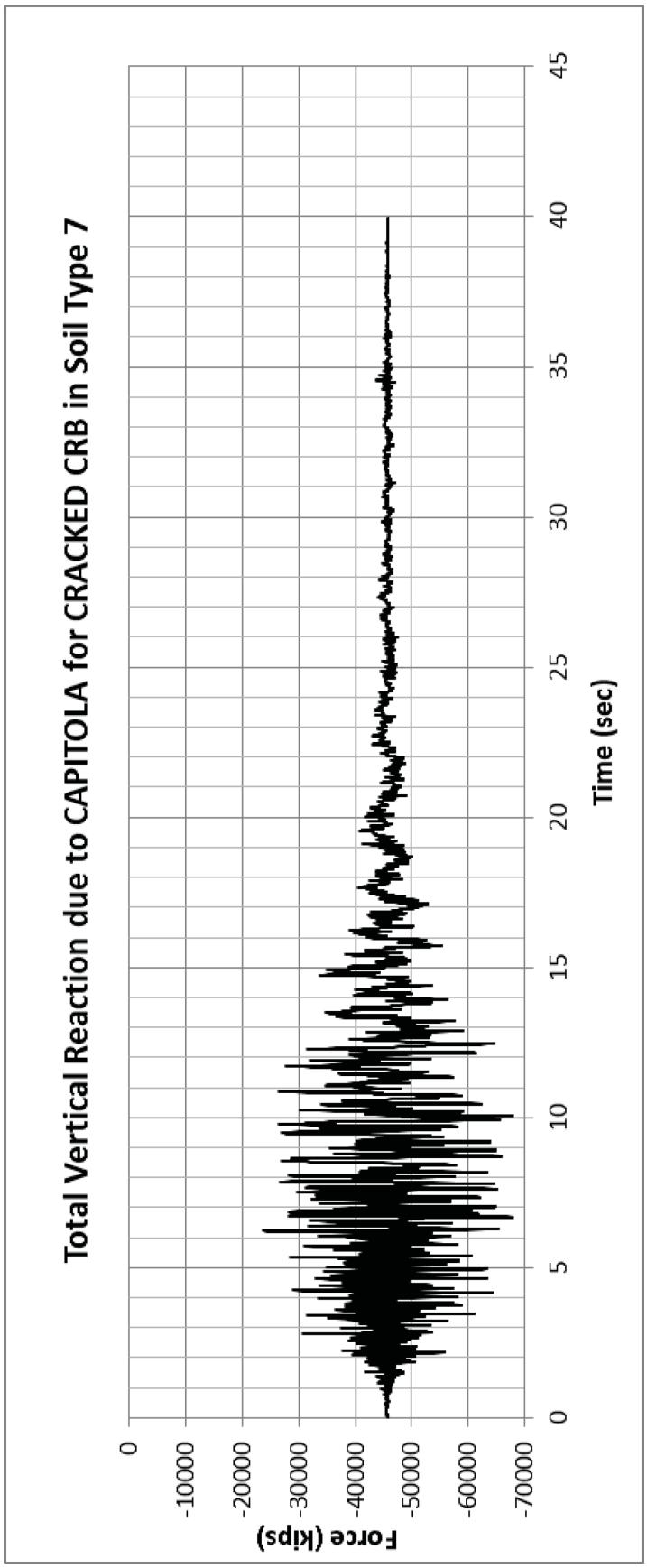

Figure 3.8.5-77: Total CRB Cracked Base Vertical Reaction Time History due to Capitola for Soil Type 7

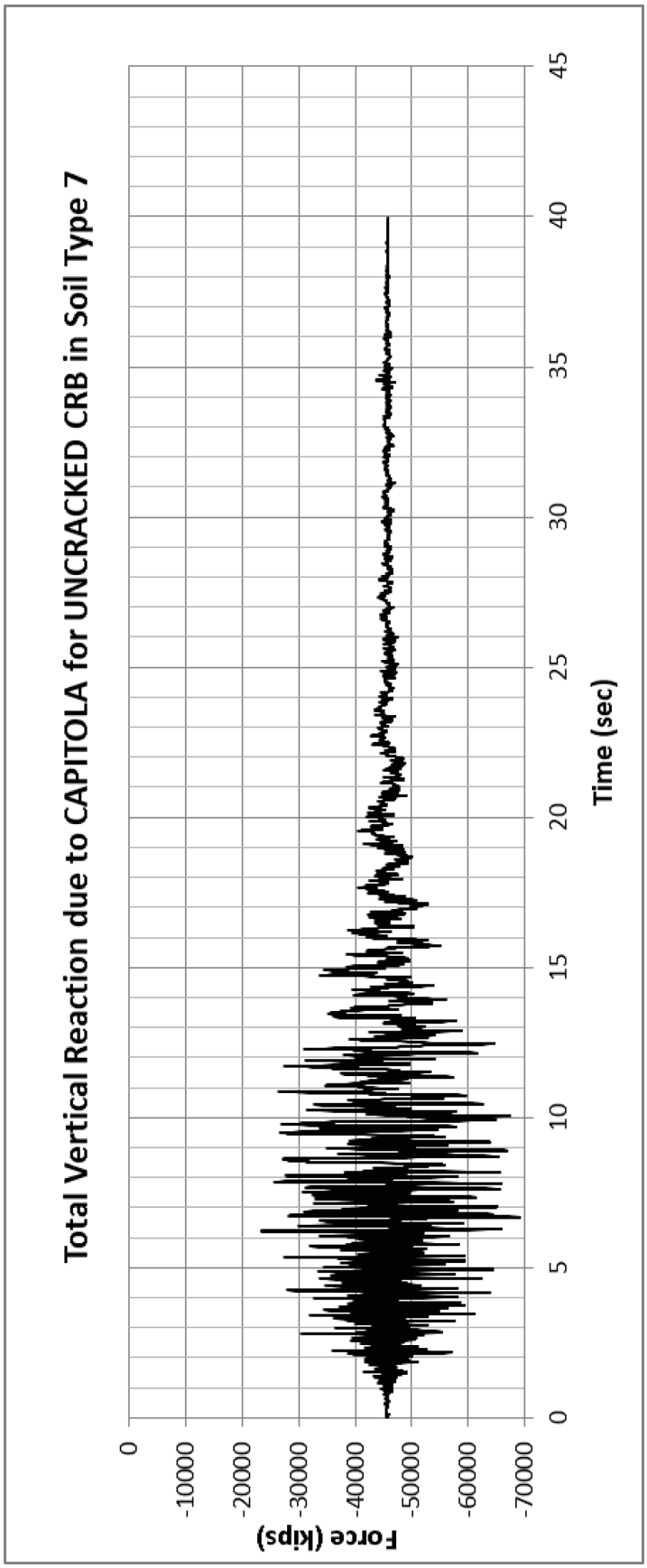

Figure 3.8.5-78: Total CRB Uncracked Base Vertical Reaction Time History due to Capitola for Soil Type 7

Figure 3.8.5-79: Total CRB Cracked Base Vertical Reaction Time History due to Capitola for Soil Type 8

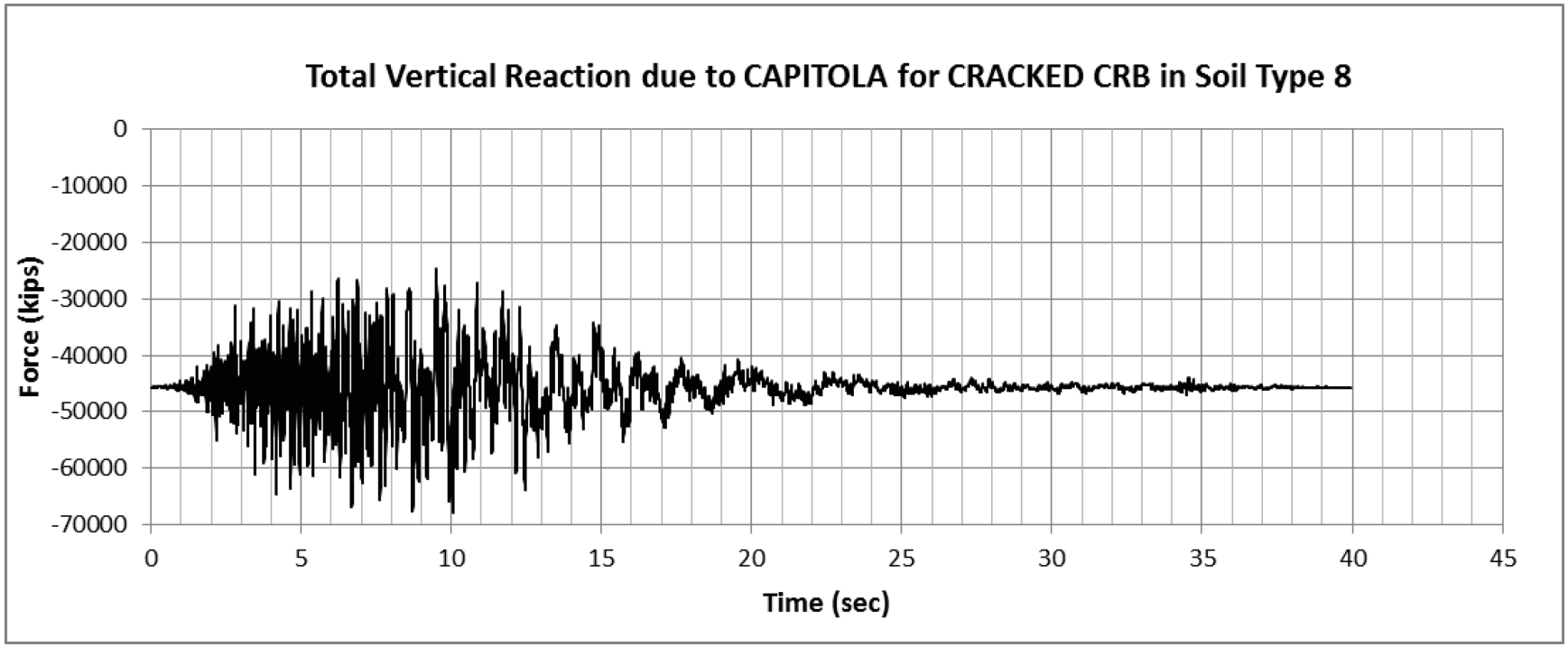

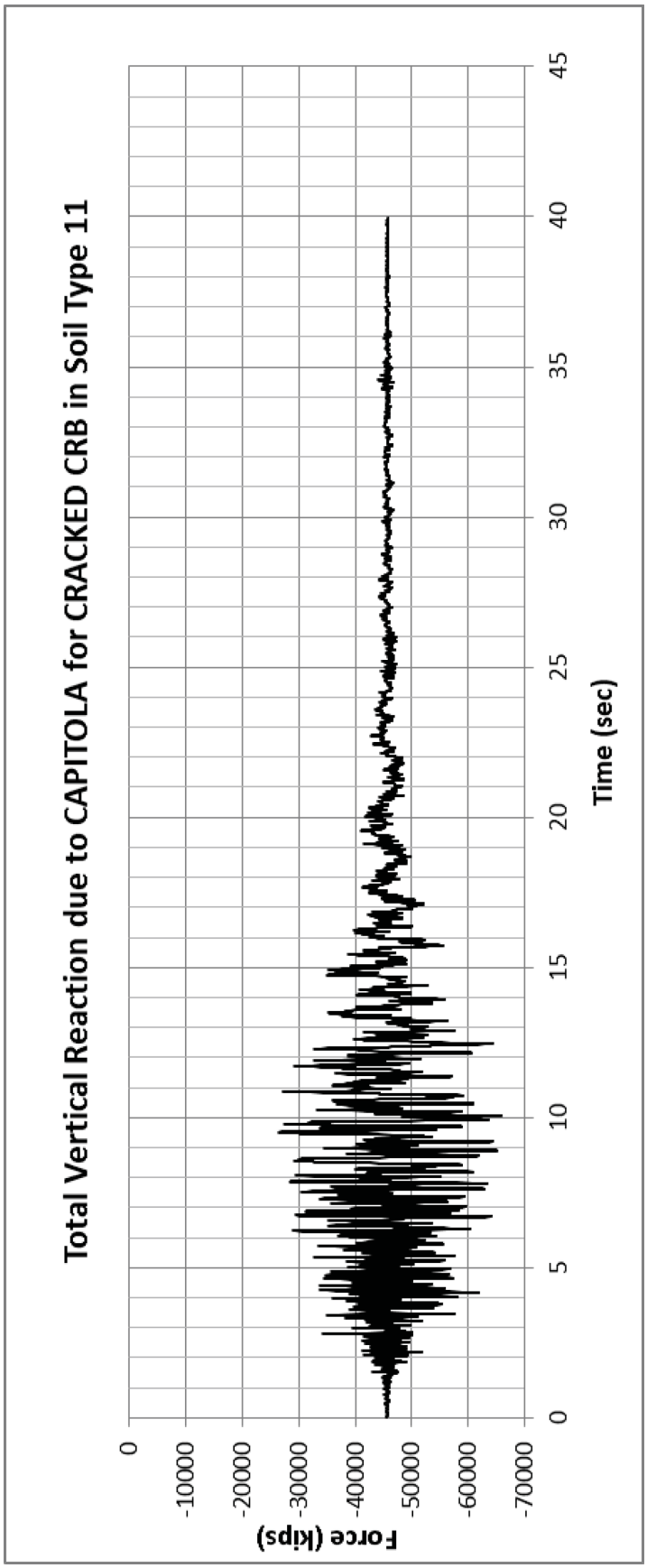

Figure 3.8.5-80: Total CRB Cracked Base Vertical Reaction Time History due to Capitola for Soil Type 11

Figure 3.8.5-81: Total CRB Cracked Base Vertical Reaction Time History due to Lucerne for Soil Type 7

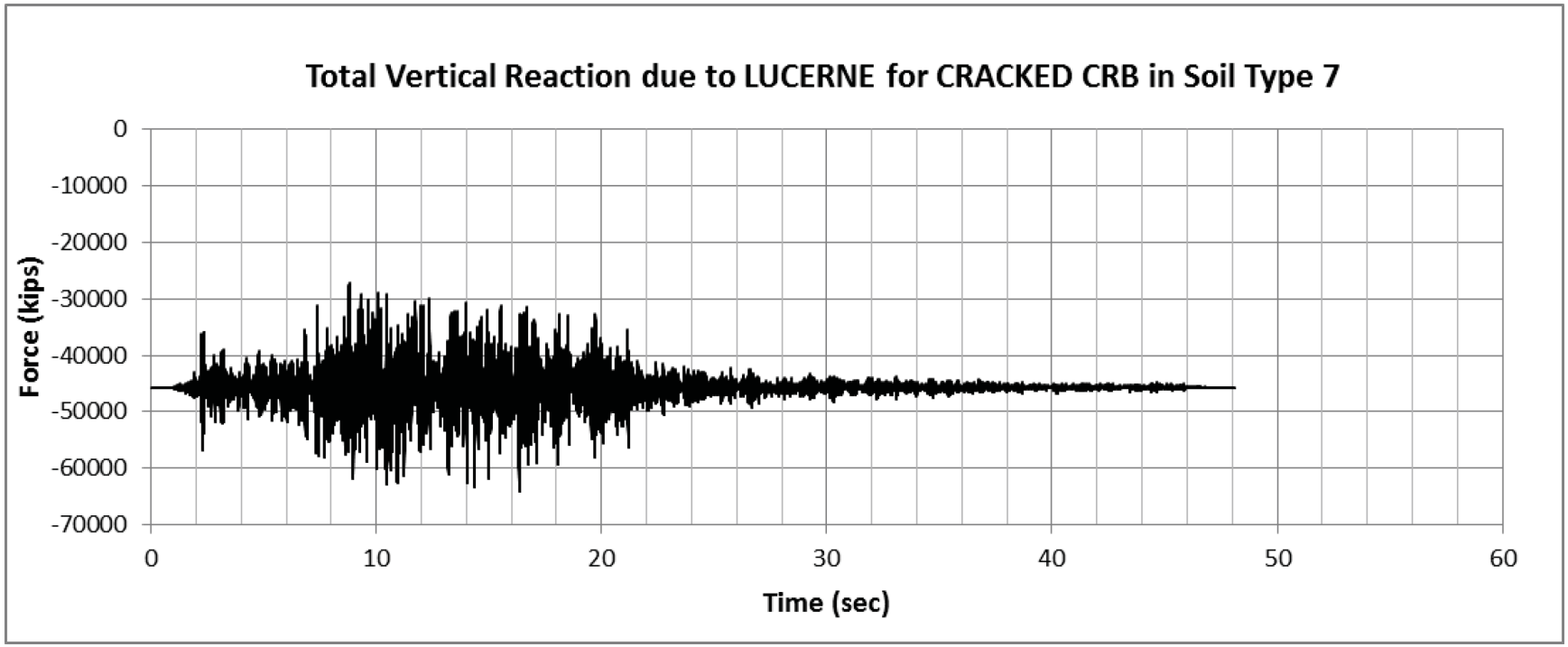

Figure 3.8.5-82: Total CRB Cracked Base Vertical Reaction Time History due to Lucerne for Soil Type 9